BRITISH ANTARCTIC SURVEY

SCIENTIFIC REPORTS

No. 78

THE GEOLOGY OF THE SOUTH SHETLAND ISLANDS:
V. VOLCANIC EVOLUTION OF DECEPTION ISLAND

By

P. E. BAKER, B.Sc., D.Phil., I. McREATH, M.A., Ph.D.,
M. R. HARVEY, B.Sc., Ph.D.,
Department of Earth Sciences, University of Leeds

M. J. ROOBOL, B.Sc., Ph.D.
Department of Geology, Imperial College of Science and Technology, London

and

T. G. DAVIES, B.Sc.
British Antarctic Survey
and
Department of Geological Sciences, University of Birmingham

CAMBRIDGE: PUBLISHED BY THE BRITISH ANTARCTIC SURVEY: 1975
NATURAL ENVIRONMENT RESEARCH COUNCIL

CONTENTS

THE GEOLOGY OF THE SOUTH SHETLAND ISLANDS:
V. VOLCANIC EVOLUTION OF DECEPTION ISLAND

By

P. E. BAKER,* B.Sc., D.Phil., I. McREATH, M.A., Ph.D.,
M. R. HARVEY, B.Sc., Ph.D.,
Department of Earth Sciences, University of Leeds

M. J. ROOBOL,† B.Sc., Ph.D.
Department of Geology, Imperial College of Science and Technology, London

and

T. G. DAVIES, B.Sc.
British Antarctic Survey
and
Department of Geological Sciences, University of Birmingham

(Manuscript received 19th January, 1973)

ABSTRACT

THE renewed volcanic activity at Deception Island appears to be closely associated with the caldera ring fault. In 1967, a submarine eruption created a new island in Telefon Bay and there was a simultaneous eruption at the land centre, 2 km. to the east. In 1969, a 5 km. fissure opened up in the glacier on the western face of Mount Pond. There were numerous vents but the most damaging aspect of the eruption was the liberation of a large volume of glacial melt water. In the 1970 eruption a series of craters built a new strip of land across Telefon Bay, partly destroying the 1967 island.

The new ejecta are remarkably variable in composition. They tend to become more basic further away from the site of the 1967 island. At any particular locality later products tend to be slightly more basic than earlier ones.

The distinctive Na-rich, K-poor characteristic apparently persists right through the history of Deception Island. Two basalt types are recognized, one rich in alumina and the other rich in iron. However, the high Na : K ratio is especially accentuated in the more differentiated post-caldera rocks, to which the recent eruptives belong.

The Deception Island suite differs in several essential aspects from the typical calc-alkali series. These differences may be explained by persistent loss of volatiles inhibiting the formation of amphibole.

* Formerly at Department of Geology and Mineralogy, University of Oxford.
† Present address: Départment de Géologie, Université de Montréal, Case postale 6128, Montréal 101, Canada.

From Livingston Island to Clarence Island the north-western side of Bransfield trough is a remarkably steep and linear feature which is almost certainly a fault line. However, neither the trough nor the escarpment are very apparent in the vicinity of Deception Island, which seems to have been constructed as a south-easterly appendage to the South Shetland Islands shelf. South of Deception Island, the submarine topography is shallower and more complex than in Bransfield trough, which, if it existed here, has since been obscured by volcanism and sedimentation. The major topographical elements of Bransfield Strait tend to fade out about 100 km. south-west of Deception Island.

Along the length of Bransfield trough is a chain of islands and shoals, lying off the South Shetland Islands shelf in a closely analogous situation to that of Deception Island. This line parallels the steep margin of the trough and runs from Deception Island, through Bridgeman Island and beyond to the north-east. Bridgeman Island, though volcanic, has no crater nor does it show signs of recent activity, but Penguin Island (off King George Island) is evidently a very recent volcano (González-Ferrán, 1971).

Three structural/topographical trends may have influenced the situation and growth of the Deception Island volcano:

i. A north-east to south-west trend is illustrated by the major fault scarp flanking Bransfield trough.
ii. A north-west to south-east trend, as shown by the prominent fault system which appears to cross Bransfield Strait, creates marked embayments in the opposing slopes of the South Shetland Islands shelf and the continental shelf off Trinity Peninsula.
iii. A less obvious north–south trend, as illustrated by the elongation of Trinity Island, and the submarine bank linking it with Deception Island.

The seismic work of Ashcroft (1972) and the gravity survey of Davey (1971) showed the South Shetland Islands with an up-faulted high-density core and a large thickness of low-density sediment forming the shelf to the north-west of the islands. Bransfield trough is a rift structure with sediments overlying an oceanic type of crust. From magnetic lineations, Barker and Griffiths (1972, p. 169) considered that in the Upper Miocene there was a spreading axis west of the Shackleton fracture zone with complementary consumption of crustal material along the line of the South Shetland Islands trench. They regarded the extensional opening of the Bransfield Strait graben as a secondary effect of plate consumption.

There are strong geological and geophysical similarities between the South Shetland Islands ridge and Trinity Peninsula. In both cases, low-velocity crustal layers are much thicker than in the intervening Bransfield Strait, where mantle velocities are encountered at about 15 km. (Ashcroft, 1972).

In the South Shetland Islands, sediments of the Miers Bluff Series, which are believed to be equivalent to the Trinity Peninsula Series of Graham Land (Hobbs, 1968, p. 17) are overlain by calc-alkaline andesites and rhyolites of an Upper Jurassic age. These older formations are invaded and altered by the Andean Intrusive Suite. Tertiary volcanism is generally more widespread in the South Shetland Islands than on the Antarctic Peninsula (Adie, 1971), but in the late Tertiary (*c.* 6–1 m. yr.) activity seems to have been concentrated along the eastern side of the Antarctic Peninsula forming the James Ross Island Volcanic Group (Nelson, 1966; Rex, 1971). There has been Recent, though not historical, volcanism on Paulet Island and at the Seal Nunataks, both of which are situated on the Weddell Sea coast of the Antarctic Peninsula.

The Deception Island basalts are compositionally similar to those of the James Ross Island Volcanic Group, though the distinctive sodic differentiates are unique to Deception Island.

Volcanism in the northern part of the Antarctic Peninsula has undergone a change from the calc-alkaline orogenic type in the Mesozoic and early Tertiary to mildly alkaline in late Tertiary to Recent times (Table I). In some respects, the volcanic rocks of Deception Island reflect this change, causing Hawkes (1961) to regard them as an alkaline deviation from the normal andesite–rhyolite association. It is possible that cessation of crustal consumption at the South Shetland Islands trench, which Barker and Griffiths (1972, p. 170) considered to have occurred during the past 8 m. yr., coincided with the change from calc-alkaline to mildly alkaline volcanism.

B. Structure and Volcanic History

Deception Island is a horseshoe-shaped island 14 km. north–south by 13 km. east–west. It reaches a height of 542 m. at the summit of Mount Pond and 459 m. on Mount Kirkwood, both of which have a permanent glacier cover. These peaks are part of an almost continuous ring of hills which encircles the sunken interior

I. INTRODUCTION

By

P. E. BAKER *and* M. J. ROOBOL

THE sudden renewal of volcanic activity on Deception Island in 1967 and the subsequent eruptions of 1969 and 1970 provided a new stimulus for scientific investigation. Much of the work has been concerned with the immediate effects and interpretation of the eruptions. However, there has been a corresponding revival of interest in the older formations of Deception Island and in its volcanic history. There are also the wider implications of volcanism on Deception Island and the northern Antarctic Peninsula area, especially their significance in terms of the current structural regime and recent lithospheric movements. In addition to geological work there have also been new biological and glaciological studies.

The eruptions have been relatively trivial events when viewed in geological perspective, though they have caused considerable damage and inconvenience. Although individually their intrinsic importance is small, taken together they have provided an unusually good opportunity of following the progress of volcanism associated with an active caldera.

Scientists from several nations have shared in the new investigations of Deception Island and a number of accounts have already been published (e.g. Baker and others, 1969; Orheim, 1970, 1971*a*, *b*, *c*; Shultz, 1970, 1971, 1972; Baker and McReath, 1971*a*, *b*, 1972; Fourcade, 1971; González-Ferrán and others, 1971*a*, *b*). The present report represents a statement of British work on the island with emphasis on the recent eruptions, together with a summary of the geology and a study of the geochemistry. Though reference has been made to the earlier studies of Holtedahl (1929) and Olsacher (1956), it is to the work of Hawkes (1961) that the authors are especially indebted. His map provided an excellent foundation for the studies presented here, and his descriptions of the geological formations and their structural relations proved of great value in spite of some differences in interpretation.

This collection of reports is based on the following periods of field work on the island:

i. 4 December 1968–10 January 1969. Study of the effects of the 1967 volcanic eruption, revision of the geological map of Deception Island and general collections for geochemistry. [P.E.B., T.G.D. and M.J.R.]
ii. 10–22 March 1969. Study of the effects of the February 1969 eruption. [P.E.B. and M.J.R.]
iii. 9–30 December 1970. Study of the effects of the August 1970 eruption. [P.E.B. and I.McR.]
iv. December 1971–January 1972. Study of the older pyroclastic rocks of Deception Island. [M.R.H.]

The investigations have been supported by the Royal Society and the British Antarctic Survey, and in the case of M. R. Harvey's study of the older pyroclastics by the Natural Environment Research Council. Logistic support has also been provided on various occasions by the Argentine Navy and the Royal Navy. Visits to the island were partly dependent on the availability of ships in the period after an eruption. After the first visit to the island in 1968, a year after the eruption, it became obvious that much would be gained by reducing such a delay, thereby avoiding the problems caused by re-distribution of the new deposits. Through the prompt support of the Royal Society and the British Antarctic Survey, it proved possible to reach Deception Island much sooner after the subsequent eruptions.

A. GEOLOGICAL SETTING

Deception Island (lat. 63°00'S., long. 60°40'W.), so called because of the concealed inner harbour of Port Foster, is the southernmost of the South Shetland Islands. The latter lie along the south-eastern edge of a broad shelf which has a depth of approximately 250 m. and extends from Boyd Strait (north-east of Smith Island and Low Island) 450 km. north-eastward to Elephant Island (Fig. 1). Davey (1971) referred to the two separate branches of the Scotia Ridge in this area, one forming the South Shetland Islands shelf and the other Trinity Peninsula. The two are separated by Bransfield trough (Ashcroft, 1972), which is defined by the 1,000 m. bathymetric contour but reaches a maximum depth of 2,800 m. North-westward on the oceanic side of the shelf is the South Shetland Islands trench where the depth reaches more than 5,000 m.

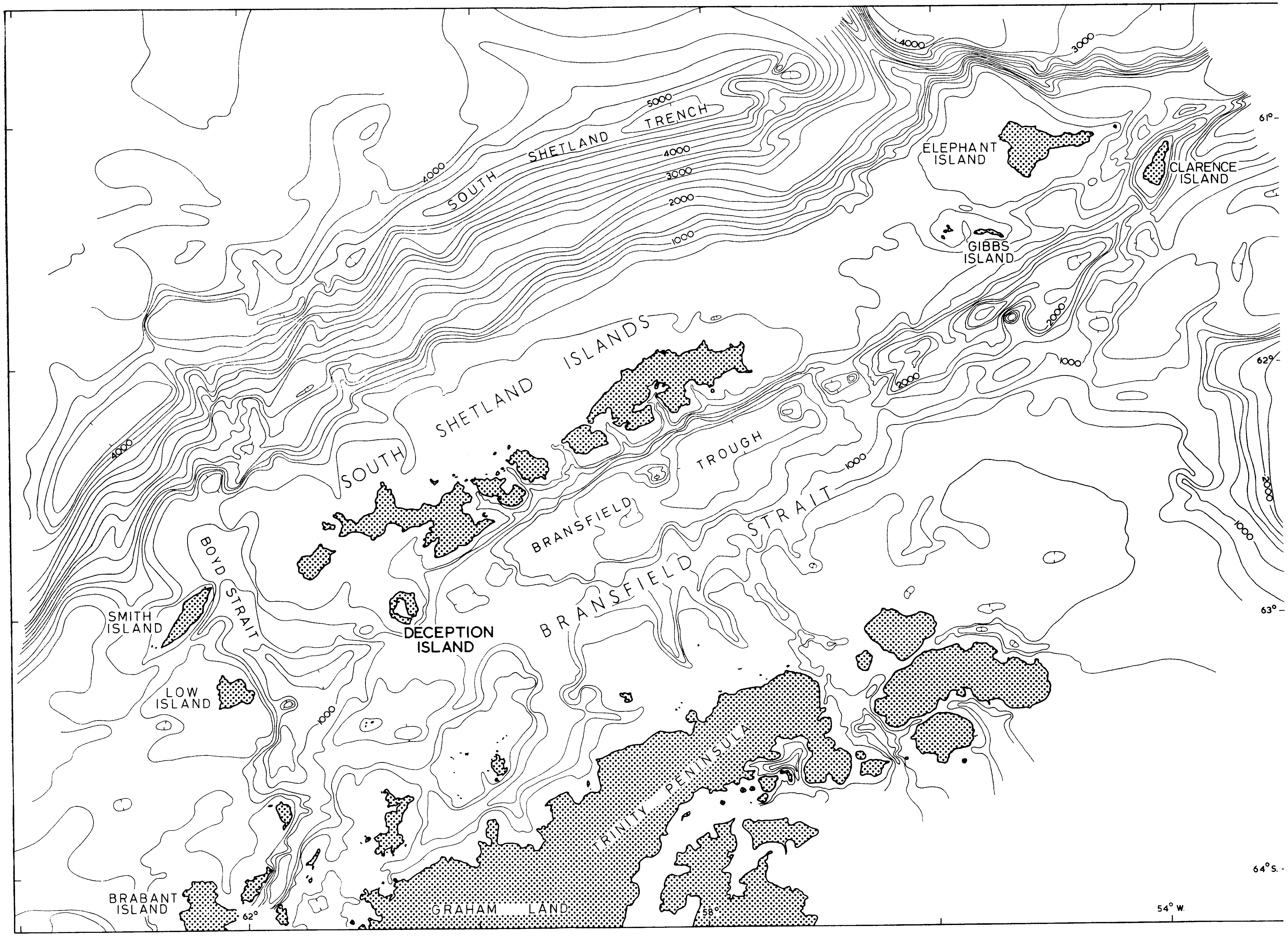

FIGURE 1

Bathymetric map of the area around the South Shetland Islands, showing the location of Deception Island.

[face page

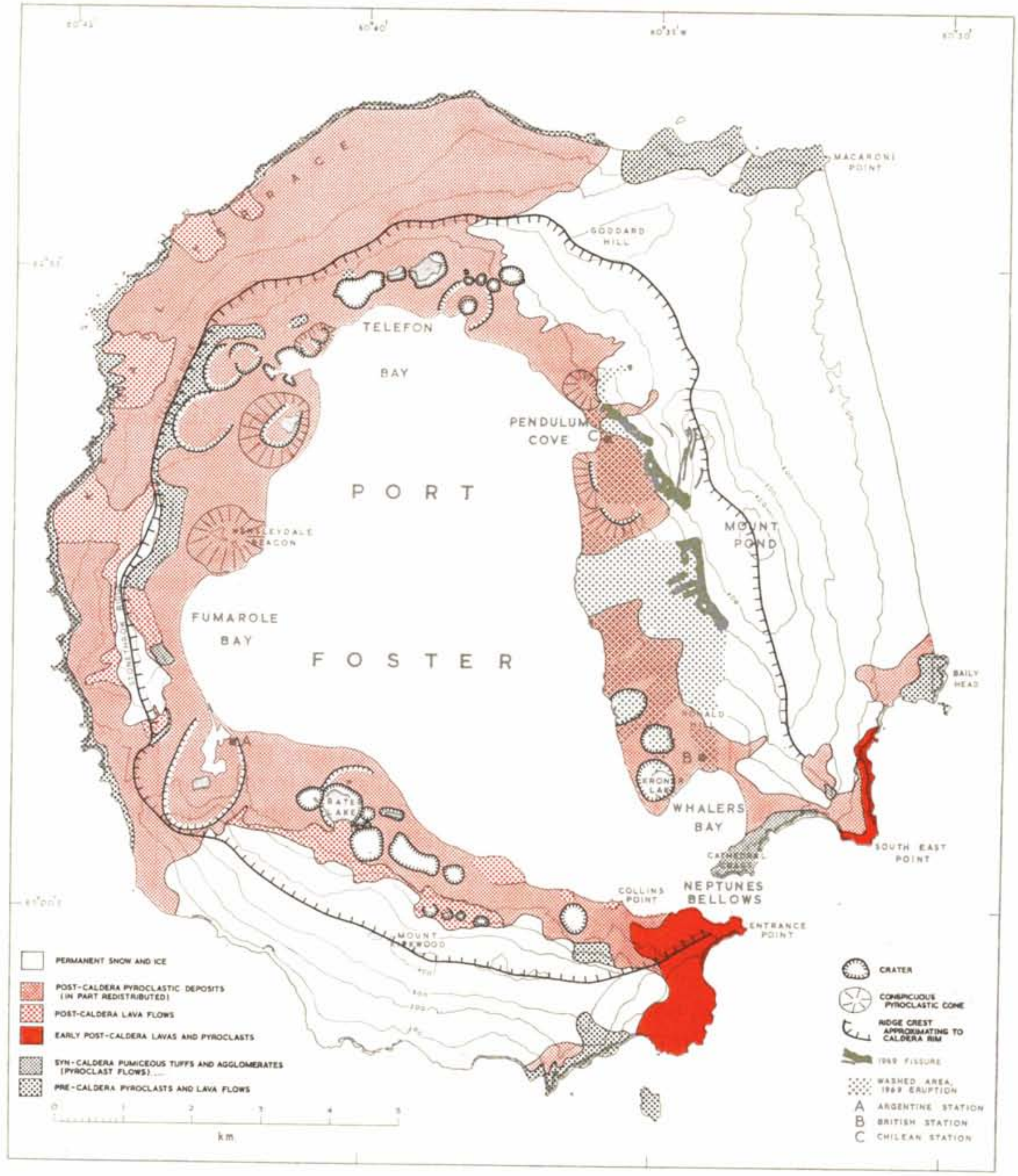

FIGURE 2
Simplified geological sketch map of Deception Island (to December 1970). (Based partly on Hawkes, 1961.)

The products of the early volcano consist of lava flows and red scoria horizons, as exposed in the caldera wall, together with the yellow palagonite-tuffs and agglomerates, exposed in the sea cliffs and referred to by Hawkes as the Outer Coast Tuff. These older pyroclastic deposits are described on p. 10. The thin lava flows, which are interbedded with the tuffs, all lack a pillowed structure and there are no palagonite-breccias of the sort described by Nelson (1966) from James Ross Island. However, many of the tuffs show evidence of shallow-water deposition and it is probable that the early volcano never rose very much above sea-level. In the well-exposed sections in the 200 m. high sea cliffs south of Neptunes Bellows (Fig. 4) and

TABLE II
GENERAL STRATIGRAPHICAL SUCCESSION ON DECEPTION ISLAND

Stage	*Localities of deposits*	*Approximate equivalent (Hawkes, 1961)*
"Historical" eruptions		
1970	Telefon Bay	
1969	Mount Pond	
1967	Telefon Bay	
1912–17	? (Orheim, 1971*c*)	
Post-1842, pre-1957	Kroner Lake, etc. (Roobol, 1973)	
1842	Mount Kirkwood	
Later post-caldera eruptions	lava flows e.g. Kendall Terrace, Stonethrow Ridge	**Whalers Bay Group**
	pyroclastic cones e.g. Crimson Hill, Wensleydale Beacon	**Pendulum Cove Group**
Earlier post-caldera lavas and scoria	Entrance Point, South East Point	**Neptunes Bellows Group**
	Main episode of caldera collapse	
Pyroclast flows preceding caldera subsidence	Fumarole Bay, Cathedral Crags	**Port Foster Group**
Parasitic cones on primary volcano	Baily Head, Macaroni Point	
Primary strato-volcano	Telefon Ridge, Stonethrow Ridge, "Outer Coast Tuff"	

also in the 100 m. cliffs at Macaroni Point (Fig. 5), the pre-caldera series consists of hills of yellow tuff draped unconformably by younger pyroclastic rocks, lavas and red scoria, which in turn are overlain by still younger tuffs. There is often a marked angular discordance between the yellow tuff and the overlying formations which could be construed as old sea stacks or as a buried landscape. In the area south of Neptunes Bellows, Hawkes (1961) mapped the overlying formation as belonging to the post-caldera Neptunes Bellows Group. Certainly at South East Point, post-caldera lavas and red scoria overlie deeply eroded yellow tuffs of pre-caldera and syn-caldera type. Not all of the unconformities seen in the yellow tuffs necessarily represent the break between pre- and post-caldera formations; there were also local breaks within the older sequence of yellow tuffs and agglomerates. Prior to caldera collapse, the picture is of a broad central volcano, intermediate in structure between a shield and a typical strato-volcano, with a number of secondary centres on its flanks.

Hawkes (1961, p. 32, 41) equated the deposition of the Outer Coast Tuff with the formation of the caldera and he suggested that after the collapse three islands remained on what was essentially a submarine caldera rim. In the present account, the Outer Coast Tuff is restricted to slightly earlier pre-caldera times. The poorly sorted chaotic pumice and scoria deposits of Cathedral Crags and Fumarole Bay have many of the properties of pyroclast flows, and are thought to have been emitted immediately prior to caldera collapse.

2. *Post-caldera events*

Hawkes (1961, p. 41) recognized an old but post-caldera Neptunes Bellows Group. Peripheral post-caldera eruptive rocks occur for example at South East Point, where red scoria and lava flows rest unconformably on pre-caldera yellow tuffs. Hawkes suggested that this phase of activity was restricted to the southern side of the caldera, but it could be that equivalent deposits elsewhere are either buried by younger volcanic rocks or hidden by ice.

The distribution of the younger post-caldera eruptive rocks, which Hawkes referred to as the Pendulum Cove and Whalers Bay Groups, appears to have been strongly controlled by the ring-fracture system.

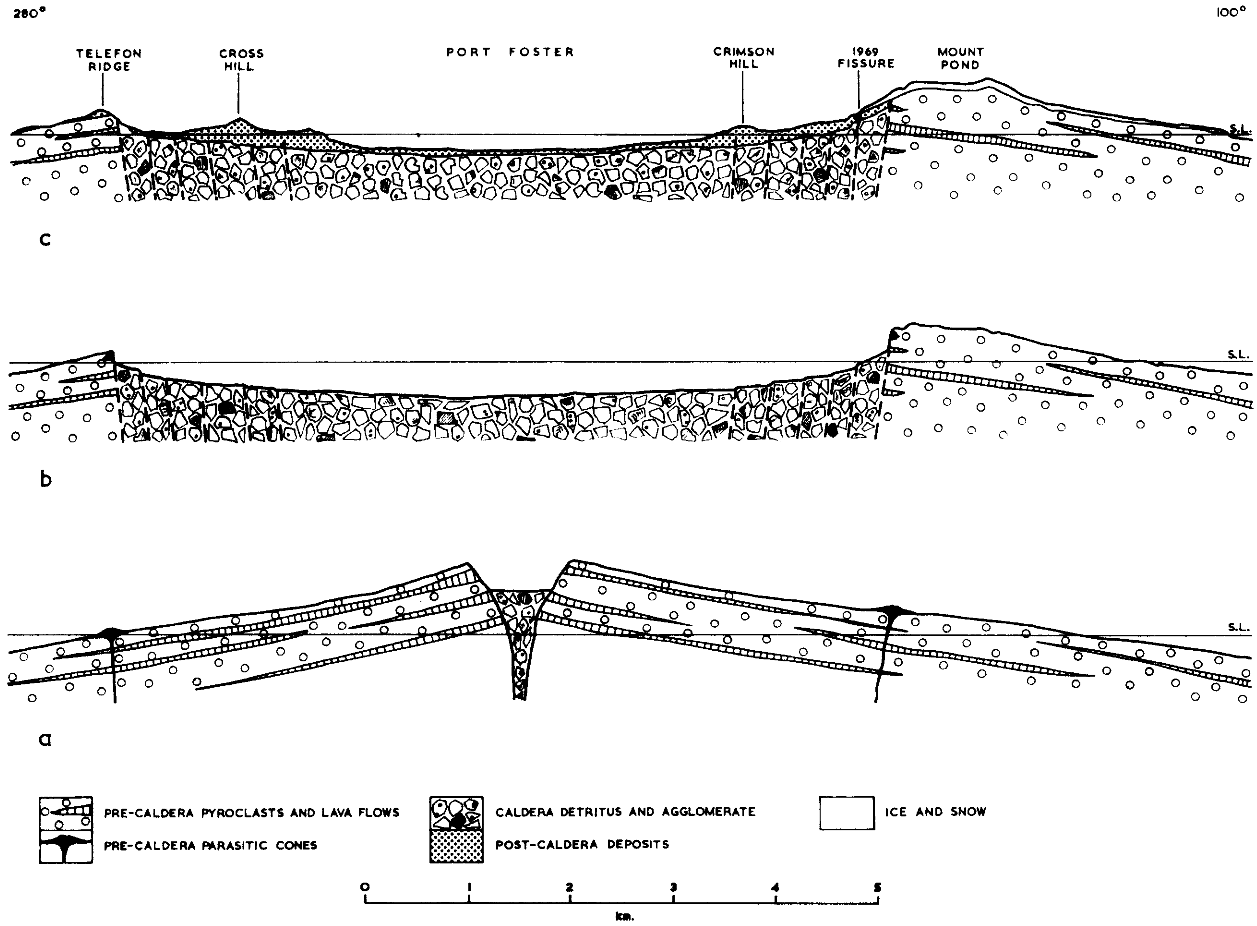

FIGURE 3

Diagrammatic sections illustrating the evolution of Deception Island. Vertical and horizontal scales are the same.

a. The original Deception Island volcano with parasitic cones marking the incipient caldera fault system.
b. After the main episode of caldera subsidence.
c. Section across the island as it is today, showing the recent development of intra-caldera cones and deposits.

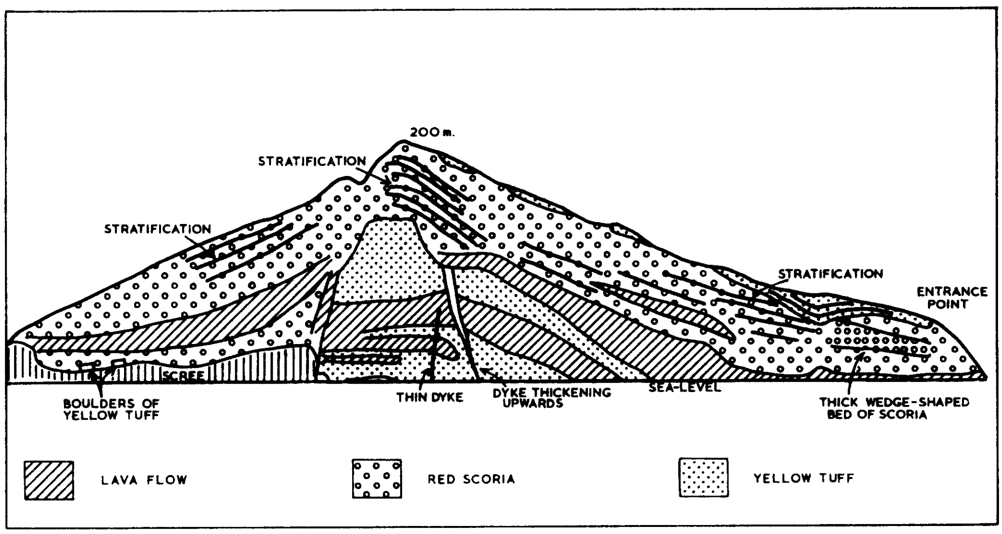

FIGURE 4

Geological sketch of a 200 m. high cliff section immediately south of the entrance to Port Foster (Entrance Point).

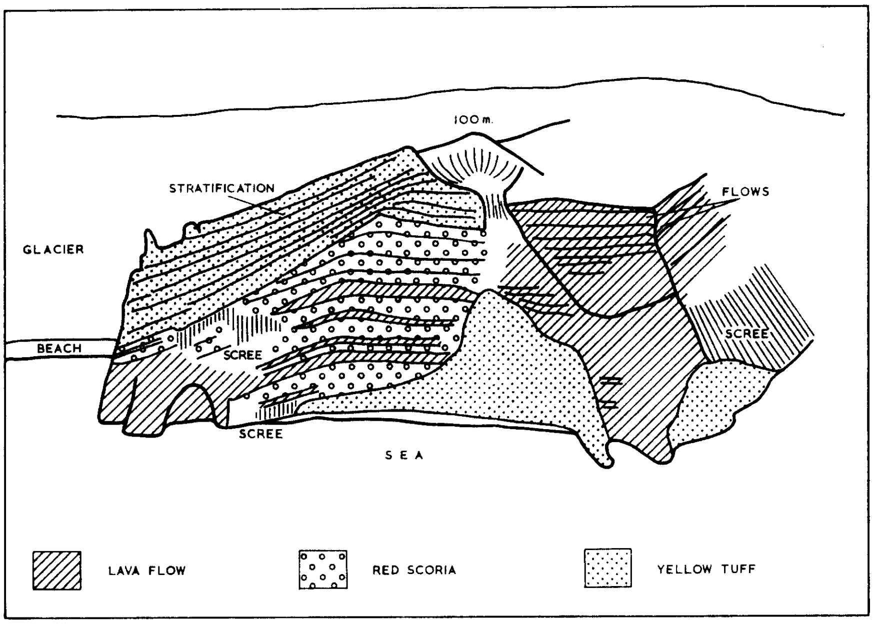

FIGURE 5
Geological sketch of the 100 m. high sea cliff at Macaroni Point.

These younger volcanic rocks include the lava flows and red scoria horizon of the high caldera rim and outer flanks such as Kendall Terrace, together with the numerous pyroclastic cones which encircle Port Foster. The unique soda-rich differentiated rocks, for which Deception Island is well known, are confined to the post-caldera series.

Hawkes's distinction between the Pendulum Cove and Whalers Bay Groups has no stratigraphical significance. The appearance of these young volcanic rocks in the form of pyroclast cones or lava flows depends on whether the vent is wet or dry at the time of the eruption. The pyroclast cones are essentially built on the lower ground around Port Foster, where sea-water had access to the rising magma. Such was the case in the 1967 and 1970 eruptions, which were partly submarine and partly in wet pyroclastic material. The 1969 subglacial eruption also produced only pyroclastic deposits, again presumably because the vent was wet though for a different reason. In contrast, the higher and drier vents emit essentially lava flows, perhaps accompanied by a little scoria and spatter.

Most of the low-level pyroclast cones consist of dark brown poorly consolidated lapilli and ash. Deposits from these centres blanket much of Deception Island and part of the material erupted during the past two centuries is also preserved within the glaciers (Orheim, 1971*c*). As seen after the 1967–70 events, much of the ash is re-distributed after each eruption and finally tends to accumulate in Port Foster.

The young lava flows are particularly conspicuous on Kendall Terrace, on the slopes of Mount Kirkwood and in the frozen cascades of Stonethrow Ridge (Plate Xa). On Kendall Terrace, sub-horizontal basaltic flows rest unconformably on loose ash and lapilli, and on the Outer Coast Tuff. Around Fumarole Bay, young lavas have poured down the caldera wall from a source high on the rim. Hawkes (1961, p. 23) illustrated a flow from the flanks of Mount Kirkwood which has built in delta fashion into Crater Lake.

Hawkes subdivided the young lavas of the Whalers Bay Group on the basis of their stratigraphical relationship to moraine and fluvio-glacial deposits. The youngest of all, the Mount Kirkwood group, rests on such deposits and they are essentially free from morainic or scree cover. These lavas are thought to have been erupted in historical times and add credibility to the report (Wilkes, 1845, p. 149) that in 1842 "the whole south side of Deception Island appeared as if on fire".

Until recently, it had been thought that the supposed eruption of 1842 was the last prior to the 1967–70 series of events. However, glaciological studies by Orheim (1971*c*), based on the recognition of seasonal wind-blown dust layers in the ice (Plate IIId), pointed to a series of pyroclastic eruptions during the period 1912–17.

II. THE PRE-HISTORIC PYROCLASTIC ROCKS

By

M. R. HARVEY

PYROCLASTIC rocks, agglomerates, tuffs and ashes form at least 80 per cent of the volume of Deception Island, though it is the subordinate lava flows that have so far received most attention. Fragmental deposits have been formed throughout the entire volcanic history of Deception Island. They comprised the bulk of the original volcano, were the most important products associated with caldera formation, and in post-caldera times have formed numerous volcanic cones around Port Foster. There are considerable limitations to the exposure of the pyroclastic rocks but at particular localities their exposure is often very good. The glaciers of Mount Pond and Mount Kirkwood conceal much of the island, whilst a good deal of the lower ground is obscured by a veneer of youthful ash and re-distributed detritus. Exposure in the cliffs around the outer perimeter of the island is excellent but largely inaccessible.

A. PYROCLASTIC STRATIGRAPHY

The stratigraphical divisions adopted here (Table II) are based partly on previous studies and partly on the author's investigation during the southern summer of 1971. Hawkes (1961) considered that Deception Island was formed by four distinct volcanoes but the majority of authors (e.g. Holtedahl, 1929; Olsacher, 1956; González-Ferrán and Katsui, 1970) have taken the view, shared by the author, that it was one major shield volcano centred over what is now Port Foster, with parasitic cones on its flanks. The principal stratigraphical sub-divisions are closely allied to the main structural events, especially that of caldera collapse.

1. *Outer Coast Tuff*

The oldest rocks of Deception Island, pre-caldera in age, are those which were termed by Hawkes (1961) the Outer Coast Tuff. Exposures of this formation may sometimes be seen in the high cliffs which in places form the caldera wall overlooking Port Foster, for example 500 m. south of Collins Point. However, the best exposures are in the cliffs of the outer coast, e.g. South Point, Vapour Col, the outlying Låvebrua Island and along the entire length of Kendall Terrace. These cliffs are in places 100 m. high and the yellow tuffs and agglomerates exposed here probably have their lateral equivalents in the remnants of the strato-volcano forming Stonethrow Ridge, Telefon Ridge and the hills around Fumarole Bay.

The rocks of this Outer Coast Tuff group consist mainly of pyroclast-fall types including thinly bedded yellow tuffs and poorly stratified agglomerates. They are thought to represent the accumulation of products erupted from a shield volcano. Judging by the presence of sedimentary structures, much of the early material was probably water-lain. Coarse agglomeratic horizons probably represent periods of more violent explosive activity, although in some cases they may simply reflect proximity to the source vent. Individual beds of the Outer Coast Tuff are laterally impersistent and the dip is generally a few degrees seaward. Extrapolation of this dip towards Port Foster would bring the beds into line with the sub-horizontal units of Stonethrow Ridge and Telefon Ridge.

Deposition of the Outer Coast Tuff probably represents by far the longest period considered here. Penecontemporaneous erosion and relative uplift of the island occurred during its accumulation, creating many non-sequences and small erosional unconformities.

2. *Parasitic centres*

Examples of secondary centres which developed on the flanks of the main volcano are well exposed at Baily Head and Macaroni Point. The relationship between these cones and the main strato-volcano tends to be obscured by the ice cover over Mount Pond. The stratified yellow tuff of the two parasitic centres bears a close resemblance to the products of the primary volcano. However, at Baily Head a tuff consisting of re-distributed ash and glass fragments, rounded by water during deposition, is particularly distinctive.

3. *Pyroclast flow deposits*

The most important structural event in the history of Deception Island was the formation of the caldera and its associated ring-fault system. The extrusion of a large volume of material mostly in the form of pyroclast flows is thought to have been closely connected with caldera subsidence. These deposits are exposed in the caldera wall itself and must therefore have slightly preceded the main period of collapse. The best examples of these pyroclast flow deposits are the unstratified massive tuffs and agglomerates of Fumarole Bay and Cathedral Crags. At Fumarole Bay, the deposits consist of poorly cemented dark grey unaltered scoriaceous fragments suggestive of a subaerial origin. The size of the constituents is variable but they may be up to 25 cm., a feature which probably led Hawkes (1961) to suggest that a vent was situated nearby. At Cathedral Crags, there is also a similar thickness of completely uniform unstratified yellow tuff containing large inclusions of black scoria. In neither case is there evidence of welding either in the field or under the microscope. The poorly sorted and unstratified nature of these thick deposits strongly suggests a pyroclast flow origin (Plate IXa). Unlike the Outer Coast Tuff, for example, these thick deposits have a very limited distribution, suggesting that they may have been emplaced like *nuées ardentes* and channelled down the valleys.

4. *Post-caldera pyroclastic deposits*

Pyroclast flow deposits appear to have been connected only with the major period of collapse which may have been a sudden event induced by the rapid emptying of the magma chamber. The caldera fault system appears to have been active to a lesser extent right up to the present time, and numerous pyroclastic centres have developed as a result of explosive activity around the fault zone. The small sea-level changes reported after the 1969 eruption, for instance, are thought to have resulted from continued, albeit slight, subsidence of the caldera. The ashes which result from sporadic eruptions around the ring fault form a veneer of loosely consolidated deposits concealing many of the older volcanic rocks. Like the yellowish Outer Coast Tuff, these younger deposits are the accumulation of ash falls but they are grey in colour and less altered. As these deposits are the result of numerous small and geographically separate eruptions, it has generally proved impracticable to place them in a strict time sequence. Naturally, the younger eruptive centres tend to have clearly defined craters but the older vents tend to be obscured by a blanket of ash. Some of these centres, like Crimson Hill, are thought to be entirely subaerial in origin but elsewhere there is clear evidence for re-distribution in shallow water, e.g. at Cross Hill and Wensleydale Beacon.

B. Re-distribution

From their sedimentary structures, it is clear that many of the Deception Island pyroclastic rocks have been re-distributed. The agents likely to have been of importance in re-mobilization have been observed in action moving the deposits which fell during the most recent series of eruptions.

1. *Submarine re-working*

Early in the history of Deception Island it is thought that most of the pyroclastic deposits accumulated in shallow seas, gradually building up into a shield volcano. Many features seen in the tuffs are ascribed to the effects of currents in shallow water (Plate VIIIa–c). Cross bedding occurs on a range of scales and many deposits are very finely laminated. Tuffaceous deposits in which there are abundant rounded boulders can be seen near the Argentine station and may mark the position of a former shoreline. Many of the older tuffs are thought to have been re-distributed by such means in a subaqueous environment but, as the evolving volcano assumed a subaerial form, other processes are likely to have become more important.

2. *Fluviatile and mudflow deposits*

Events of the past 5 years testify to the importance of surface water in re-distributing fresh pyroclastic deposits. The seasonal melt, which normally occurs during December and January, may be enhanced by a thin covering of black ash on the glaciers and much of the debris may be moved down-slope by sheet run-off or temporary streams. Where a larger volume of water is available, especially where the glaciers are suddenly melted under the influence of volcanic heat, enormous volumes of detritus may be moved in flash floods or in the lahars that follow. During and after the 1967 eruption, for example, numerous small rivers and lahars were responsible for constructing a series of alluvial fans out into Port Foster between Pendulum Cove and the land centre. There is a close resemblance between these modern mudflow deposits and those observed at Ronald Hill and in the small crater adjacent to the Argentine station.

3. *Aeolian re-distribution*

Dry volcanic dust and ash is particularly susceptible to transport by the strong winds which are so prevalent at Deception Island. During the recent activity it was apparent that much loose ash and even lapilli could be moved over very considerable distances by the strong winds. Deposits of older yellow tuffs showing aeolian cross bedding have also been recorded (Plate VIIId), indicating that this process operated in the past though it was probably less important than movement by water.

C. Grain-size Characteristics

The deposits of Deception Island show a large variation in grain-size. Beds range from those consisting essentially of very fine material, less than 0·25 mm. in diameter, to agglomerates where the blocks are mostly greater than 32 mm. Lapilli-tuffs (4–32 mm.) are fairly common but in most tuffs there is usually some very fine-grained matrix. The grain-size is sometimes uniform within very thin beds but mostly it is extremely variable. As has been demonstrated in the case of the 1967 deposits, the grain-size within a particular unit may diminish with increasing distance from the vent. The 1969 deposits are exceptional in having a fairly uniform grain-size distribution regardless of distance from source. Subaerial primary pyroclast falls like these are generally relatively well sorted and unimodal. Many of the older tuffs which show numerous thin beds are well sorted in this way, but the massive stratified pyroclast flow deposits of Fumarole Bay and Cathedral Crags are very poorly sorted and polymodal. The grain-size distribution may be affected by re-distribution factors as for example when very fine-grained wind-blown dust infiltrates amongst previously deposited lapilli.

D. Composition of the Pyroclastic Deposits

1. *Glasses and their alteration products*

As a general guide, the colour of the rock gives an indication of its stratigraphical position and affinities. In general, the older the rock the more distinctly yellow it appears. The Outer Coast Tuff, for example, is yellow whilst the more recent pyroclasts are brown or grey. The yellow colour is due to the secondary growth of palagonite which develops from the pale brown basaltic glass, sideromelane. This process is known to be time-dependent and could explain the distinction between the older yellow rocks and the younger, post-caldera, brown pyroclastic rocks. On the other hand, the depositional environment has been different in the two cases, for the pre-caldera pyroclasts are essentially submarine, whereas the post-caldera ones are subaerial. Pyroclastic fragments found as inclusions in younger deposits always appear to be a brighter yellow colour indicative of the more extensive development of palagonite on sideromelane. Occasionally, especially in the finer-grained rocks, all of the sideromelane may have been altered in this way. The relationship certainly suggests that the reaction is not solely temperature-dependent, as suggested by Bonatti (1965), but develops with increasing time and the availability of an aqueous phase after deposition of the glass (Moore, 1966).

The formation of sideromelane itself suggests that the hot ash came into contact with water and this may have meant that the initial reaction to palagonite may also have been accelerated only to be retarded again immediately on quenching. Ashes which fell into water and formed sideromelane during the 1967 eruption show no sign of palagonitization. At Deception Island, it is thought that most of the hydration of sideromelane takes place during the short southern summer when some of the ice and snow melts and the porous rocks permit the downward percolation of water.

Glass is the most important constituent of all the pyroclastic rocks of Deception Island and includes both the distinctive sideromelane and its alteration products together with black and red scoriaceous material. Most of the deposits may therefore be classified as vitric tuffs. In most cases, glasses form more than 80 per cent of the volume of a rock, with the remainder consisting of primary and secondary minerals, including the cement, and a variable proportion of lithic fragments which are generally basic volcanic rocks.

Sideromelane, quenched basaltic glass, is the principal component and is generally pale brown or slightly greenish when viewed in thin section (Plate Xb); when fresh it is completely isotropic. It is difficult to identify in the hand specimen owing to its finely disseminated occurrence and to the fact that it is often camouflaged by alteration minerals. It usually occurs as well-rounded near spherical or ellipsoidal fragments but is sometimes more irregularly shaped. The size of these fragments ranges from less than 1 mm. to large lapilli-sized pieces between 4 and 32 mm. in diameter. Within a particular rock most of the larger fragments tend to conform to a similar size but there is a complete range in sizes of the fragments composing the matrix which may form 40 per cent of the total.

Sideromelane is rarely found unaltered in the older pyroclastic rocks. Normally, the larger fragments (greater than 1 mm.) have margins which are altered to yellow palagonite (Plate Xc). The degree of alteration can be expressed in terms of the rim formed around the glass; it is generally less than 0·1 mm. wide but occasionally in the older rocks the entire fragment of glass may be palagonitized. The smaller sideromelane fragments, i.e. those with a larger surface area/volume ratio show a higher degree of alteration.

In contrast to sideromelane, the abundant fragments of black, dark brown or red scoriaceous material rarely show signs of alteration. These dark basaltic glassy fragments are thought to have chilled subaerially and only subsequently come into juxtaposition with the sideromelane fragments. Although the two types of glass in any particular rock may be contemporary, in some instances re-distribution may have resulted in particles with quite different histories being brought together in a reconstituted deposit. Usually the darker scoriaceous fragments have a more irregular outline than the rounded pieces of sideromelane. Glassy fragments show varying degrees of vesicularity. In sideromelane the vesicles are often of the order of 0·1 mm. across but in the darker scoriaceous glasses they are usually about 0·3 mm. Most of the vesicles are rounded but some of them are elongate or elliptical, presumably reflecting compression prior to solidification. Apart from the very rare appearance of calcite, no other secondary mineral has been observed developing in the vesicles.

2. *Crystalline components*

Microlites are generally detectable in the sideromelane, at least under high magnification, and they are even more distinct in the dark scoriaceous glasses. The proportion of crystalline material usually amounts to 20 per cent or less of the total but in some instances it may total about 50 per cent. The variability of this microlite development exists not only from one sample to another but it also varies between different grains of the same sample. Most of the microlites are small needle-shaped laths of plagioclase about 0·1–0·3 mm. long. Some of the larger ones have a composition in the labradorite–bytownite range.

Small pyroxenes also appear in some of the glasses but they are less abundant than the plagioclase. They are generally small (0·1–0·3 mm.) euhedral crystals of clinopyroxene and rarely orthopyroxene. Microlites may be aligned in a flow texture around the small phenocrysts but often their orientation is random.

The groundmass, which consists of very fine ash and dust, usually forms less than 20 per cent of the total volume of the rock. A variety of constituents is present and includes altered and unaltered glasses, small primary crystals, lithic fragments and clay minerals. Often much of the sideromelane has been transformed to palagonite. The crystalline components of the groundmass generally comprise 5–10 per cent of the total rock. The crystals are mainly abraded fragments of calcic plagioclase (sometimes zoned), clinopyroxene, and occasionally orthopyroxene and olivine. Quartz makes a very rare appearance.

It is the groundmass which is responsible for the lithification of the pyroclastic rocks and their frequently compact nature. However, it is the groundmass which is also most susceptible to weathering and disintegration. The secondary calcite has filled in some of the pore spaces, perhaps arresting the growth of the palagonite phase (Brew and Muffler, 1965) and aiding the compaction of the rocks. Invariably, this secondary deposition is the result of water percolating through the rocks and it may be connected with the alteration of sideromelane. Calcite, though usually absent, may in some cases form up to about 5 per cent of the total volume of the rock and it is often concentrated in particular areas. One example, from Ronald Hill, is exceptional in having about 10 per cent of calcite which can even be distinguished in the hand specimen.

3. *Lithic fragments*

Lithic fragments are an integral component of most of the pyroclastic rocks. The most abundant type of lithic fragment is basaltic, holocrystalline and fine-grained though there are some of intermediate composition as well. They are interpreted as fragments of the vent walls torn off during the explosive discharge of the magma. The frequency of occurrence of lithic fragments appears to depend on the proximity to the source vent. In general, the size of the lithic fragments is comparable with that of other clasts but occasionally they are conspicuously larger; they are angular or slightly rounded. Lithic fragments are rarely absent from a pyroclastic rock but generally they constitute less than 5 per cent of the total volume.

4. *Chemical composition*

Five new chemical analyses of the pre-historic pyroclastic rocks from Deception Island are given in Table III. These have been recalculated on a water-free basis in order to compare, so far as possible, the

TABLE III

CHEMICAL ANALYSES (XRF) OF DECEPTION ISLAND PYROCLASTIC ROCKS; RECALCULATED TO 100 PER CENT ON A WATER-FREE BASIS

	B.803.4	B.809.1	B.814.1	B.825.1	B.802.1
SiO_2	53·98	49·92	51·33	53·81	53·18
TiO_2	1·61	1·69	1·47	1·76	1·83
Al_2O_3	16·77	18·54	18·57	16·42	16·87
Fe_2O_3	9·17	9·61	8·67	9·98	9·88
MnO	0·16	0·16	0·15	0·17	0·17
MgO	4·32	6·28	5·39	4·40	4·56
CaO	7·90	8·84	10·00	8·34	8·12
Na_2O	5·08	4·16	3·60	4·13	4·40
K_2O	0·72	0·54	0·59	0·79	0·70
P_2O_5	0·29	0·26	0·23	0·29	0·29

B.803.4 Outer Coast Tuff; 1 km. south of the Argentine station. } **Pre-caldera**
B.809.1 Outer Coast Tuff; south end of Stonethrow Ridge.
B.814.1 Pyroclast flow; Fumarole Bay. } **Syn-caldera**
B.825.1 Pyroclast flow; between Cathedral Crags and South East Point.
B.802.1 Tuff; 0·5 km. south of the Argentine station. **Post-caldera**

original compositions of the deposits. Four of the samples (B.803.4, 809.1, 814.1 and 825.1) had about 12 per cent of water but the other sample (B.802.1), belonging to the post-caldera group had only 3·91 per cent of water. This undoubtedly reflects the lack of secondary palagonite in the latter rock type. Palagonite is thought to be mainly responsible for incorporating water into the structure. Chemically, these rocks have a basaltic composition as suggested also by their mineralogy in thin sections, but they show no obvious grouping in relation to their stratigraphy. The early magma appears to have remained more constant in composition in comparison with the highly variable nature of the post-caldera products. The maximum silica difference of 4·06 per cent is between two rocks of the Outer Coast Tuff group. An important characteristic of these rocks, shared by the entire Deception Island suite in general is their high soda content (Hawkes, 1961; Baker and others, 1969). The high soda content of the older pyroclastic rocks demonstrates that this distinctive feature has persisted throughout the entire evolution of Deception Island and that it is not simply a phenomenon of the Post-caldera group.

E. CONCLUSIONS

There is a very large lithological overlap between pyroclastic rocks of different ages on Deception Island. Rocks of all ages show the same range in proportions of glass, scoria, lithic and crystal components. Re-distributed pyroclastic rocks of similar appearance have evidently formed repeatedly throughout the history of the volcano.

A major grouping of the pyroclastic rocks can, however, be made in relation to the principal structurally determined sub-divisions and it is possible to distinguish:

i. A pre-caldera group.
ii. A syn-caldera group.
iii. A post-caldera group.

Groups i and ii are distinguished by the presence of palagonite which imparts a yellowish colour to the rocks. Rocks of group iii lack palagonite and calcite, and are generally brown in colour. The distinguishing features of group ii, the syn-caldera pyroclasts, are best observed in the field and include a lack of stratification, poor sorting and an association of yellow and black deformed pumice fragments. Group i are pyroclastic rocks belonging to an early stage in the development of the Deception Island shield volcano and are thought to have been essentially submarine in origin. Group ii are the pyroclast flows associated with the formation of the caldera. Group iii are the deposits from the post-caldera cones, which are mainly subaerial in origin. Chemically, all of these pre-historic tuffs are soda-rich basalts which are comparable in composition with the lava flows. They confirm the persistence of this sodic character throughout the geological history of the island.

III. THE 1967 ERUPTION

By

M. J. ROOBOL, T. G. DAVIES *and* P. E. BAKER

A. EVENT CHRONOLOGY AND OBSERVATIONS OF THE ERUPTION

The following account of the 1967 eruption has been compiled from records of the British Antarctic Survey, from previously published British and Chilean reports, and from statements made by members of the British Antarctic Survey who either witnessed the activity or were on the scene shortly afterwards.

Earthquakes were recorded at the British Antarctic Survey station on Deception Island in late April 1967. Further tremors were experienced throughout the following November and these increased in frequency and intensity, culminating in the eruption which began at 22.40 hr. G.M.T. on 4 December 1967. Table IV,

TABLE IV

SEQUENCE OF EVENTS DURING THE VOLCANIC ERUPTION AT DECEPTION ISLAND ON 4–5 DECEMBER 1967

hr. G.M.T.	
4 December 1967	
22.46	Chilean station called on radio but no contact.
22.54	A very large cloud was observed developing in the north.
22.58	Commenced sending radio calls for help.
23.05	Ash falling heavily at British station and visibility reduced to 30 yd. [27·5 m.].
23.10	Ash of all sizes from coarse sand to fine dust falling.
23.15	Decision to prepare to evacuate station if the situation deteriorated. Ash still falling. Build-up of cumulo-nimbus cloud.
23.30	Severe storm which seriously hindered preparations for evacuation of station and radio communications.
5 December 1967	
00.15	Radio contact with Stanley stating island had erupted and preparations made to evacuate.
00.51	British station at the Argentine Islands acknowledged distress signals and kept watch until evacuation of the island.
01.00	Ash and large hailstones falling heavily. The sky was completely black and continuous heavy thunderstorm.
01.15	Received position of *Piloto Pardo*; due to arrive at Deception Island at 03.00 hr.
01.20	Requested permission to evacuate with Argentinians if necessity arose.
01.25	*Piloto Pardo* stated intention to enter Whalers Bay if possible.
01.31	Informed Stanley of intention to evacuate on *Piloto Pardo* when arrived at Deception Island.
01.39	Received radio information that Chilean station members on their way to British station. This was the first news of the safety of the Chileans.
01.50	Amount of ash falling had decreased and visibility had improved. For the first time, it was observed that the water level in Whalers Bay was rising and falling at a very rapid rate. Approximately 5 ft. [1·5 m.] rise and fall, and time between rise and fall between 30 sec. and 2 min.
01.58	Enquired of *Piloto Pardo* whether there was any news of Argentine station.
02.00	Static black-outs in radio communication.
02.23	Informed *Piloto Pardo* that water in Whalers Bay was still rising and falling rapidly.
02.32	*Piloto Pardo* requested information on station personnel and possibility of using boats through Neptunes Bellows.
02.33	*Shackleton* advised arrival time as 15.00 hr. local time.
02.39	Informed *Piloto Pardo* that there was a very strong current through Neptunes Bellows and that the water in Whalers Bay was still rising and falling rapidly. Also that British personnel unharmed but nothing further had been heard from either the Chilean or Argentine stations.
02.49	Informed *Piloto Pardo* that Chileans had arrived at the British station.
03.00	Visibility 300 yd. [274 m.], heavy continuous thunder, lightning, hail, blowing dust and pseudo-fog; vertical visibility 50 ft. [15·2 m.].
03.01	27 Chileans arrived in very tired and distressed state, having taken 2 hr. for the journey. There were no casualties and they were immediately re-clothed, made comfortable and fed.
03.05	Informed all stations that Chilean personnel reported eruption centre north-west of Telefon Bay.
04.20	Because of poor visibility, *Piloto Pardo* postponed rescue attempts until morning when rescue would be by helicopter. 42 personnel at British station.
04.23	Received news from *Piloto Pardo* that all Argentine personnel were safe and that *Bahia Aguirre* due to arrive at 05.10 hr.

TABLE IV—*continued*

5 December 1967—continued	
06.22	Wind speed 0–15 kt [0–7·7 m./sec.] with variable direction and visibility 2 km. to south. The sea had been normal during the past hour.
07.22	Radio communication with *Piloto Pardo.*
07.38	*Piloto Pardo* cruising south of Deception Island with *Yelcho* awaiting improvement to lower boats.
10.00	Advised *Piloto Pardo* against the use of small boats inside the island because of the rapid rise and fall of the water.
10.24	*Piloto Pardo* reported to be sending helicopters within 1 hr. Full weather report given.
11.12	Situation reported to Stanley.
12.04	Helicopters arrived and the Chilean party evacuated first.
12.26	Radio station closed down.
12.50	Last two British personnel evacuated. Fresh eruptions were observed while the last flights were being made. Later on distinct volcanic cloud columns were observed above stratus and cumulus cloud. *Piloto Pardo* and *Yelcho* stood by while the Argentine party was evacuated by helicopter to *Bahia Aguirre.* Both Chilean ships proceeded to Discovery Bay, Greenwich Island, where rendezvous with *Shackleton* had been arranged.

compiled by R. J. Adie, shows the sequence of events as seen from the British station at Whalers Bay.

According to Valenzuela and others (1968), men at the Chilean station at Pendulum Cove saw a column of black ash and vapour break through the partial ice cover of Telefon Bay, and expand rapidly to a height of more than 2,500 m. At about the same time, voluminous dust clouds also rose from the vicinity of the Chilean refuge on the east side of Telefon Bay. In Pendulum Cove itself, the sea began to boil and there was a pungent sulphurous odour; the sea-level oscillated up to 1·5 m. above its normal level every 2 or 3 min.

Meanwhile, at the British station at Whalers Bay, the initial moments of the eruption were obscured by the intervening Ronald Hill and the ridge north of Kroner Lake. But at 22.52 hr. the large eruptive cloud was noticed and photographed. Subsequent re-orientation of the photographs shows that the cloud was over the eastern side of Telefon Bay and that it corresponded to the cloud reported by the Chileans to have risen from near their refuge hut rather than from the submarine source on the western side of Telefon Bay.

To the accompaniment of an electrical storm, the eruptive clouds quickly enveloped the Chilean station, causing almost total darkness. By 23.01 hr., about 20 min. after the start of the eruption, the cloud had reached the British station, reducing visibility to about 10 m. Fragments falling at Pendulum Cove were up to 10 cm. across but only coarse sand to fine dust-grade debris fell at Whalers Bay. Observers on the Chilean ship *Piloto Pardo*, then about 10 km. to the north-east of Deception Island, saw the eruptive cloud assume "the form of a curtain stretching in a west to east direction probably because of the influence of the prevailing wind coming from the north-north-west (velocity 15–20 kt)" (Valenzuela and others, 1968, p. 8).

By 23.30 hr. the activity had waned sufficiently to allow the Chileans to make their way to the British station, which they reached at 02.47 hr. on 5 December. At 01.48 hr. the sea in Whalers Bay was noted to be rising and falling through 1·5 m. every minute or two, but this movement had ceased by about 06.00 hr. At 05.00 hr., ash and large hailstones were falling heavily on the British station. British Antarctic Survey and Chilean personnel were evacuated by helicopter from Whalers Bay to *Piloto Pardo* between 12.00 and 13.00 hr. G.M.T. on 5 December. Men from the Argentine station at Fumarole Bay were evacuated to *Bahia Aguirre*. Eruptive clouds were observed throughout the day.

At 10.35 hr. on 6 December the crew of a Chilean Air Force aircraft on a flight over Deception Island observed a new island in Telefon Bay (Plate Ib) and reported that explosions from the island were hurling debris to over 300 m. whilst a column of steam was rising to 6,000 m. The second or land centre on the shore between Telefon Bay and Pendulum Cove, near the Chilean refuge hut, was emitting steam to a height of over 10,000 m.

On 7 December, R.R.S. *Shackleton* returned to Deception Island to close the British station. Photographs taken at 21.30 hr. G.M.T. show voluminous clouds of steam rising from both the new island and the land centre. At about 22.30 hr., *Shackleton* sailed to within about 3·2 km. of the active centres and went sufficiently near to Pendulum Cove to see the Chilean huts. Capt. D. H. Turnbull reported that there was a steady emission of steam from the new island but the explosions had apparently ceased. However, the land centre was more active and two separate vents could be distinguished: one on the shore and the other about 400 m. inland. The latter was discharging bursts of vapour about every 3–4 min. and steam was rising to about 10,000 m. but there was no ash. The vent by the shore was less regular in its behaviour and was emitting dark explosion clouds of ash and vapour from which bombs were accelerating leaving black trails behind them. These dark clouds collapsed into white cauliflower-shaped mushrooms of steam. Film taken at the time shows that, in addition to the rising column there was also a well-developed basal surge moving laterally from its lower part.

Later, from about 48 km. off the island, Capt. Turnbull reported seeing a column of vapour rising to around 10,000 m. above Deception Island, penetrating stratus cloud which was probably at about 5,000 m. He stated that there was a slight ash cover on Livingston Island and probably on Greenwich Island too. About 2 weeks later he saw an ash-coated iceberg near Elephant Island about 200 km. to the north-east of Deception Island.

I. Curphey, also on board *Shackleton* during the visit of 7 December, confirmed the observations made by Capt. Turnbull but added that, viewed from Whalers Bay, there seemed to be a third column of steam rising from a point well to the east of the land centre, possibly on the outer slopes of Deception Island. Whereas about 4 days previously Deception Island had appeared white with the fallen snow, now most of the island was covered by ash. There seemed to be more ash falling on the ship as it approached from the east than when it came in through Neptunes Bellows. Curphey described the explosion which he witnessed at the land centre "as spurts of black ash followed by steam". He stressed the lack of noise even when the ship was close by in Pendulum Cove. He also reported that vapour may have been coming from Telefon Ridge and that there was no evidence of any sea ice remaining in the northern part of Port Foster.

Three Chilean geologists returned to Deception Island immediately after the eruption and made a brief reconnaissance survey (Valenzuela and others, 1968). R.R.S. *John Biscoe* visited Deception Island during the period 14–18 December 1967 and preliminary investigations of the effects of the eruption and topographic changes were made by the Survey's scientists (Clapperton, 1969). G. Higgins reported that on 15 December 1967 puffs of steam were still being emitted from the land centre and that the new island, though steaming, was more quiescent. He also stated that the western side of Deception Island between Crater Lake, on the slopes of Mount Kirkwood, and Telefon Bay was apparently free from debris, whereas elsewhere there were varying degrees of ash cover (Fig. 6).

B. THE NEW ISLAND

Situated in the north-western corner of Telefon Bay, the new island (Plate IIa) was elongated in a north-east to south-west direction and was built partly on an older submarine platform. The south-western end was 80 m. from the shore of Deception Island whilst the north-western side was 150 m. away at its nearest point. It had maximum dimensions of 934 m. by 366 m. and reached 62 m. a.s.l. Essentially, the island consisted of three overlapping pyroclastic cones with water-filled craters (Plate IIb). Clapperton (1969, p. 85) stated that another small islet rising about 3 m. a.s.l. lay about 9 m. off the north-eastern end of the new island, but by December 1968 it had been re-distributed to form a hooked spit connected with the larger island. By this time, cliffs up to 18 m. high had formed along the exposed south-eastern side of the island, whilst the opposite sheltered side had cliffs only 1–3 m. high. Fig. 7 is a contoured sketch map of the new island as it was in December 1968. For reference purposes, the craters are numbered from south-west to north-east.

Crater 1 was a low-lying feature open to the sea at its western end. It had an oval plan with its major axis parallel to the elongation of the island; at low tide its outer dimensions were 210 m. by 180 m. and its interior ones 190 m. by 140 m. Parts of the rim were submerged at high tide but not on the southern side where the rim was 7 m. above low-water mark. This cliff provided the best exposure of the crudely stratified pyroclastic deposits emitted from crater 1.

The small flooded crater 1A was located at the north-eastern edge of crater 1 and had been blasted out of the flanks of crater 2. It formed at a very late stage in the eruption since the ash emitted from it coated the south-western inner and outer slopes of crater 2, indicating a south-westerly wind at the time.

Crater 2 was almost circular, had a diameter of about 230 m. and was the largest and most complex of the three craters. The outer slopes of its cone had a gradient of about 32°. The summit and higher parts of the new island were formed by the rim of this crater, which was probably the site of the major explosive activity. The original crater 2 was partly filled by debris from the later eccentrically situated crater 2A, which contained a greenish lake measuring 130 m. by 100 m. Soundings suggested that this was only a few metres deep. Crater 2B was a small flooded offshoot 20 m. wide on the north-eastern edge of crater 2A. Like crater 1A, its ash deposits covered the area to the north-east, and the two were probably contemporaneous representatives of the final activity at the new island.

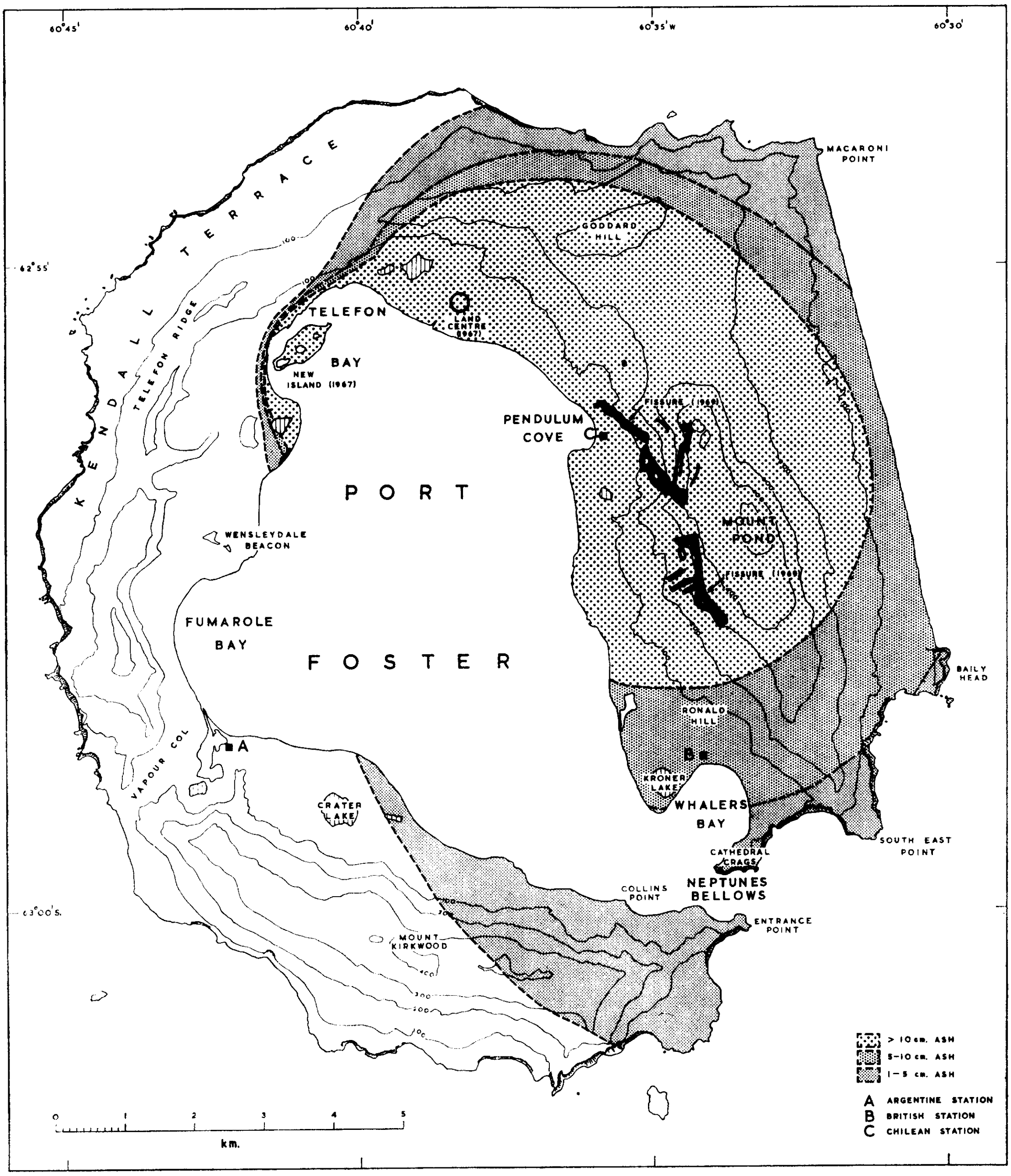

FIGURE 6
Distribution of the 1967 pyroclastic deposits on Deception Island. (For details of measurements and isopachs see Fig. 15.)

Crater 3 was slightly oval in plan, again with its longer axis parallel to that of the island, and it had a diameter across the rim of 200–220 m. The outer slopes of its cone were inclined at only about 18°, which was considerably less steep than those of crater 2. The inner walls were plastered with ash deposits and the stratigraphy was poorly displayed. The inner south-western wall of crater 3 had been straightened and steepened by the coarse bombs and lapilli thrown over from crater 2A. There was a small irregularly shaped lake on the broad flat bottom of crater 3. Clapperton (1969, p. 84) showed the position of the small low islet to the north-east of the new island, which was subsequently re-worked and attached to the latter in the form of a hooked spit. The original offlying islet was probably not a separate eruptive centre but simply represented the accumulation of new pyroclastic debris in shallower water on the edge of the submarine bank. Clapperton (1969, p. 85) also referred to small (5–8 cm.) scoria ridges on the beaches. Similar ridges were observed forming around the shores of Port Foster in 1969. They were caused by the

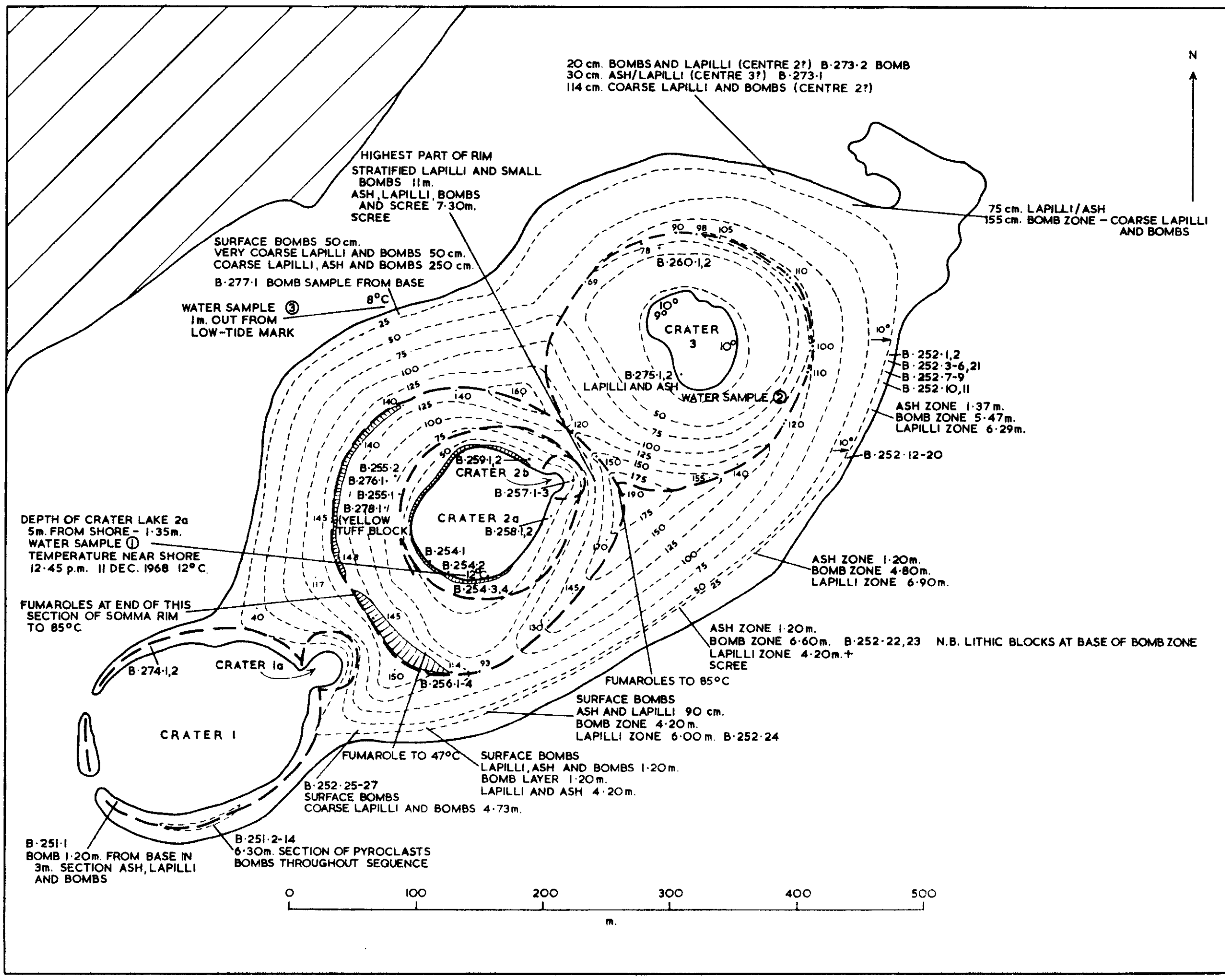

FIGURE 7

Annotated sketch map of the 1967 island in Telefon Bay (orientation and outline from an Argentine air photograph of 21 January 1968 and Royal Naval Survey of December 1968). Geological notes and topography are from the Royal Society/British Antarctic Survey expedition, December 1968–January 1969. Contours and aneroid spot heights are in feet. Sample collecting sites are shown as B.252.1, etc.

successive stranding of beach ridges as the tides decreased and they were destroyed when tide levels subsequently increased to their monthly maximum.

In cross-section, the island was distinctly asymmetric in form with all of the crater rims being higher to the south-east. This suggests that during the construction of the island the dominant wind was from a north-westerly direction, which is consistent with the isopachs compiled on the basis of measured sections of the pyroclast fall deposits (Fig. 15). Longitudinal and cross-sections of the island are shown in Fig. 8.

Fig. 9 is a bomb-density map showing the relative concentrations of bombs over the surface of the island. It illustrates that the last major bomb episode in the development of the island was associated with crater 2A. The distribution of bombs appears to have been unaffected by wind direction, since the maximum concentrations are both to the north-west and south-east of the crater (Plates IId and IXc). The absence of bombs on the inner eastern slopes of crater 2A was probably due to the steepness of the slope. The summit would also tend to shield the south-eastern part of the island from the volley of bombs. A contoured map showing the maximum size of bombs found on the surface in different parts of the island is given in Fig. 10. The figures quoted represent the mean diameter as calculated from three dimensions measured on the three largest bombs in any particular traverse from the crater rim to the coast.

The sequence in which the vents ceased activity was: first crater 3 followed by craters 1 and 2A, and finally craters 1A and 2B which produced the fine ash blown in a north-easterly direction.

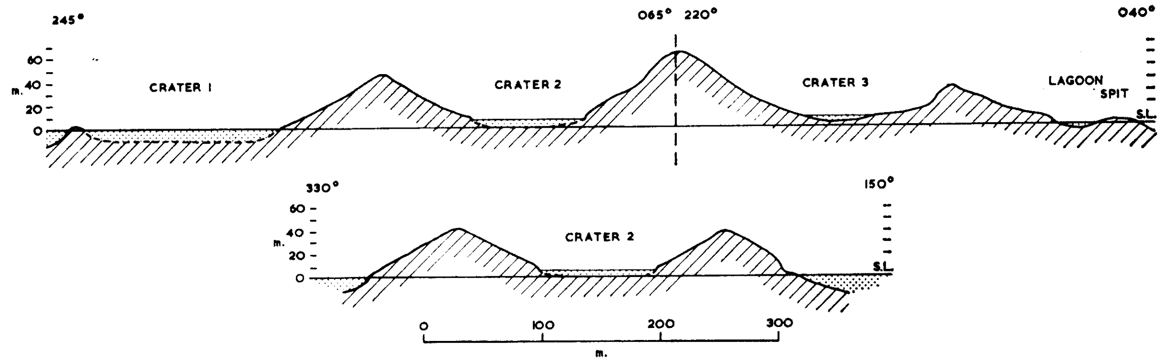

FIGURE 8
Topographical profiles across the 1967 island in Telefon Bay. (Based on a survey in December 1968.)

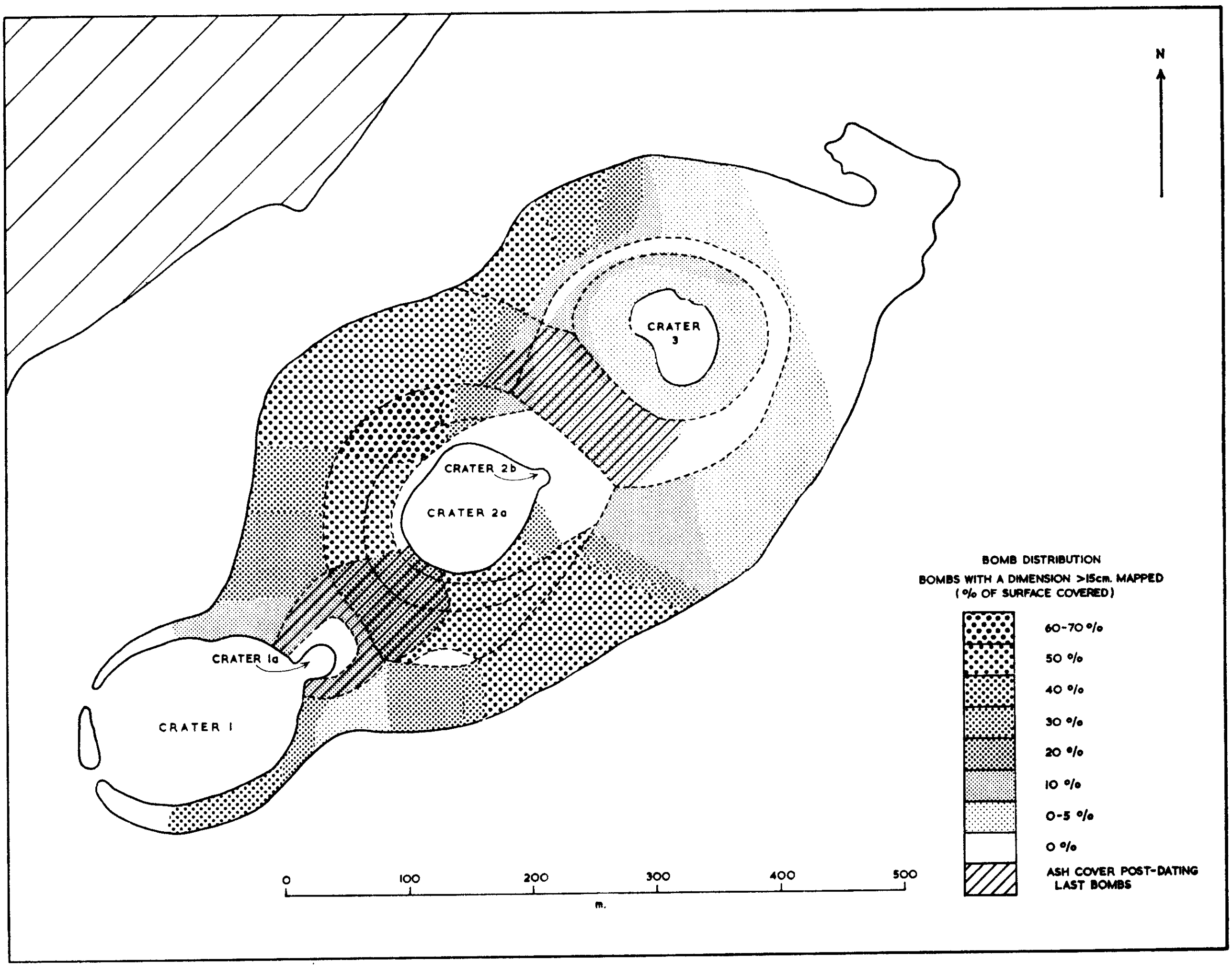

FIGURE 9
Density distribution of volcanic bombs on the surface of the 1967 island.

C. THE LAND CENTRE

The term "land centre" is used to identify the second 1967 eruptive centre which was situated 2 km. east of the new island on the shore of Port Foster between Telefon Bay and Pendulum Cove (Plate IIc). From the observations of the activity reported earlier and from the evidence presented by Clapperton (1969,

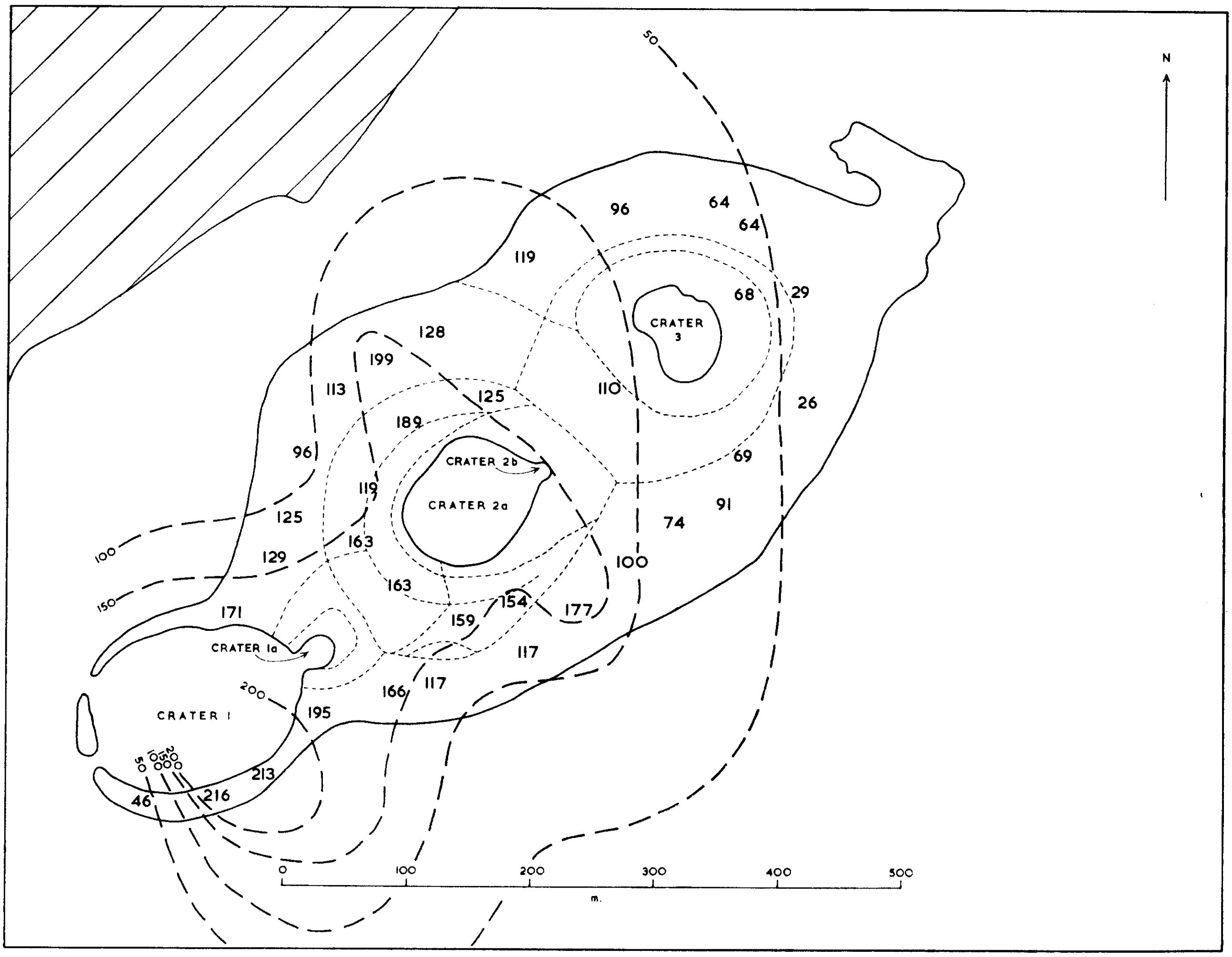

FIGURE 10

Size variation of volcanic bombs on the surface of the 1967 island. The "contours" link maximum sizes obtained in different parts of the island. The values shown (in cm.) represent the mean diameter (as calculated from three dimensions) of the three largest bombs encountered in any particular traverse from crater rim to coast. Note that because of the thick deposits at the island these dimensions apply only to bombs discharged in the closing phases of the activity.

p. 88–89), it is clear that two distinct vents were operative at the land centre. The new craters opened up within a much older crater measuring about 1,100 m. by 800 m., which forms part of the zone of pyroclast cones encircling Port Foster. Around most of its circumference the old crater is bounded by walls up to 135 m. high but on the south-west side it is open to the sea. The crater floor rises gently inland towards the north-east.

The first of the new vents was represented by a water-filled crater which occupied the centre of the old amphitheatre. The lake was roughly circular with a diameter of about 200 m. and was enclosed by vertical walls which were about 8 m. high along the southern edge, diminishing to only about 1 m. on the northern side. Stratified pyroclastic deposits exposed in the southern wall were similar in aspect to those of the new island.

The second land-centre crater was marked by a sharp indentation in the coastline where a newly formed bay 400 m. long reached to within about 100 m. of the main crater lake (Plate IIc). The sea in the new bay was very discoloured and fumaroles were active around its margins. A hydrographic survey party from H.M.S. *Endurance* sounded the bay in December 1968 and found that the floor shelved gently seawards with no evidence of a continuous rim or deep crater-like form. However, since the eye-witness accounts seem to suggest that this was an eruptive centre, it may be that its crater was filled in by later pyroclastic deposits from the main land-centre crater or by debris brought in by longshore drift during 1968.

The area around the land centre was blanketed by new pyroclastic material which had smoothed out many of the local topographic irregularities. Part of an ice cap to the north-east of the land centre, together with two melt-water ponds at its edge, were obliterated as was the Chilean refuge hut to the north. Figs. 11 and 12 show the distribution and size variation of bombs in the immediate vicinity of the land centre. The contours reveal that the final event was the discharge of bombs from the main crater which was subsequently occupied by the lake.

The pyroclastic deposits in the vicinity of the land centre were disrupted by open fissures arranged roughly concentrically to the walls of the crater to produce a stepped topography. These fissures extended up to 1 km. away from the land centre, were up to 2 m. wide and 800 m. long, and often accompanied by vertical displacements of up to about 1 m. The crater floor immediately to the east of the crater lake was also cut by two groups of north–south fissures spaced a few metres apart. These were the site of extremely active fumaroles in December 1968, and also in March 1969, but they had disappeared in December 1970.

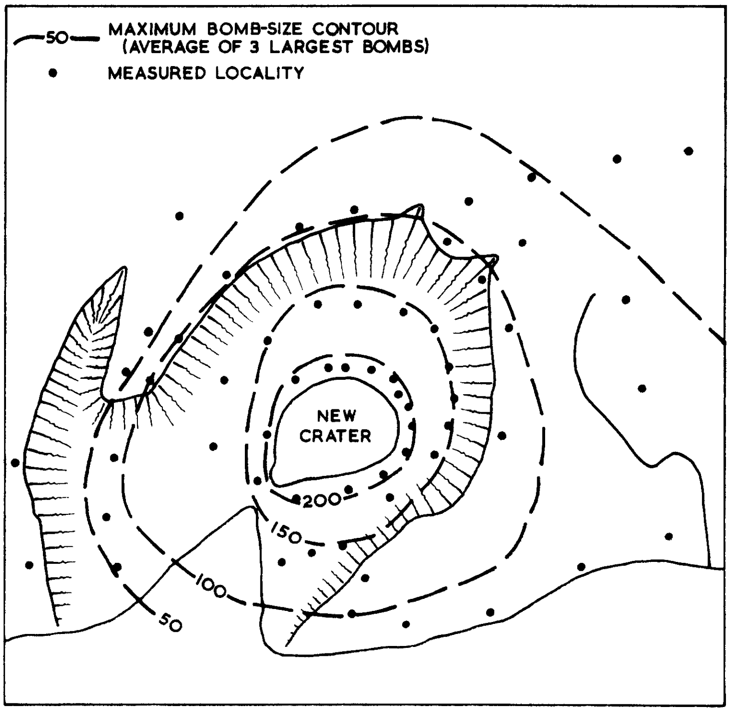

FIGURE 11

Sketch map of the 1967 land centre with maximum bomb-size "contours" in centimetres. Values are based on the mean diameter of the three largest bombs at any particular locality.

On the north-western side of the crater floor were two small collapse features or pit craters, the largest of which had a diameter of about 10 m. and a depth of 4 m. A third collapse feature 5 m. deep was situated 500 m. north-west of the land centre in an area greatly disturbed by two sets of intersecting open fissures. Both the fissures and the collapse features are thought to have been due to the compaction of the unconsolidated pyroclastic deposits, perhaps aided on occasion by earth tremors.

D. SURFACE WATER MOVEMENT DURING THE ERUPTION

There is good evidence to suggest that large volumes of water passed down the slopes in the vicinity of the land centre during the 1967 eruption. A new 300 m. long gully cut into unconsolidated pyroclastic deposits ran down into a sharp recess in the north-western wall of the old amphitheatre which partially encircled the new crater lake. This gully does not appear on air photographs taken in 1956. At its lower end it was 17 m. deep and 25 m. wide, passing upwards into a series of short branching gullies about 2 m. deep. The lower part was observed by Clapperton (1969, p. 88) when he visited the area in December 1967 and a year later it was partly filled by snow and scree. The gently inclined area extending from the mouth of the gully was composed of tongues of re-distributed pyroclastic debris gradually becoming less distinct as they

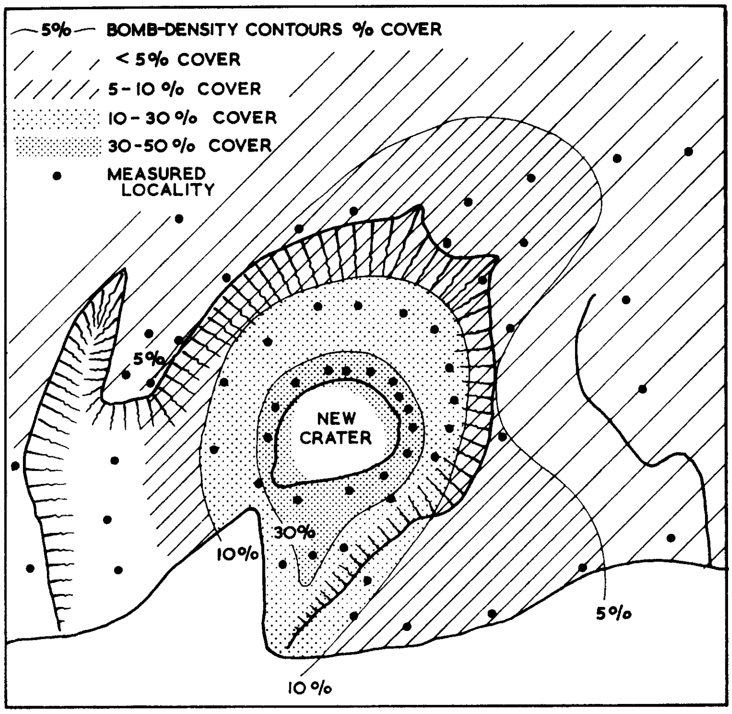

FIGURE 12
Density distribution of 1967 volcanic bombs at the surface of the land centre.

approached to within about 50 m. of the shore. As illustrated by Clapperton (1969, p. 89), the lobes often had a distinct zonation with a coarser darker margin and finer lighter-coloured interior. They were interpreted by Clapperton as mudflow deposits and this was substantiated by analogy with numerous comparable lobes which were seen forming in several places along the eastern side of Port Foster during the period December 1968–March 1969.

Although some of the water probably came down the new gully as a flood, the residue appears to have emerged as mudflows which came to rest before the end of the 1967 eruption. The mudflows clearly post-date the main pyroclast falls, since they are essentially free of ash cover, but impact craters including bomb fragments indicate that the explosions had not entirely ceased when they formed. There were many other smaller gullies cut into the walls of the land-centre amphitheatre, suggesting that there had been a fairly general deluge across this area (Fig. 13).

About 800 m. west of the land centre, lakes filled two older craters which were separated by a narrow strip of low ground. Another deep gully led down into the larger of the two lakes with a drop of 50 m. to the water surface. Immediately above the lake, the gully was 16 m. wide and 8 m. deep, but it dwindled to nothing on the flat surface between the lakes and the land centre. There was yet another gully on the slope to the north of the land centre; it ran towards the larger of the twin lakes and had a maximum depth of 5 m. and a width of 13 m. The Chilean geologists, who visited the area immediately after the eruption, reported that the two lakes had coalesced to form a single body of water 750 m. by 200 m. (Valenzuela and others, 1968). However, by December 1968 there were again two separate lakes. It would appear that the floods of water which created the series of new gullies during the 1967 eruption also caused a temporary union of the two crater lakes.

The position of the gullies in each case coincides with an abrupt change in gradient and it would seem that, although the water passed without noticeable effect over the gently inclined surfaces, it cut deeply into the loose pyroclastic deposits where the slope steepened.

From the sector affected by the floods and lahars, the water originated from somewhere to the north-east of the land centre. Possible sources of the large volume of water are:

i. Displacement of water from the two small lakes shown on the 1961 map (Hawkes, 1961) to the east of the land centre.

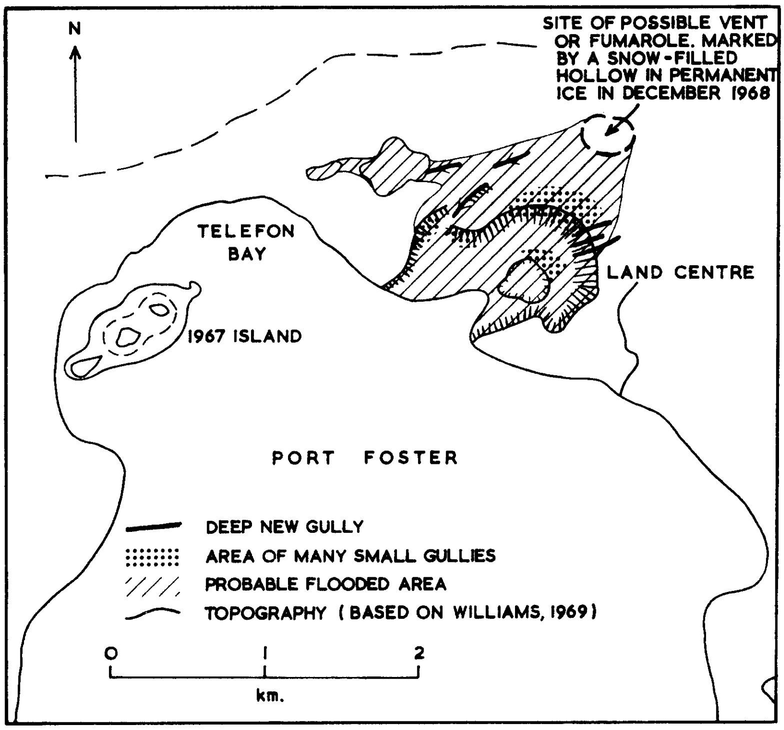

FIGURE 13

Probable extent of the flooded area and positions of new gullies around the 1967 land centre. The possible source of the melt water is also indicated.

ii. Heavy rainfall induced by the 1967 activity.
iii. Melting of the glacier to the north-east of the land centre by a heat source associated with the volcanism.

The two small lakes were probably filled by falling debris but their volume was small and their positions with respect to the land centre make it improbable that they were responsible for the floods. The rainfall hypothesis is also unlikely for, although hail fell on witnesses, there was no mention of rain. Even if some rain fell after observers left Deception Island, it is doubtful whether it would have provided surface water on the scale required. On the other hand, there was no evidence in December 1968 of any further vents in the ice slopes above the land centre, though by then this area was thickly blanketed by snow which had fallen during the intervening winter. However, this hypothesis must be considered seriously in the light of what happened during 1969, when immense floods were generated from the glaciers. Equally significant is the fact that one of these 1969 craters, 60 m. in diameter and 37 m. deep, had disappeared when the area was re-visited in December 1970.

E. Topographic Changes in the Vicinity of the Land Centre

Difficulty was encountered in attempting to distinguish the deposits of the 1967 eruption from the older pyroclastic deposits in the area around the land centre. The nearest deposits resting on a snow base were found on the shore of Telefon Bay 340 m. to the north-west. From a comparison of the terrain in 1968 with that portrayed on the 1961 topographic map and the 1956 air photographs, it became clear that the changes were more substantial than initially suspected.

The site of the land centre was originally occupied by a crater in pyroclastic material, one of many such features which encircle Port Foster. A braided stream channel ran across its floor, cutting through the low south-western rim before entering the sea on an almost straight stretch of coast. The old crater measured 850 m. north-east to south-west by 700 m. north-west to south-east, whereas the new land centre measured 1,100 m. by 800 m.

When the new outline of the land centre is superimposed on that of the old crater (Fig. 14), the changes become apparent and it can be seen that the new centre was displaced south-eastward relative to the older one. Excluding the new embayment, the coastline now had a curved form and had been extended as much as 200 m. into Port Foster. On the eastern side, the crater rim now reached a height of 135 m. compared with 80 m. for the older crater. This increase in height might be explained by general inflation of the pre-existing topography during the eruption or by the accumulation of pyroclastic deposits. If the latter was the case, 55 m. must have fallen on the eastern rim and also a substantial volume of material closer to the vent must have disappeared, presumably by subsidence, to account for the absence of a new cone. On the other hand, there was no independent evidence to support the suggestion that such a thickness of pyroclastic material had in fact fallen on the eastern rim and the change may be largely a consequence of inflation and localized subsidence.

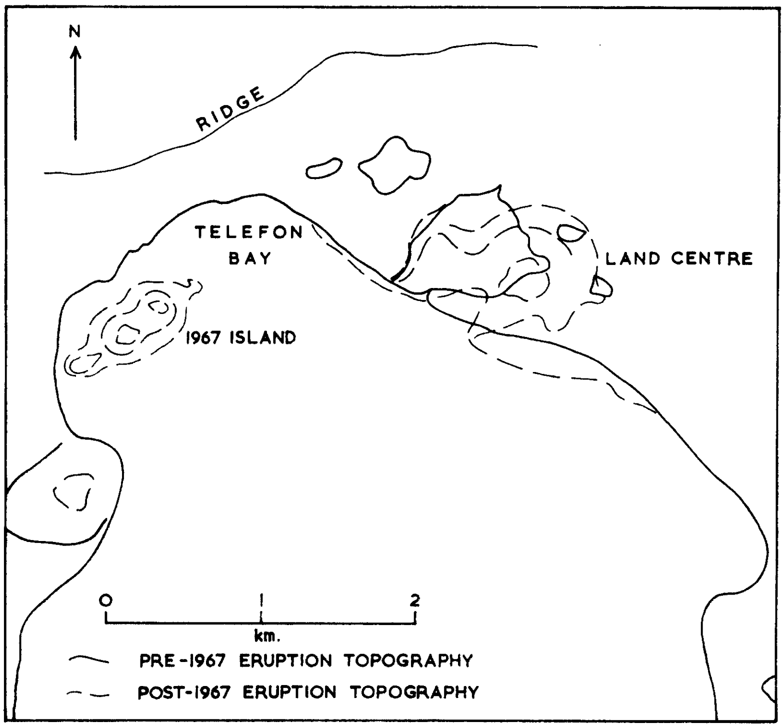

FIGURE 14

Topographical changes in the Telefon Bay area resulting from the volcanic activity of December 1967.

F. THE PYROCLASTIC DEPOSITS

The 3 day eruption produced *no* lava flows, *only* bombs, blocks, lapilli, ash and dust, the total volume of which is computed from the isopach map (Fig. 15) to be about 0·05 km.^{3}. The largest individual fragment was a bomb found on the inner north-eastern slopes of crater 2 of the new island which measured 440 cm. by 275 cm. by 75 cm. and must have been in a plastic condition on impact, since it was moulded over underlying debris (Plate IXb). It has a black, highly vesicular core, is lighter coloured towards the margin and has a fragile outer skin of black glass.

Ash and lapilli from the eruption were found over most of Deception Island except for the area between Kendall Terrace and Crater Lake. Thicknesses of the pyroclastic deposits were measured at frequent intervals over the remainder of the island, where the base could often be identified by the underlying layers of snow, ice, penguin feathers, moss, pebbles or scoria (Figs. 16 and 17).

A contoured isopach map was compiled from these measured thicknesses (Fig. 15). The south-eastward elongation of the isopachs indicates that throughout the eruption the dominant wind was from the north-west, and this is consistent with the observations made on 4 December. However, in the declining stages of

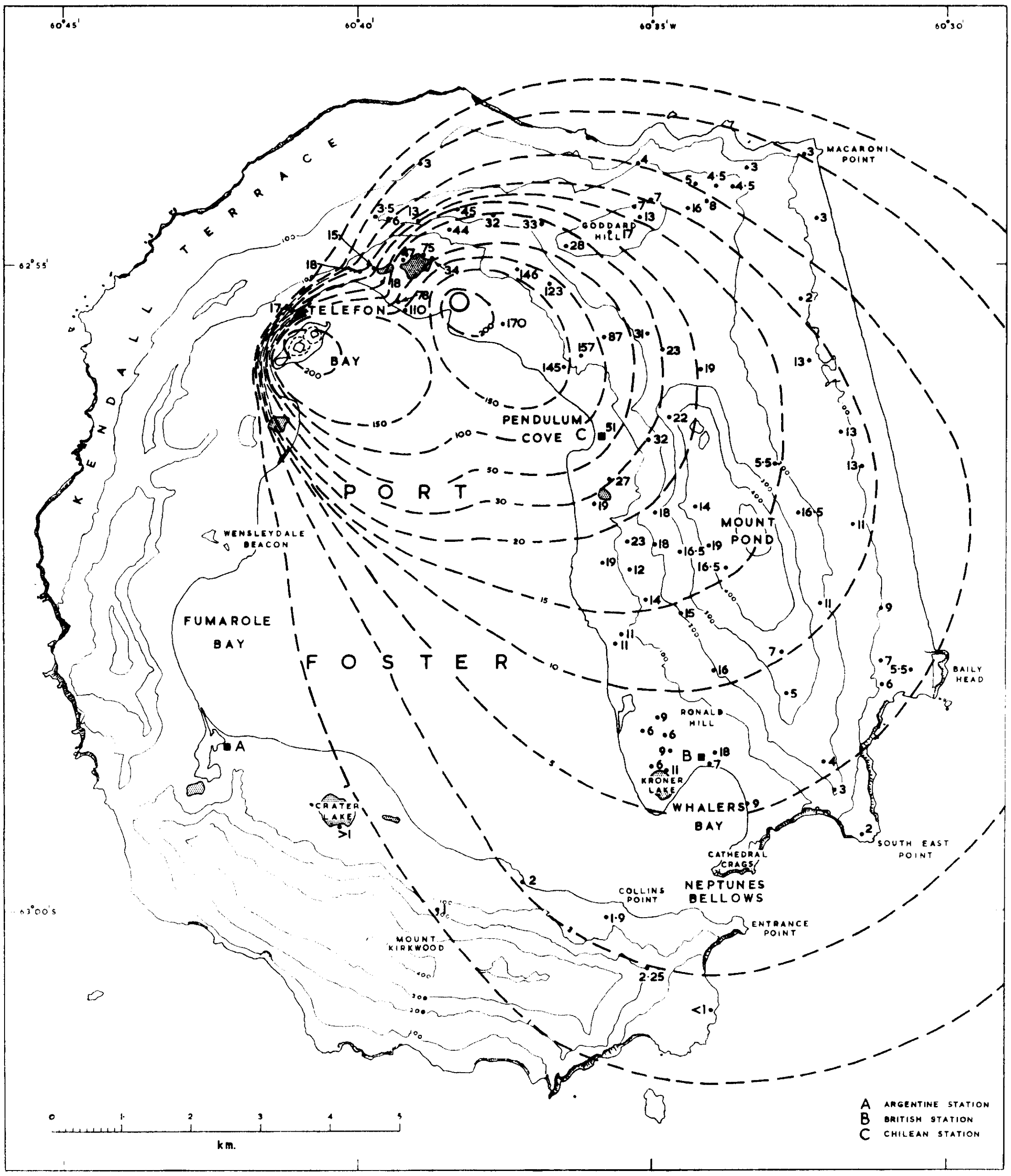

FIGURE 15

Distribution of the 1967 pyroclasts. Isopachs (in cm.) are based on the measured thicknesses shown.

activity, there is evidence that the wind changed to a south-westerly direction as suggested by the distribution of the final ash deposits of the new island from craters 1A and 2B. Witnesses on *Shackleton*, on 7 December, also reported that material being emitted from the land centre was drifting north-eastward. However, the influence of the late south-westerly wind is scarcely apparent from the isopach map, presumably because the quantity of pyroclastic material emitted at this stage was minimal in comparison with that erupted earlier.

In order to study the distribution of the largest fragments, three dimensions were measured on the five largest specimens at each locality except near the vents where the bombs were very large and only three specimens were measured. An average was obtained for these dimensions and the results are plotted in

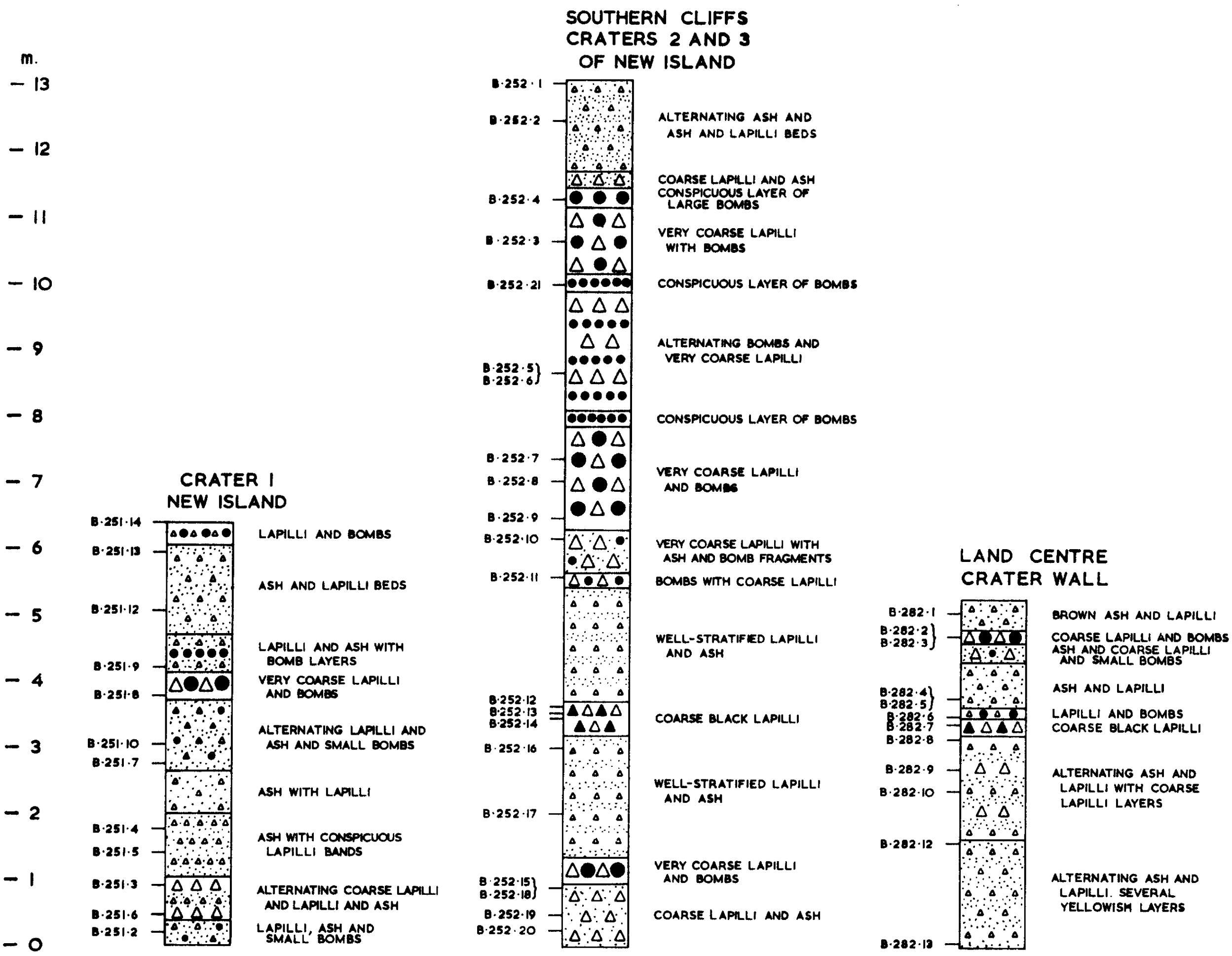

FIGURE 16

Generalized pyroclastic stratigraphy at the 1967 eruptive centres, showing the stratigraphical locations of samples (e.g. B.251.14).

Fig. 18. These contours differ from those of the isopach map in showing an eastward elongation; this is probably because the isopachs incorporate data for the entire eruption, whereas the size-distribution data are compiled essentially from fragments at the surface, representing the final stages of activity. The data suggest that the larger bombs were thrown further from the new island than from the land centre but allowance must be made for the fact that there is heavier blanketing of late-stage finer ash and lapilli around the land centre.

Grain-size analyses were carried out on a number of samples from the 1967 eruption and various parameters were calculated. Ideally, the objective was to examine samples from a single horizon across as wide an area as possible but there were severe limitations to this. No single unit selected at a distance from the island or land centre could be traced to one of the vast number of beds exposed at the centres themselves. Away from the centres it was not possible to distinguish deposits from the island from those of the land centre. As a practicable compromise, it was decided to take the coarsest unit in each of the exposed sections. This occurred near the base of the succession and graded from cindery lapilli near the land centre to a coarse ash at Whalers Bay. The samples were sieved, the fractions weighed and the grain-size distribution was analysed from histograms and cumulative curves. The conclusions were as follows:

i. The modal grain-size diminishes south-south-eastward away from the land centre, showing a general correspondence with the isopach map (Fig. 19).

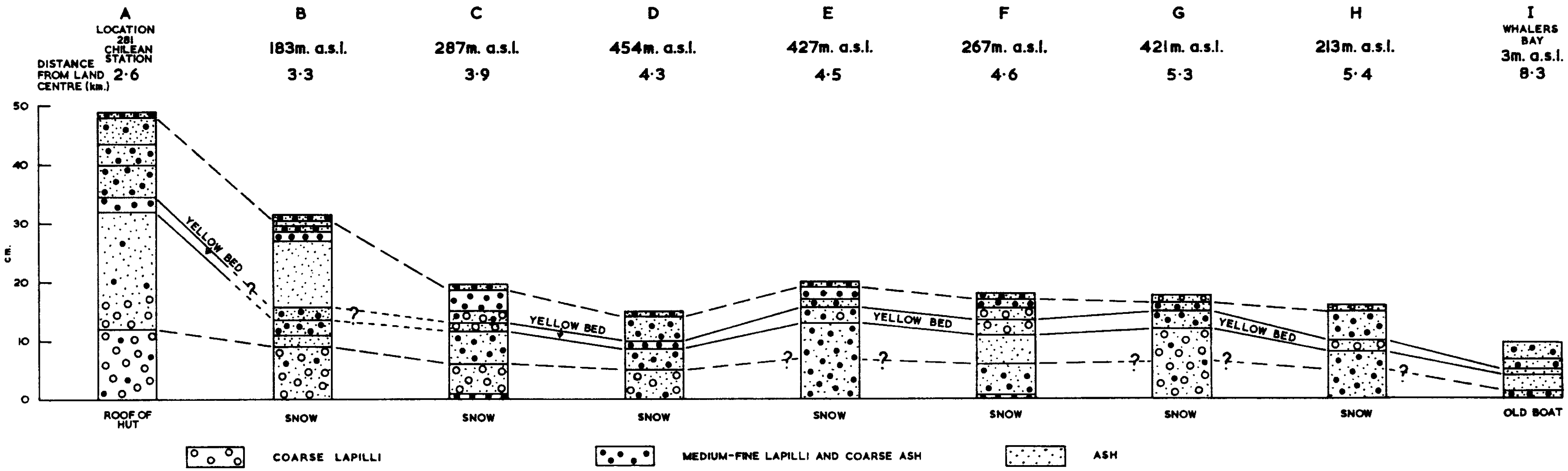

FIGURE 17

Stratigraphical correlation of the 1967 pyroclastic deposits along the eastern side of Deception Island from Pendulum Cove to Whalers Bay. Localities A–I are shown on Fig. 22.

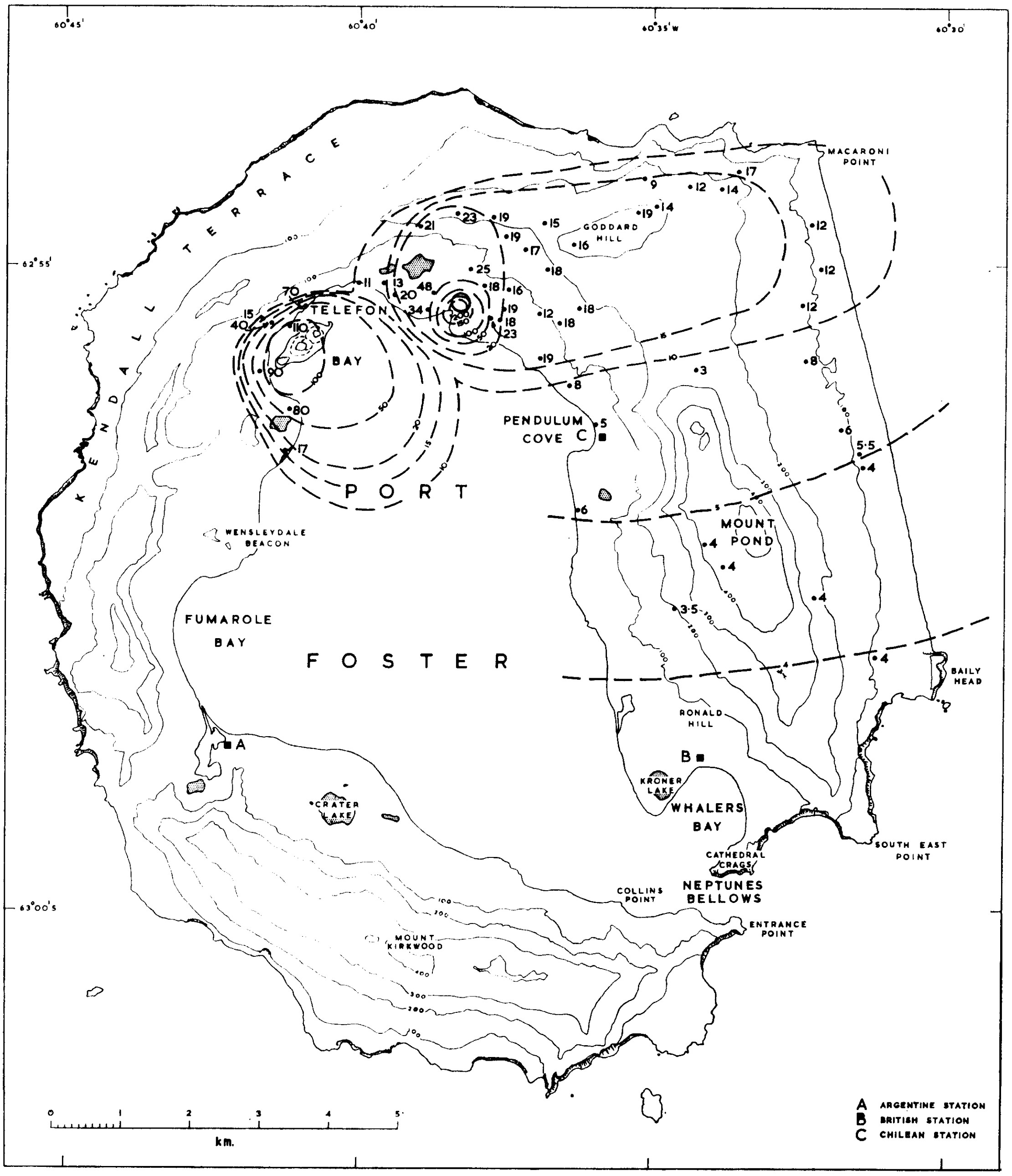

FIGURE 18

Distribution of the largest 1967 pyroclasts. Figures represent the mean diameter (in cm.) of the five largest pyroclasts obtainable at each locality. Values obtained close to the eruptive centres are omitted from this map but they are shown on Figs. 10 and 11. There are slight differences in the positions of some of the contours near to the centres. In this figure, away from the vents where the deposits are thin, the dimensions represent the maximum sizes for the entire eruption, whereas near to the vents only bombs emitted in the closing phases of activity were accessible for measurement.

ii. "Contours" showing the percentage of material coarser than 2 mm. (Fig. 20) show a distinct elongation eastward from the land centre and are similar to those of Fig. 18 based on the largest fragments at particular localities.

iii. Sorting generally improves with distance from the land centre but there is an anomalous area of relatively poorly sorted material on the outer slopes of the island to the north-east of Mount Pond (Fig. 21). This area does not coincide with any recognizable eruptive centre though its position

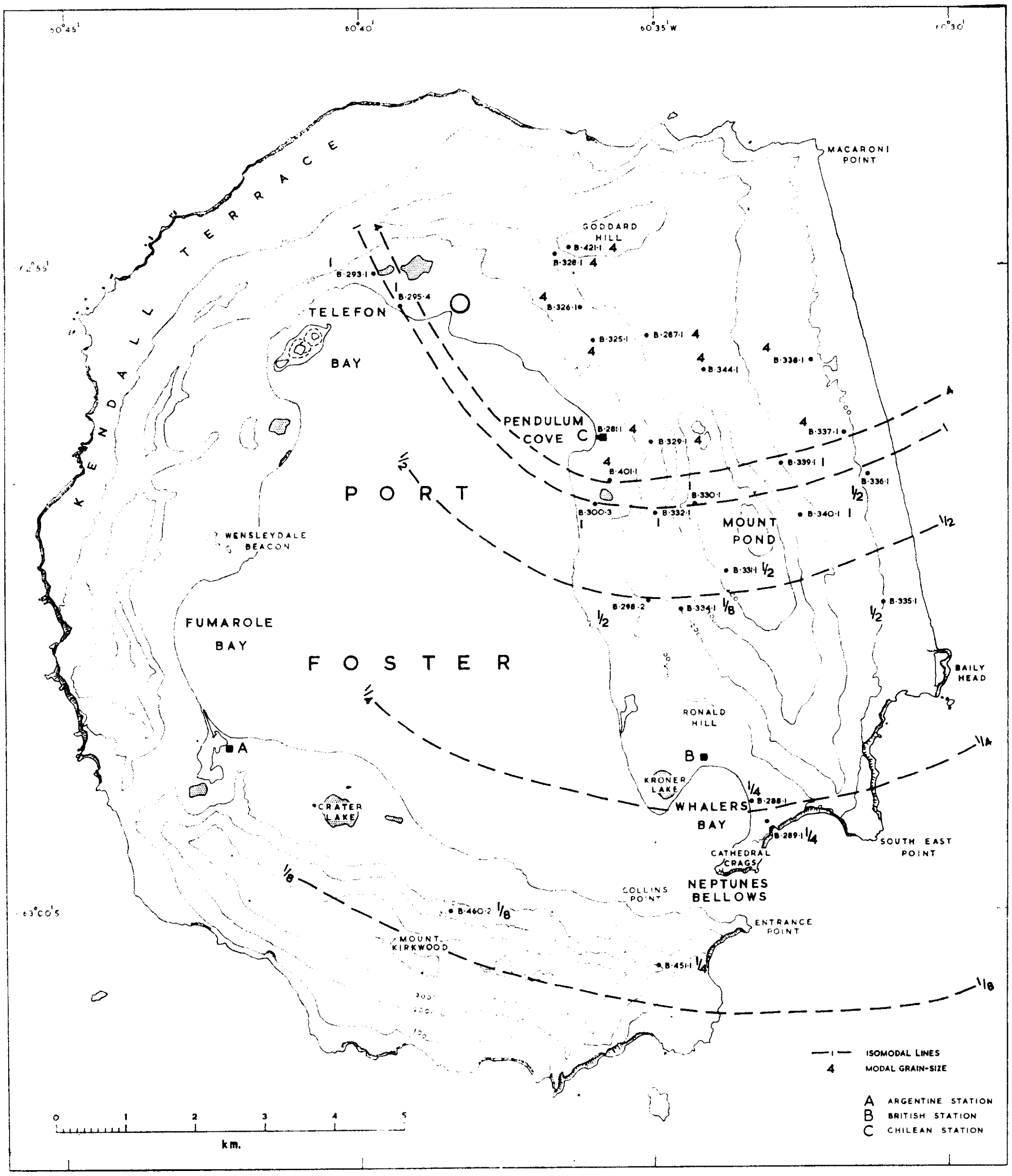

FIGURE 19

Modal values (in mm.) and isomodal lines for sieved specimens of the 1967 pyroclasts.

would correspond approximately with that of the third column of vapour reported by I. Curphey east of the land centre (p. 18).

iv. The grain-size distribution within a particular sequence of pyroclast fall deposits, such as the well-defined group lying on top of the huts at the Chilean station, illustrates that the coarsest material of all lies at the base of the succession, that it becomes progressively finer in the central part and then somewhat coarser again towards the top. The much abbreviated sequence from the shore of Whalers Bay suggests a similar pattern. It seems, therefore, that the initial outbursts were the most powerful, that activity then waned somewhat but increased again towards the end of the eruption. Comparative sections through the pyroclast sequence at various localities are illustrated diagrammatically in Fig. 17.

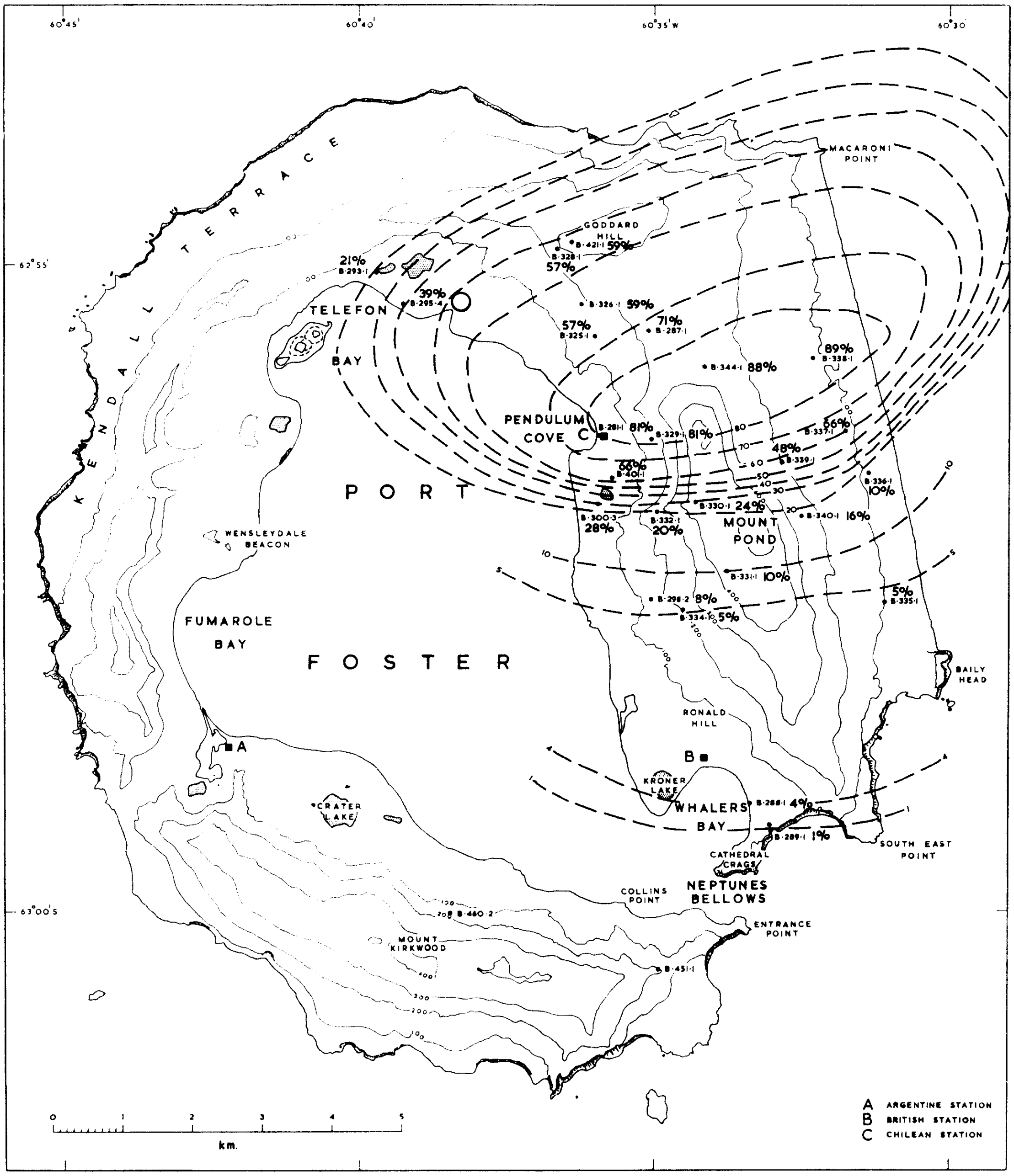

FIGURE 20

Percentage of material coarser than 2 mm. in sieved samples of the 1967 pyroclastic deposits.

v. The sorting of many of the samples (e.g. B.338.1 and B.281.3) is characteristic of pyroclast fall material. However, there are often distinct departures from this (e.g. B.326.1 and B.281.11) which may be accounted for by one or more of the following factors: (a) The finest material is all included within a single size category of <1/16 mm., since separation into finer grades by settling velocities was not carried out. This may account for the apparent bimodality in some of the finer samples (e.g. B.335.1 and B.288.1). (b) Falling snow and hail may have selectively removed some of the finest material from the eruptive clouds and accentuated the finer fractions in the deposits. (c) In some instances a sample is bimodal in fractions coarser than 1/16 mm. (e.g. B.281.11 and B.421.1).

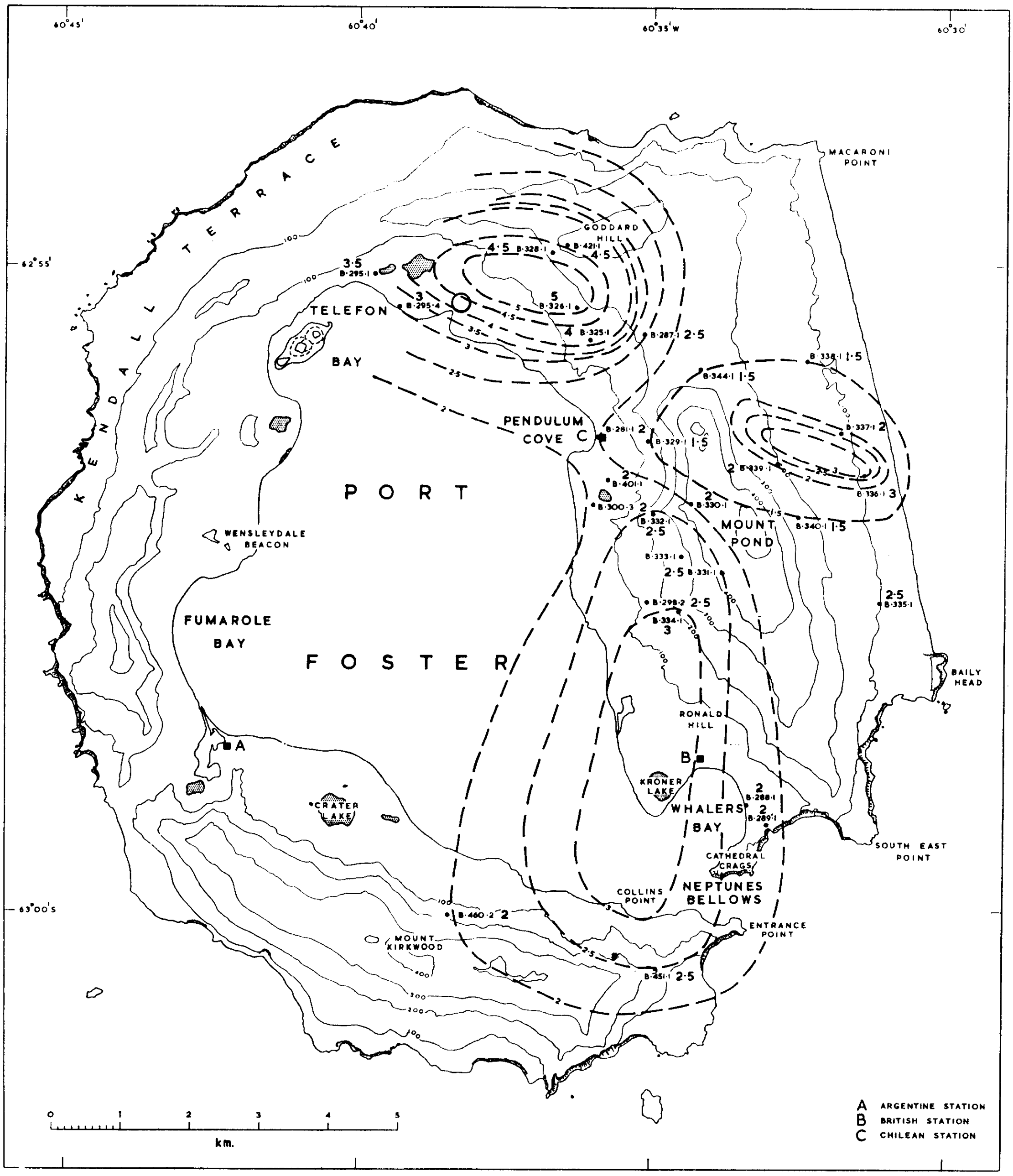

FIGURE 21

Sorting coefficients ($(Q_3/Q_1)^{\frac{1}{2}}$) for the 1967 pyroclasts. Note the anomalous area of poorly sorted deposits north-east of Mount Pond.

These are probably composite samples containing components erupted contemporaneously from the two centres or in some cases it may mean that a single sample was erroneously collected across the boundary dividing separate eruptive units. The sample of material which fell on *Piloto Pardo* 10 km. north-north-east of Deception Island on the night of 4 December 1967 is also distinctly bimodal since small bomb fragments fell with the finer ash and dust (Valenzuela and others, 1968, p. 12). This suggests either that pyroclasts from two sources were falling at the same time or that fine wind-blown ash was falling with larger fragments erupted explosively but slightly later from the same vent.

It is also worth noting the close correspondence between the histogram for a sample from the Chilean station presented by Valenzuela and others (1968, p. 12, fig. 3) and that obtained by the writers on a sample (B.281.4) from the top of the succession on the roof of one of the Chilean huts.

1. *Composition of the 1967 pyroclastic rocks*

The 1967 samples contain fragments composed mainly of two distinct types of glass. First, there is a dark scoriaceous glass, which comprises the larger bombs and also forms varying percentages of the lapilli. Secondly, there are fragments of a clear pale brown glass ($n = 1 \cdot 542 \pm 0 \cdot 003$) which is very abundant in some lapilli samples (e.g. B.294.1 and B.273.1). It is thought that the pale brown glass represents chilled magma erupted from a submarine vent, whereas the darker scoriaceous material is indicative of subaerial conditions. Many of the pyroclastic samples show a mixture of both glasses which is perhaps to be expected in a situation where the vents are close to sea-level.

Apart from the glass there are microphenocrysts of plagioclase zoned within the andesine range (An_{50-40}) and smaller plagioclase laths, very abundant in some samples, which have an oligoclase composition (ca. An_{30-25}). In addition there are scattered microphenocrysts of grey-green clinopyroxene and even rarer olivines ($\sim Fo_{45}$) (Plate Xd).

From a series of complete or partial chemical analyses of samples from the new island, the land centre, a sequence of pyroclast fall units on the huts at the Chilean station and an abbreviated sequence at the old whaling station at Whalers Bay, the following points may be made:

i. All samples from the land centre are distinctly more basic than those from the new island.
ii. Analyses of pyroclasts from various stratigraphical levels in the new island all fall within a very close compositional range (60·2–61·2 per cent SiO_2), though there is a slight suggestion that they become marginally more basic towards the top.
iii. All bombs analysed from the land centre fall within the range 57·5–57·8 per cent SiO_2 and there is no evidence of any systematic compositional change.
iv. Samples from the Chilean station are again within a tight compositional bracket (54·9–56·8 per cent SiO_2). They are distinctly more basic than those from the new island and slightly more basic than those from the land centre. Within this sequence there is a tendency for the beds to become more acid upwards.
v. At Whalers Bay the thin units are generally more basic than elsewhere but again they show a change from a more basic base to a more acid top.
vi. No systematic differences could be detected between analyses of whole-rock pyroclasts and those of the 1/16 mm. fraction.

The differences in composition of large bombs from the new island and the land centre are considered significant and must certainly reflect a real difference in the composition of the magma at these two centres. Away from the source vents it was not possible to draw a distinction between the products of the new island and land centre, though from the isopachs and from their composition it seems probable that most of the pyroclastic deposits on the south-eastern areas of Deception Island came from the land centre. However, the deposits apparently become progressively more basic in composition with increasing distance from the centres. Although one explanation would be that the sampling procedure failed to pick out the more basic units represented in the thick sequences at the centres, this does not seem very plausible. It is more likely that the pyroclastic debris was subjected to a form of mechanical differentiation whilst in flight. This apparently resulted in the winnowing out of the more siliceous material, and at least within the confines of Deception Island itself this process was more effective with increasing distance from the vent. Presumably, the more acid fraction would have been lifted high in the eruptive column and most of it carried far from Deception Island, though the acid pumice (B.317.1) collected from the beach near the new island may be representative of this fraction.

It was noted that pyroclastic successions at Pendulum Cove and Whalers Bay showed a tendency to become more acid upwards, although no corresponding changes could be detected in sequences at the eruptive centres themselves. Such variations may again be attributed to fractionation, since, if the energy of the eruptions diminished as time went on or if the wind velocity decreased, winnowing processes would be less effective and the resultant deposits would be less basic.

2. *Re-distribution of the 1967 pyroclastic rocks*

At the time of the 1967 eruption much of the previous winter's snow lay on Deception Island and was covered and preserved by the pyroclast fall deposits. The material was then buried by the snow which fell during the winter of 1968 so that when visited at the of end that year the new pyroclast layer was preserved dry but buried by snow. The dry nature of the deposits enabled samples for sieving to be collected without difficulty. However, when the overlying snow melted during the summer of 1968–69, the pyroclastic material became waterlogged and was partly re-mobilized; later it was frozen solid. The following observations were made during the summer of 1968–69.

At first the effects of the melt were felt only near sea-level but by January 1969 they were obvious up to 300 m. a.s.l. Steep-sided gullies were rapidly cut in the loose pyroclastic debris and were particularly in evidence between the land centre and Pendulum Cove where the ash fall had been heaviest. One such gully was 13 m. wide at its mouth and its stream discharged across a newly formed delta which had already been built out about 50 m. into Port Foster. There were several new deltas along this stretch of coast. The streams flowed in pulses caused by the periodic collapse of the unconsolidated gully walls. For the same reason, there were rapid fluctuations in the proportions of water and solid material, so that the discharge varied between a normal stream flow with most fragments in suspension and a dense mudflow when the stream was heavily choked with debris.

The water, charged with pyroclastic debris, raced across the braided surface of the delta, changing course every few minutes and plunging down steep foreset beds into Port Foster. There was apparently very little mixing, since the turbulent muddy current was sharply delimited from the clear greenish sea-water. On the delta, the movement and abrasion of the pyroclastic fragments generated a continuous clattering and hissing sound.

The large volume of pyroclastic debris that was swept down the slopes added greatly to the beaches, especially on the eastern side of Port Foster; for instance, an entirely new beach 20 m. wide at high tide was formed at the foot of Crimson Hill.

Immediately north-west of the land centre there were four or five new beach ridges around high-water mark which were composed entirely of vesicular and fairly complete bombs up to about 1 m. in diameter. Similar, though less well-developed ridges of bombs, this time usually greater than 1 m. across, occurred along the beach opposite the new island. It is thought that these bombs were thrown from the vents directly into the sea but on account of their own density were washed ashore to form the beach ridges. The low density was apparent when several of the bombs were thrown into the sea to test this hypothesis; they floated to the surface, remained there for a few seconds and then sank amid streams of bubbles.

Before the eruption, a crater immediately below Cross Hill was occupied by a shallow lagoon connecting through a narrow channel with Telefon Bay. By November 1968, the entrance to the lagoon had been blocked and a small lake was left in the crater. There was only a very light fall of pyroclastic debris in this area and the blocking of the lagoon was undoubtedly caused by longshore drift, which also created a much wider beach along this part of the shore.

The thaw that occurred in late 1968 was regarded as unusually rapid by those who had experienced other summer melts on Deception Island, or alternatively remarkably little snow fell during the earlier part of the year. Although there was a great deal of snow around the lower levels of the island in December 1967, at the same time the following year there was almost no new snow on top of the pyroclastic deposits. At the Chilean station, for instance, there was no snow at the surface in December 1968 but the deep snowdrifts of the 1967 winter were preserved beneath the 50 cm. layer of ash (Plate Va). The new ash cover over Deception Island appears to have exerted two different influences, depending on its thickness. The dark ash clearly absorbs more solar radiation than the ice and snow. Where the ash cover was thin or incomplete, this heat was transferred to the underlying snow and melting was accelerated. On the other hand, when the thickness of the ash exceeded more than a few centimetres, it had the opposite effect of insulating the snow and prevented melting, as clearly happened at the Chilean station.

G. Fumarolic Activity

Reports of fumaroles are to be found in the earliest accounts of Deception Island. In order to establish some reference for any subsequent changes in the pattern of activity, the locations of existing fumaroles together with their temperatures were mapped by A. Bushell in December 1968 (Fig. 22).

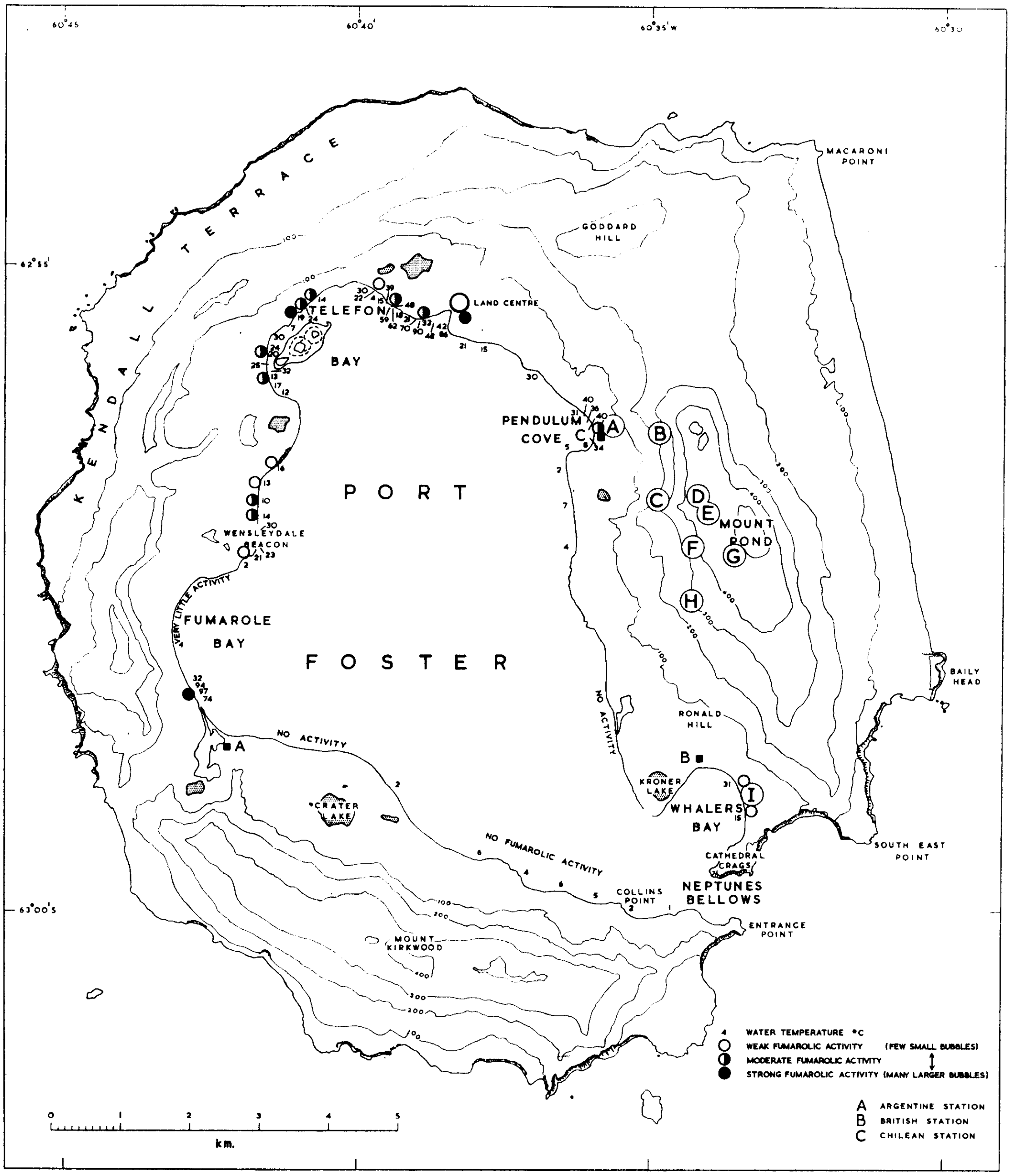

FIGURE 22

Water temperatures around Port Foster, 14 December 1968–2 January 1969 (recorded by A. N. Bushell). Localities I–A refer to the stratigraphical sections shown in Fig. 17.

Many of the fumaroles, such as those around Whalers Bay and Fumarole Bay, have been established for a long time and there were no indications of increased activity in 1968. But the submarine fumarolic activity in Pendulum Cove, though not new (Casertano, 1964), certainly appears to have increased during the recent event, and clouds of steam and sulphurous vapours were continually swept inland over the Chilean station.

The most active of the new fumarolic areas was on the floor of the land centre, where large volumes of vapour issued from a series of north–south-trending fissures.

In December 1968 there was a considerable amount of new fumarolic activity around the shores of Telefon Bay, especially in the new embayment alongside the land centre. The hottest spots were in the shallowest water which was often bubbling vigorously and where temperatures up to 97° C were recorded.

The zone of hottest water was always at the shallowest depths and it migrated to and fro with the tide. Presumably, a fairly broad zone was in fact subject to fumarolic heating but wherever the water reached depths of about 1 m. the heat was then dissipated. Right on the shoreline a much smaller volume of water would remain over the hot spots for a longer period of time.

Between the new island and the northern shore of Telefon Bay, streams of bubbles rose in cold water that was more than 5 m. deep. In a few places the bubbling also occurred in shallow water where the temperature was as low as 5° C. The gas was odourless and in all probability it was simply air bubbles released from the vesicular pyroclastic deposits which had accumulated in Port Foster.

IV. THE 1969 ERUPTION

By

P. E. BAKER *and* M. J. ROOBOL

LITTLE more than a month after field studies of the 1967 eruption had been completed, Deception Island erupted again. This time the only occupants of the island were five members of the British Antarctic Survey living at Whalers Bay. The following account of the eruption is based on the eye-witness accounts of these five men. The subsequent investigation of the effects of the eruption and the description of the new volcanic centres are based on a brief survey made during the period 10–22 March 1969 by a small party supported by the Royal Society and the British Antarctic Survey.

A. EVENTS PRECEDING THE ERUPTION

In January 1969, men at the Argentine station on Fumarole Bay apparently experienced a number of small tremors which were not felt at the British Antarctic Survey station on Whalers Bay but in early February tremors were felt at both stations. At Whalers Bay, D. Snell constructed a simple but effective seismograph consisting of a weighted boom linked to a barograph pen recorder. From 7 February onwards a more or less continuous record of the tremors exists, including those which occurred on the day of the eruption (Plate XIII). Increased fumarolic activity was also noted at Kroner Lake; in January 1969 its temperature was 5° C but shortly before the eruption steam was rising from its surface. In view of these premonitory signs, it had already been decided that the five British Antarctic Survey men should be evacuated from Deception Island as soon as possible.

At 03.34 hr. local time on 21 February 1969 all five men at the British station were suddenly awakened and vigorously shaken by a particularly strong earthquake. This was followed by many others so that as soon as it was light, at about 06.00 hr., the base commander, remembering events of the previous year, sent everyone out to look for signs of an eruption. Visibility was good and there were no signs of new volcanic activity. A fall of rock from Ronald Hill was observed and it had probably been loosened by the tremors. At 07.20 hr., the men returned to the station but continued seismic activity prompted them to radio R.R.S. *Shackleton* and ask for her arrival at Deception Island to be put forward. At 07.33 hr., as a result of the continuing strong seismic activity, assistance was also sought from the Chilean ship *Piloto Pardo*, which was nearer Deception Island than *Shackleton*. At about this time a wind blew up from the east and snow flurries began to fall, reducing visibility. At 08.32 hr., the tremors reached a new maximum and swung the roof of the aircraft hangar 1 m. out of line, also spilling 10 cm. of water from the station kitchen tank which was previously filled to within 5 cm. of its top. At this point, it was decided to abandon the station and to move to the outer coast of the island. It was considered that this would facilitate evacuation, since during the 1967 eruption the oscillating water level in Port Foster had made navigation in the narrow Neptunes Bellows very hazardous. The ships were informed accordingly, the station was abandoned and the five men set off towards South East Point.

B. THE ERUPTION

At 09.50 hr., the men were climbing the snow-covered slopes overlooking Whalers Bay, heading towards South East Point when a large white eruptive column was seen rising from the vicinity of Pendulum Cove up towards the cloud base over Mount Pond. A few minutes later the column darkened and debris began to fall from it. A deep rumbling was heard and a second column now rose about 1 km. to the east of the first one. The two columns merged and an intense electrical storm began with lightning dancing along "Little Pond ridge", discharging on to the high points from the clouds above.

Snow began to fall and darkness set in as coarse lapilli-sized material rained down on the five men, knocking one of them to the ground. They sheltered under their rucksacks throughout the first shower, which lasted about 20 min. and consisted of lapilli with a coating of ice. No further observations of the eruptive columns were possible because of the poor visibility. As the first fall of debris abated, the party moved to the nearest rocks where they sheltered from the second shower which lasted 35–40 min. This time there was no ice on the lapilli which were warm to the touch.

During the second lull, the men moved down to the shelter of an old corrugated iron whaling shed on the shore of Whalers Bay. When they arrived there at 11.00 hr., they could see the lights of the station hut and they also noticed that some of the large storage tanks from the old whaling station had been moved down into Whalers Bay. As they sheltered in the shed, showers of lapilli of 10–20 min. duration continued to rattle down on the roof, whilst in the poor visibility it seemed that Whalers Bay was "boiling" with the impacts of the falling lapilli. Every now and then a larger missile would create a much bigger splash. Birds were seen flying through the curtains of falling debris towards shelter.

As their portable radio had been damaged, at 11.45 hr. the men decided to head back along the beach and use the station radio. They ripped sheets of corrugated iron from the walls of the shed and ventured out holding them over their heads for protection. Farther along the beach they were again forced to take shelter in a wooden hut as the fall of debris increased. From this point the station hut was obscured by a row of very large storage tanks belonging to the whaling station.

At 12.05 hr., they moved into one of these large tanks which had an entrance cut in the side and had been used as a storehouse. Blocks of ice up to 1 m. in diameter were strewn both around and inside the tank and 20 cm. of water now covered the floor of the tank which had previously been dry. Wet marks on the sides of the tank indicated that 2·5 m. of water had passed by shortly before. From this vantage point the men were able to establish that the station lights were now out. They also noticed that a stream of ochre-coloured water 20 m. wide and 15 cm. deep with newly incised 1 m. gullies was flowing between the tanks and the station; earlier that morning only a small melt stream had flowed gently across this area.

Coarse lapilli continued to fall until about 12.40 hr. when the group left the tank and moved towards the station huts. Only then did the full extent of the damage become apparent. A strip of ground about 50 m. wide between the station huts and the old whaling station had apparently been levelled off. Material from the higher parts, including the cemetery, had been eroded away and deposited lower down, extending the shoreline about 90 m. seawards from its former position. The surface of this eroded zone was littered with large boulders of ice. Much of the old whaling station had been swept away and some of the tanks were lying partially submerged in Whalers Bay (Plate Vc).

The jetty had been destroyed and most of the British Antarctic Survey's buildings were damaged. The worst hit was "Biscoe House", the older wooden part of the station which looked out across Whalers Bay (Plate Vd). Both the back and front walls had been breached and much of the contents carried away. Blocks of ice were strewn inside the hut as well as on the ground outside. The newer fibreglass extension to "Biscoe House" was partly choked with the debris from a mudflow, consisting of small sub-angular blocks of ice now fused together into a solid mass. This ice-block lahar had apparently entered through the back wall and passed along the corridor, pushing into rooms on either side as it went. The generators were partly buried in the mudflow debris, which accounts for the failure of the lights whilst the men were returning along the beach. Tractors parked in front of the huts had been swept away and one of them was found partly buried near the remains of the jetty.

The party collected some food from an undamaged hut and at 13.10 hr., just as a fine black ash began to fall, they moved into the aircraft hangar which was essentially undamaged. Drums of aircraft fuel with cotton wicks provided beacons whilst the party remained in the hangar until 16.30 hr. The electrical storm stopped as the lapilli fall came to an end but during the afternoon rumblings could be heard in the distance. Snow flurries combined with the falling ash and dust to form a dense coating on the windows and walls of the buildings. At 16.30 hr., after the local cloud base had lifted slightly, the five men were evacuated by two helicopters to the Chilean ship *Piloto Pardo*. The rescue was performed under extremely difficult flying conditions with ash and snow falling in a strong easterly wind. Before they left, they noticed that the concrete apron in front of the hangar was not completely covered by ash. From the helicopter they also noticed that Kroner Lake was now breached on its seaward side and linked with Port Foster.

On the ship the men were given every assistance and learned that, although *Piloto Pardo* had arrived at Deception Island some time before, conditions had prevented the helicopters from taking off. Although the ship had waited to the south-east of Deception Island, ash had fallen on board suggesting that, in addition to the easterly surface wind, high-level winds were from the north-west.

The men subsequently transferred to *Shackleton* and on the morning of 23 February returned briefly to Deception Island to collect their belongings. During this visit visibility was very poor because of low cloud but no debris fell and no tremors were felt. It was noted that there was now "about six inches" of debris in front of the aircraft hangar. The runway had been severely eroded and a 2 m. deep gully leading to Kroner Lake had been cut across it while the surface was partly covered with ice blocks up to 2 m. in diameter. Professor L. C. King, also aboard *Shackleton* at the time, climbed Ronald Hill and saw a large cavity in the ice behind it. Before leaving the island, Capt. D. H. Turnbull took his ship around Port Foster and noticed that the Chilean station, abandoned a few months earlier, now seemed to have been totally destroyed. Whilst they were off Pendulum Cove, the cloud parted briefly and a few men on the ship glimpsed a new steaming crater behind the former Chilean station.

C. Subsequent Investigation of the Eruption

Prompt action by the Royal Society and the British Antarctic Survey enabled the writers to return immediately to Deception Island so that the effects of the activity could be studied before they were obscured by the coming winter's snow. The following description of the eruptive centres and interpretation of events are based on observations made during the period 10–22 March 1969.

The eruption had occurred along a 5 km. arcuate fissure which had opened up in the permanent ice cap on the inner slopes of Mount Pond, on the east side of the island (Plate IIIa). A number of elongate open chasms totalling 3·5 km. in length had formed in the glacier, as shown in Fig. 23. Separate stretches of the fissure do not fall upon a smooth arc but are slightly angled or offset. There are also two smaller centres, which lie to the north and south of the main fissure.

D. The Fissures and Vents

The term "fissure" is used in a descriptive way in this account for an open gash in the ice or rock. The elongate open chasms in the glaciers are not strictly "fissures" in the volcanic sense but in this case they are a surface expression of volcanic fissures enlarged through melting.

For reference purposes, sections of the fissure and associated features are labelled A–F from south to north on Fig. 24 and the particular features of each part are described below:

A. The most southerly expression of the fissure is a new fumarole at 150 m. a.s.l. north-east of Whalers Bay. It has developed through 30 m. of permanent ice and appears on the surface as a 3 m. wide irregular hole with overhanging edges. It was emitting steam and sulphurous gases in March 1969.

B. 100 m. to the north of the fumarole at an altitude of 180 m. is a large cavity in the glacier, first observed by Professor L. C. King a few days after the eruption (Plate IVb). It measures 200 m. from north to south and is about 100 m. east–west. Though it is backed by a 30 m. high ice cliff to the east, it is open to the west. Volcanic bombs are scattered down-slope from the feature, substantiating its eruptive origin. The floor of this cavity in the ice is covered by waterlain deposits of black and red ash and lapilli somewhat disturbed and tilted by a series of north–south-trending open fissures.

C. About 500 m. north-west of B is the beginning of a 1·5 km. long open fissure. It trends north-north-east across the ice, rising slightly from 320 m. a.s.l. at its southern end to 370 m. at its northernmost point. About 100 m. south of this stretch of the fissure is a small depression in the ice suggesting further subglacial activity; it also emphasizes the offset relationship of B and C. The southern 800 m. section of C is generally about 70 m. deep and 100 m. wide but with an irregular outline in detail. Towards its southern end, it starts to branch but the composite 170 m. wide chasm terminates abruptly in a series of ice walls. The floor of the fissure is a jumble of ice blocks accumulated from the often overhanging ice walls. Avalanches from these walls were heard during March 1969.

   Near its central part the chasm is almost closed by a barrier of ice which reaches most of the way across its width. Immediately north of this, a section 300 m. long and 100 m. wide is largely filled by a number of overlapping pyroclast cones which bury the lower or western edge of the chasm to a maximum depth of about 20 m. A 70 m. deep vent is present in the southern part of these pyroclastic deposits and to its north are a number of smaller vents 10–20 m. deep. The eastern edge of the fissure is formed by an ice cliff 50 m. high which is overlain by 2 m. of debris. Falls from this cliff built a scree of ice blocks which partly covers the cones. A considerable volume of volcanic ejecta was emitted from this short section of the fissure and, from the observations of D. Stocks, it

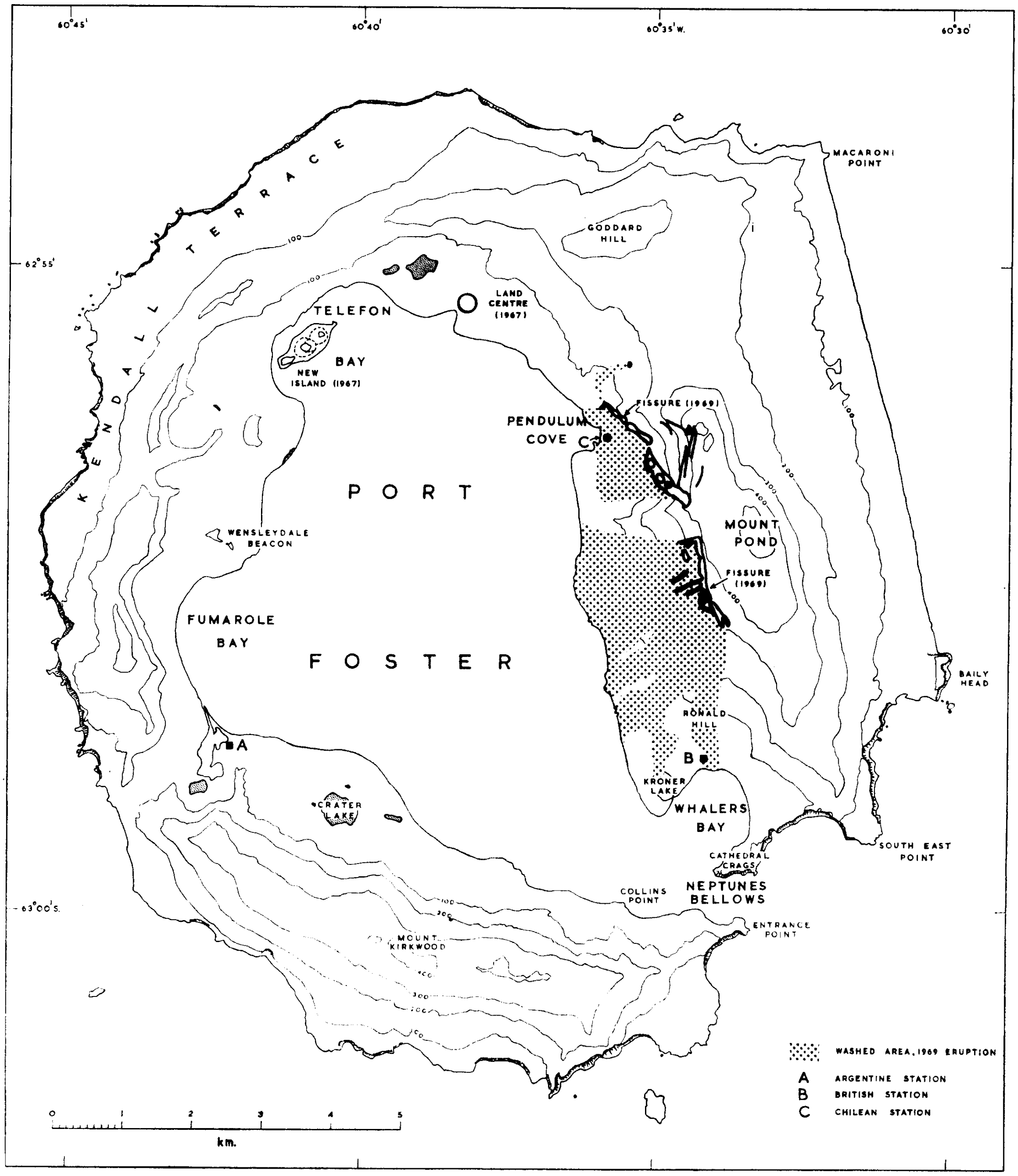

FIGURE 23
Location of the 1969 fissures and the area affected by the flood of melt water.

was probably the site of the second eruptive column seen on 21 February. Much fumarolic activity was taking place here in March and a series of fissures trending north–south in the pyroclasts revealed red glowing, though solid, material to within 1 m. of the surface. It was apparent that only a thin layer of debris was necessary to insulate the glowing matter from the underlying ice.

The northern 300 m. of this part of the fissure are open and ice-floored; at the north end two deep gullies lead down-slope through the ice.

D. This is a small but elongate vent lying at 270 m. altitude immediately down-slope from the most active section of C. It is 230 m. from north to south, 100 m. wide and 40 m. deep with vertical ice walls. The flat floor is covered by a layer of black air-fall lapilli, through which steam was escaping along two north–south-trending fissures.

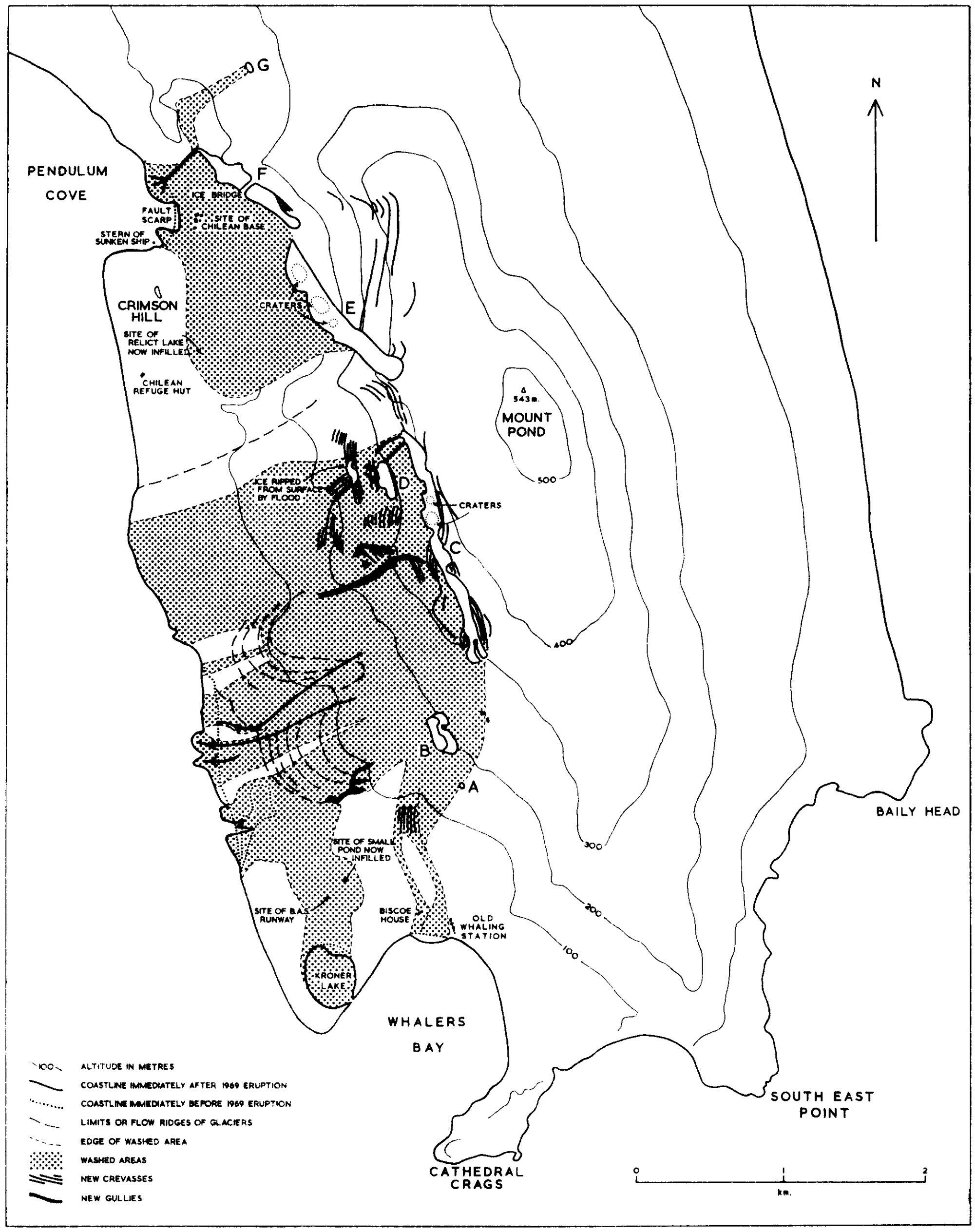

FIGURE 24

Sketch map showing details of the 1969 eruptive fissure system and features associated with its activity.

E. This is a 1 km. long fissure extending in a north-westerly direction from 470 m. a.s.l. near the top of Mount Pond down to 70 m. a.s.l. at Pendulum Cove. Crossing the 450 m. gap between sections C and E of the fissure are a series of new open crevasses. The high southern end of this section of the fissure is 200 m. deep and 170 m. wide. Since the glacier is here only 50 m. thick, the underlying bedrock is now exposed in the lower part of the new chasm. The freshly exposed rocks include yellow tuffs and red scoria overlain by what appears to be black frozen ash and lapilli. Blocks of the overlying ice have slipped westward down this interface to accumulate on the floor of the fissure.

The northern two-thirds of this section of the fissure are about 200 m. wide. Several separate or overlapping craters are discernible and the fissure is almost entirely filled with bombs, lapilli and ash. These deposits extend over the lower western edge of the fissure, covering to a depth of 50 m. the ice slopes which lead down to Pendulum Cove. The higher eastern edge is formed by a 50 m.

high ice cliff overlain by 10 m. of new debris. On the west edge of the fissure there was vigorous fumarolic activity in March 1969 and red-hot scoria was observed in a series of north-west-trending cracks. This part of the fissure with its large volume of coarse pyroclastic deposits was clearly the site of the most active vents during the 1969 eruption and was almost certainly the source of the first eruptive column observed on 21 February (Plate IIIb and c).

F. This section of the fissure is located immediately inland from Pendulum Cove, trending in a north-westerly direction from a height of 135 m. a.s.l. at its south-eastern end down to 30 m. at its north-western end. It is 900 m. long and half-way along its length it is divided by an ice bridge (Plate IIId). The two sections of the fissure are linked by only a very low tunnel on the floor of the chasm. The sides of the fissure are vertical ice walls 50–100 m. high. Sheets of ice were spalling from these walls and the bottom of the chasm was a jumble of fallen blocks. At its north-western end, the fissure takes an abrupt right-angle turn and passes into a newly eroded valley or gorge leading down to Port Foster. There were no visible vents along this length of the fissure and no sign of erupted debris on the edge.

G. This lies well outside the arcuate or *en échelon* pattern of the other sections of the fissure and it is 650 m. north-east of the northern end of F at an altitude of 170 m. It is a semi-circular hole in the ice 50 m. in diameter and 40 m. deep, with its floor covered by ice blocks. Large volcanic bombs are scattered around its edge, and a trail of bombs and lapilli extends down-slope from it over the ice.

E. The Crevasses and Fissures

Prior to the 1969 eruption the crevasses on the smooth west-facing slopes of Mount Pond ran parallel to the ridge though on the isolated hills they formed a crossed pattern. Section C of the new fissure is largely parallel to the crevasse direction and there is no obvious interaction between them except where crevassed slices of ice lean into the chasm. More striking changes occurred where the flood of water from the vents ran down-slope across the trend of the crevasses, and are described below. Section E of the new fissure system lies below the steepest and highest slopes on the western side of Mount Pond and it is here, above the fissure, that crevasses have opened up in response to the general slip which took place at the weakened base of the glacier. In March 1969, new ice cliffs up to 20 m. high were seen where large blocks of ice had slipped a short way down-slope. The new fissures and crevasses are shown in Fig. 24.

The fissures which opened up during the 1969 activity appear to have formed essentially by the removal of ice and are not dilatational or tensional features. This view is supported by the abrupt termination of the fissures in ice walls up to 100 m. across and also by the presence of an ice bridge in section F, and an almost comparable link in section C. These features indicate that there was virtually no separation across the width of the fissure. From the profile of the ice slopes on either side of the fissure, it is also clear that there were no significant vertical displacements either.

F. The Flood

There is much evidence to suggest that an enormous volume of water rushed down-slope from the zone of the vents into Port Foster and that in some areas this was followed by mudflows. Most of the terrain between Pendulum Cove and Whalers Bay was covered by the flood (Figs. 23 and 24). The washed areas have largely been covered by later air-fall deposits but they are readily identified where this cover is less than 1 m. thick because of large stranded ice blocks (Plate IVd) and deep gullies cut into the steeper slopes.

Floods of this type are well known in Iceland where many of the high volcanoes have permanent ice caps. When these volcanoes erupt, the ice is melted and water rushes down the flanks in floods known as "hlaups" or "jökulhlaups". They accompanied the 1362 and 1756 eruptions of Oraefajökull—a large volcano, 2,044 m. high, on the south-eastern coast of Iceland. An eye-witness account of the 1756 hlaup (Thorarinsson, 1958) is very similar to that of the events at Deception Island on 21 February 1969. The effect of the floods on the upper ice-covered slopes will be considered separately from those on the lower near-shore area.

1. *Effect of floods on the ice slopes*

Leading down-slope from the fissures are gullies cut in the ice and trending normal to the crevasse direction; they are best seen on the down-slope side of section C (Plate IVa) and again at the northern end of F. Those below C extend for about 500 m. from the lower edge of the fissures (370 m. a.s.l.). The gullies are steep-sided, often vertical, and up to 10 m. deep; they are linked by open crevasses parallel to the fissure. Locally, e.g. below the north end of section C, the surface is greatly disturbed and ice blocks have been ripped out of the surface and carried away. The eroded area is about 30 m. in diameter and this, together with the gully and surface scatter of ice blocks, bombs and lapilli, is a new feature. Prior to the 1969 eruption, the ice in this area was broken up mainly by open crevasses following the contours of the slope. These crevasses were widened during the 1969 eruption and several new ones were opened up. The lower crevasses are probably the result of the earth tremors but those above the fissure may have opened as the ice slipped down-slope into the open chasms.

Scattered over the washed surfaces are blocks of clear glassy ice similar to that in the walls of the fissures. On flatter surfaces and in depressions are deposits, often with mudflow or alluvial structures, composed of black and red ash and lapilli. Below 170 m., the surface flattens out and down-slope of section C is a glacier with a capping of ash and lapilli which extends into Port Foster. The surface of this glacier is very uneven and ice blocks are very abundant with some perched on the tops of hills 17 m. above the adjacent valley, though other hills only 10 m. high appeared to have escaped the deluge. Before arriving in this hilly area the water had descended through a vertical distance of 300 m. down a 12° slope. The edges of the washed areas were identified by the concentration of small ice blocks a few centimetres in diameter, which made up a continuous ridge. The area is covered with lapilli from the 1969 eruption but during March all ice blocks smaller than 30 cm. diameter melted, while the lapilli between remained frozen, leaving a characteristic pitted surface over the washed areas. Digging below the air-fall deposits in the washed areas revealed a water-lain deposit of red and black ash and lapilli.

The relations below the most active part of the fissure (E) above Pendulum Cove cannot be seen because of the thick surface cover of pyroclastic debris. Large gullies lead down-slope from the northern end of section F, while smaller ones less than 2 m. deep lead down-slope from many other stretches of the fissure.

An enormous volume of water carrying ice blocks together with red and black cinders appears to have swept down the ice slopes from the vents and across the open crevasses which are commonly more than 2 m. wide and 30 m. deep. Not only must these crevasses have been filled but locally blocks of ice were ripped out from this surface and carried away. After the initial flood, which appears to have run off as a sheet, the water was probably concentrated in the newly established gullies leading down-slope from the lowest points of the fissures.

2. *Effect of floods on the lower ground*

The lower part of the island is composed of yellow tuffs and lava flows largely buried by unconsolidated pyroclastic deposits from the younger post-caldera centres. Much of this debris is in the permafrost zone though in summer the thaw reaches to a depth of about 1 m. The changes brought about by the flood involved gullying and erosion of the steeper slopes and a levelling off of the lower ground by deposition in hollows. Narrow valleys such as that between Ronald Hill and the glacier to its north were widened and blocks of ice and permafrost were torn up. The flood branched around Ronald Hill and a relatively small volume passed into Whalers Bay, just reaching far enough to damage the British station. The wash deposits are again covered by air-fall debris but the water-lain red and black ash and lapilli can be seen on the dried-up stream beds, indicating that some water continued to flow after the eruption ceased. The washed areas are easily recognized by using the criteria mentioned earlier. Undoubtedly, some of the black cinders of these deposits are re-worked but much of the red material, which is uncommon in the air-fall deposits, must have been carried out from under the ice cap.

A larger volume of water passed to the north of Ronald Hill and formed a temporary lake in the crater depression below the hill. However, some of the water entered Kroner Lake and breached its south-eastern side to enter Whalers Bay. Numerous ice blocks were stranded in this area and scattered across the British Antarctic Survey's runway. The temporary lake lasted until after the eruption ceased as mud deposits overlie the air-fall lapilli. As it drained into Kroner Lake, a gully 2 m. deep and 10 m. wide was cut across the runway and a broad delta was built into Kroner Lake. West of Ronald Hill, ice and permafrost blocks up to 4 m. in diameter were stranded on the washed surface (Plate IVc). North of Kroner Lake, a strip 550 m. wide was levelled and a small lagoon was filled in. The northern edge of this area is an arcuate bank along which the edge of the washed area is clearly marked. The highest point reached by this mark is 4·5 m. above the level of the plain, though there are in fact several wash marks, suggesting that the flood passed by as a series of surges. Farther north, a number of strips and "islands" escaped the wash.

Little can be seen of the surface effects in the Pendulum Cove area because of a thick cover of air-fall debris which has caused the infilling of Relict Lake. The coastline of Pendulum Cove, which in January 1969 was smooth and arcuate with a gently shelving beach, now had a new delta immediately east of Crimson Hill which extended 20 m. into the sea. This is undoubtedly due to the flood of water from section E of the fissure which must have been channelled into Pendulum Cove at this point by Crimson Hill. Immediately west of this delta, the stern of a sunken ship previously not visible at low tide, but marked on the Admiralty charts, now stands permanently above sea-level. This is thought to have been tilted to its present position by the same flood of water responsible for the formation of the delta. A second new delta extends 30 m. into Pendulum Cove below the gullies leading from the northern end of section F of the fissure. Between the two new deltas the shoreline is marked by a new 3 m. high straight cliff composed for the most part of pre-1969 material. The boat house and jetty of the former Chilean station had disappeared and a concrete slipway, which previously ran down the shore into the sea, was now hanging over the edge of the cliffs. The shoreline was closer to the remainder of the Chilean station than it had been in January 1969. The cliff line appears to be a fault scarp marking the edge of a block which has subsided a few metres into the sea. Similar subsidences, though unaccompanied by an eruption, occurred in Whalers Bay in 1921 and again in 1930. In January 1969, the Chilean station, which had been abandoned in December 1968, was still essentially intact though partly buried by snow and 50 cm. of the 1967 pyroclasts. By March 1969 it had been almost totally destroyed; most of the buildings and their contents had disappeared and all that was left was a few charred and smouldering remains (Plate Vb). Some of the missing furniture, etc., together with that from the British Antarctic Survey station and parts of the old whaling station, were found scattered along a 2 km. stretch of shore south of Fumarole Bay. The Chilean station had evidently been destroyed by floods of water from sections E and F of the fissure and what remained had been ignited by bombs from the vents of section E. None of the debris washed ashore had been burnt.

Most of the coastline between Pendulum Cove and Whalers Bay, except for the faulted part and that below the glacier which enters Port Foster, had been extended by up to 200 m. This extension was not uniform but took the form of a series of fans coinciding with the mouths of the main channels followed by the flood water. In early March, the tides were dropping so that the edges of these areas were marked by a series of low beach ridges but later, when the tides began to rise, an ever increasing pile of debris was pushed inshore. Another interesting effect was seen on the breached side of Kroner Lake, which had now become tidal as it was linked with Port Foster by means of a narrow channel 5 m. wide and up to 1 m. deep. Water entering the lake with each flood tide had, by 20 March, built a large delta extending 15–20 m. into the lake. No corresponding delta was present on the seaward side of the breach presumably because the movement of material is largely one way.

There is then ample evidence that an enormous volume of water laden with ice blocks and cinders rushed down the inner slopes of the island from the new fissures. Observations of the debris in Whalers Bay on 21 February fix this as taking place in the first hour of the eruption and the mudflow which damaged the generators and extinguished the station lights as forming in the second hour of the activity. The flood appears to have been 2·5 m. deep in Whalers Bay, 4·5 m. deep north of Kroner Lake, and as much as 17 m. deep on parts of the glacier below section C of the fissure.

It seems probable that this flood marked the opening of the vents through the ice cap, and it is significant that the first observed emissions were of white steam columns and not black explosion clouds as seen in the 1967 eruption of Deception Island. Furthermore, the first showers of lapilli were coated with white ice. The presence of the gullies probably means that the fissures were full of water and that the water was probably warm. The eruption had presumably commenced with melting at the base of the glacier, sometime before it was actually observed. At 09.50 hr., the ice cap was penetrated by explosive columns of steam containing wet lapilli, and the flood of water and fragmented ice was released. Observations of the two eruptive columns and of the damage to the British station suggest that at least sections B, C and E of the fissure system formed about 10.00 hr. on 21 February.

G. Products of the Eruption

The February 1969 eruption, lasting probably less than 48 hr., threw out 0·02 km.³ of pyroclasts and left another 0·01 km.³ in the vents in the ice cap. The volume of material beneath the ice cap is unknown and the surface deposits are about half those of the 1967 eruption.

The main products away from the vents are vesicular black lapilli with a small percentage of red lapilli. Volcanic bombs are scattered along the edge of the fissure, attaining their largest dimensions and greatest abundance near the principal eruptive vents in sections C and E of the fissure. The largest bombs reaching 4 m. across occur beside section E of the fissure above Pendulum Cove. Typically, the bombs have a dark brown glassy outer surface which may show an irregular ropy structure and a black frothy interior. At Pendulum Cove, many of the bombs have a black exterior and a flight-twisted spindle form of a type

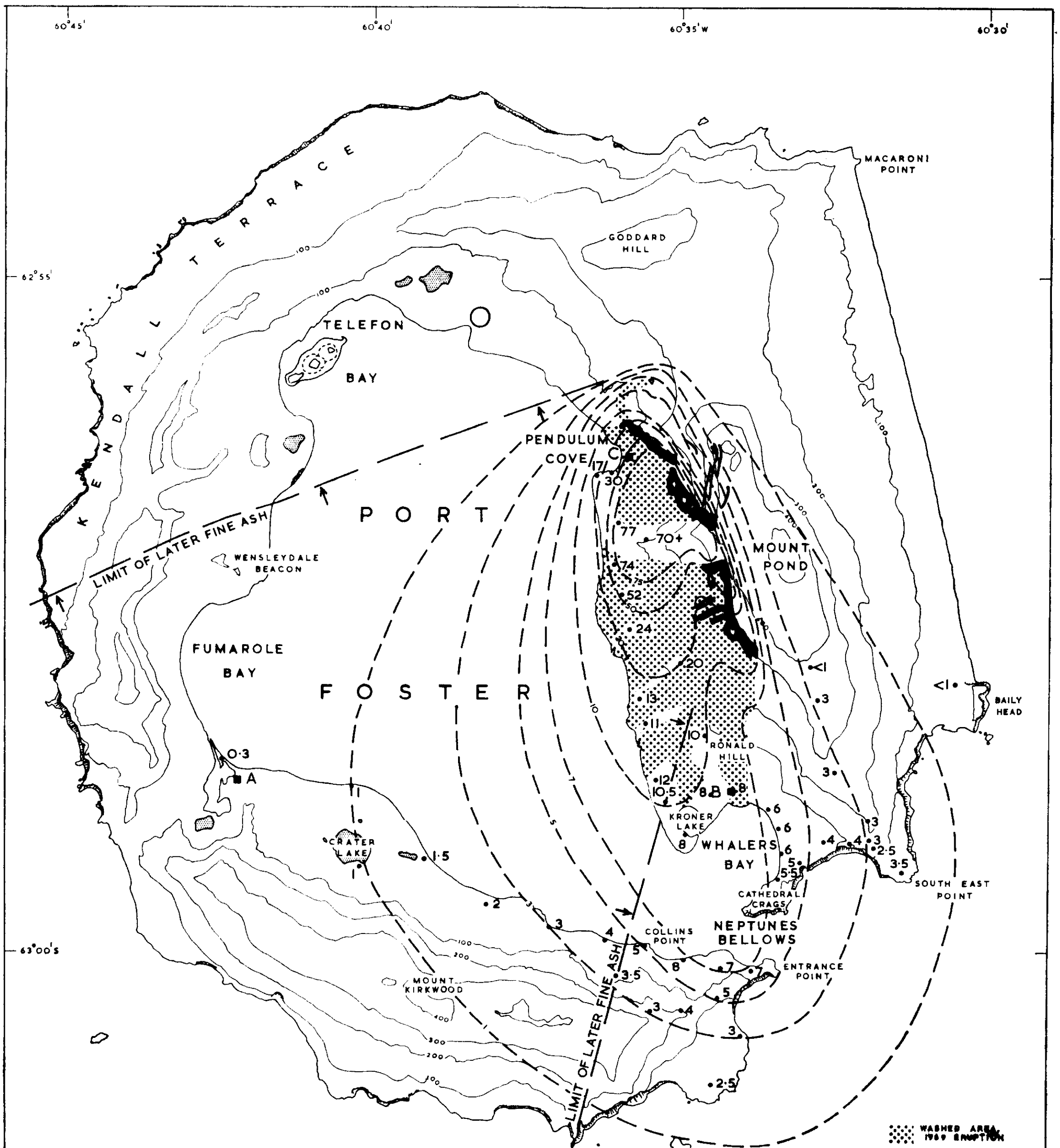

FIGURE 25

Distribution of the February 1969 pyroclasts. Measured thicknesses and isopachs are in centimetres.

not found among the 1967 products, which suggests that the 1969 magma was more fluid and more basic There are also blocks of dense brownish lava ranging from fused and streaked to friable aggregates identified as 1969 magma because of the presence of ragged clots of olivine, plagioclase and pyroxene, as found rarely in the air-fall deposits. Equally important are the deposits of red and black cinders, and scoria up to about 10 cm. in diameter, carried out by the flood of water from beneath the ice. The dense brown blocks and the red cinders are thought to be the products of the initial subglacial phase of activity.

Seen in thin section, the 1969 bombs are composed for the most part of dark scoria, in which are set sparse microlites of plagioclase, mostly oligoclase, and clinopyroxene.

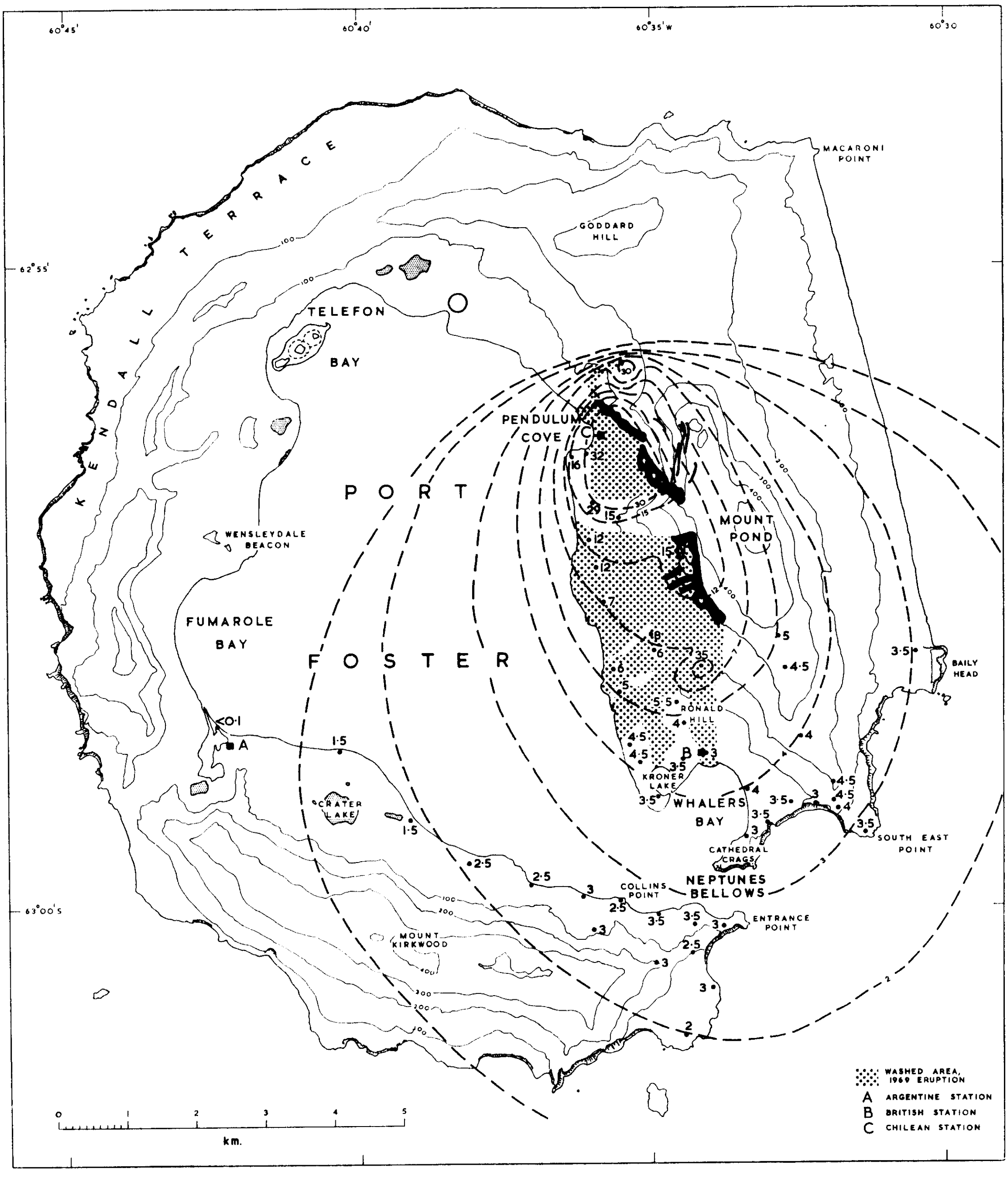

FIGURE 26

Distribution of the largest pyroclasts of the February 1969 eruption. Figures represent mean diameter (in cm.) of the five largest pyroclasts at each locality. Contours are based on the measurements shown.

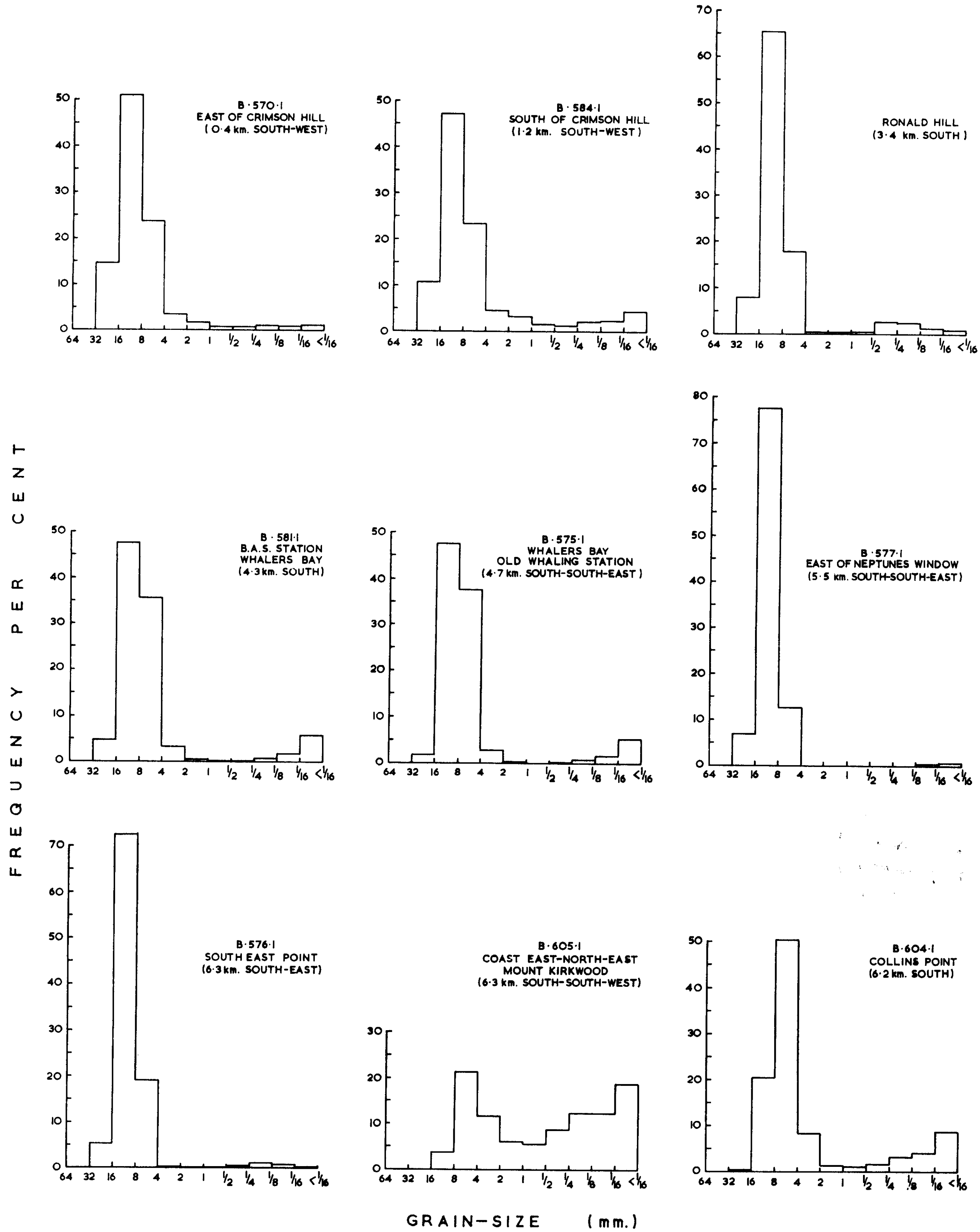

FIGURE 27

Histograms illustrating the grain-size characteristics of the 1969 pyroclast fall over Deception Island. Figures in parentheses indicate the distance from the principal vent above Pendulum Cove. Note (i) the persistence of the coarse mode (+8 −16 mm.) in all but two of the most distant samples; (ii) reproducibility of results as indicated by two samples from different parts of Whalers Bay (B.581.1 and B.575.1); (iii) the increase in the (+16 −32 mm.) fraction nearer to the probable source vent; (iv) the slight bimodal tendency in several of the samples which becomes particularly marked in B.605.1 and is the result of an additional and slightly later ash fall from vents in section C of the fissure.

1. *Distribution and size characteristics of the 1969 pyroclastics*

An isopach map for the air-fall deposits of the 1969 eruption is shown in Fig. 25. Difficulty was encountered in the washed areas, where the original thickness of the pyroclast-fall material had often been substantially reduced by erosion. So far as possible, care was taken to ensure that measurements were taken only at localities which had for one reason or another escaped the flood. The isopachs show a very distinct elongation in a north–south direction and appear to focus on section E of the fissure, which independent evidence suggests was the site of the principal eruptive vents. The zone of significant pyroclast

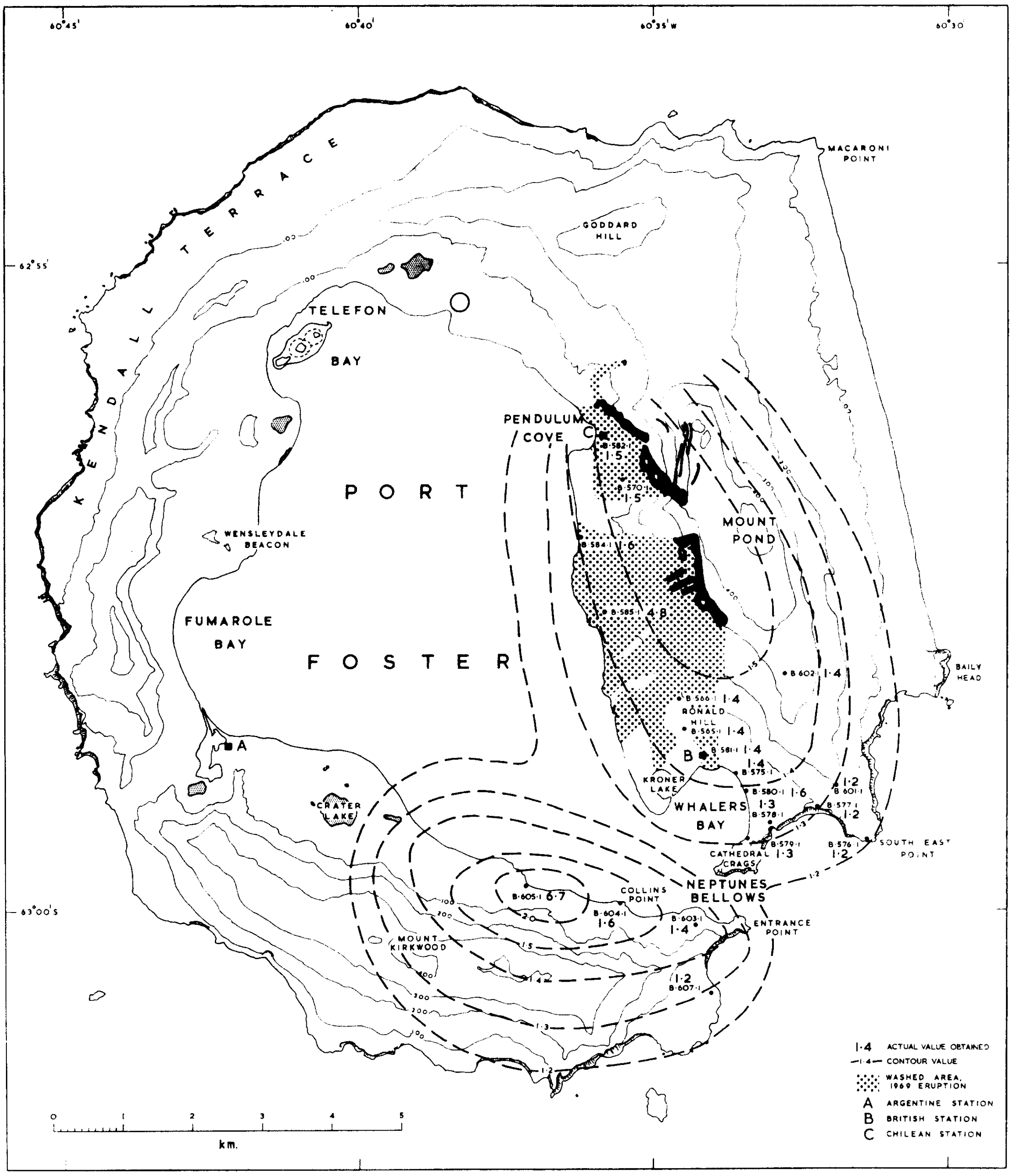

FIGURE 28

Sorting coefficients $((Q_3/Q_1)^{\frac{1}{2}})$ for the 1969 pyroclastic samples. Sorting shows a general improvement southward along the east side of the island. This simple pattern is complicated by the admixture of the late fine ash which has its maximum effect in reducing the degree of sorting on the south-west side of the island below Mount Kirkwood. The sorting "contours" are very approximate especially west of Neptunes Bellows.

fall is very restricted and was clearly controlled by a strong northerly wind, in spite of the fact that surface winds are known to have been from the east early on 21 February.

There is, however, a second unit to the 1969 deposit, which consists of a thin layer of black ash which is found coating the earlier cinders on the slopes immediately below the fissure, and was also deposited over the other side of the island between Collins Point and Wensleydale Beacon. This late ash appears to have been discharged from vents in section C of the fissure and was apparently distributed by a north-easterly wind.

The distribution of the largest pyroclasts was also mapped by averaging the mean diameters of the five largest fragments at any one locality, and the results are shown in Fig. 26. Contouring these points reveals a pattern not unlike that of the isopach map but more symmetrical about the fissure.

One of the remarkable features of the 1969 pyroclastics is the generally coarse grain-size. The modal value is either 4 or 8 mm. at every site sampled and, although the thickness of the deposits diminishes with distance from the vent, there is no obvious corresponding decrease in grain-size (Fig. 27). At Baily Head, for example, there is no meaningful thickness, since the cover is incomplete and lapilli are scattered over the surface with a spacing of about 2 m.; yet individual fragments have an average diameter of 3·5 cm.

Allied to this is the extremely well-sorted character of the great majority of the 1969 samples. The sorting coefficient for primary fall samples is mostly in the range 1·5–1·2 with a tendency for those samples more distant from the vent to be slightly better sorted than the nearer ones (Fig. 28).

2. *Chemical composition*

Chemical analyses of volcanic bombs collected from different parts of the new fissure system are shown in Table V. All are more basic than the products of the 1967 island and all but the northernmost sample are

TABLE V

CHEMICAL COMPOSITION OF 1969 BOMBS

	B.556.1	B.561.1	B.567.1	B.568.3	B.571.1	B.571.1*	B.560†
Distance from south end of fissure (km.)	0	0·5	1·0	1·3	3·0	3·0	4·4
SiO_2	56·2	55·0	55·4	55·1	54·9	54·80	59·1
TiO_2	1·97	1·95	2·03	2·04	2·07	1·95	1·73
Al_2O_3	15·9	15·6	15·8	16·0	16·1	16·83	16·0
Fe_2O_3‡	9·77	9·70	10·2	10·2	10·7	2·34	8·25
FeO	—	—	—	—	—	7·39	—
MnO	0·17	0·17	0·17	0·17	0·17	0·17	0·18
MgO	3·12	3·20	3·45	3·66	3·67	3·31	2·30
CaO	6·47	6·46	6·94	7·30	7·25	7·27	5·23
Na_2O	5·36	5·25	5·94	5·01	5·02	4·83	5·72
K_2O	0·85	0·84	0·77	0·75	0·73	0·65	1·04
H_2O+	—	—	—	—	—	0·11	—
H_2O-	—	—	—	—	—	0·06	—
P_2O_5	0·34	0·35	0·29	0·28	0·29	0·30	0·41
TOTAL	100·15	98·52	100·99	100·51	100·90	100·01	99·96

XRF analyses by I. McReath and A. Gray.
* Gravimetric/colorimetric analysis by J. Wigley.
† Mean of B.560.1 and 2.
‡ Single figure denotes Fe_2O_3 total.

more basic than the 1967 land centre. There is a significant variation in the composition of the bombs emitted from different parts of the fissure. Those from the central sections are more basic than the ones at either end. However, this could also be interpreted as meaning that where the activity was at its maximum the erupted products were more basic. In contrast, where activity was slight, at the northern ice pit (G) or the southern cirque (B), the products were more differentiated.

H. CONCLUSIONS

The linear distribution of the vents is a clear indication of the southerly extension of activity from the site of the 1967 eruptions along the eastern side of the caldera. The relation of the new vents and fissures to the caldera fault is clearly shown. The variation in composition of the ejecta argues against an origin directly from a single magma chamber; on the contrary, it suggests that separate batches or pockets of magma, differentiated to varying degrees, are migrating up the caldera fault zone. The eruption further emphasized the special hazards involved when a volcanic eruption occurs beneath a glacier.

V. THE 1970 ERUPTION

By

P. E. BAKER *and* I. MCREATH

As this eruption occurred during the southern winter, when Deception Island was unoccupied, there were no eye-witnesses to the event. Preliminary information about the eruption came from J. Croom, a U.S. exchange scientist at the Soviet station Bellingshausen on King George Island and also from the British Antarctic Survey. The information was channelled through the Smithsonian Institution Centre for Short-lived Phenomena and was released as event 70-70 on cards 990, 991 and 995. These reports stated that ash fell on the Chilean station Arturo Prat on Greenwich Island and also on Bellingshausen station early in the morning of 13 August 1970. Both stations also reported a sulphurous odour.

The seismograph at the British Antarctic Survey station on the Argentine Islands recorded an earthquake, believed to have been located near Deception Island, at 17.42 hr. G.M.T. on 12 August. According to reports from O'Higgins and Petrel stations, there was an electrical storm in the vicinity of Deception Island on the morning of 13 August 1970. Final confirmation of the eruption came from the photographic reconnaissance flight made by the Argentine Air Force on 28 August. These photographs showed that considerable changes had taken place in the Telefon Bay area and that there was a virtually complete ash cover on the inner slopes of the caldera from Goddard Hill to Telefon Ridge and also on the outer slopes across Kendall Terrace.

The ground survey, which is described here, was carried out during the period 9–22 December 1970. It was made possible through the financial support of the Royal Society and the courtesy of the Instituto Antártico Argentino and the Argentine Navy, who organized an Argentine-sponsored expedition to Deception Island on board the vessel *Zapiola*. The expedition included geologists, N. H. Fourcade and J. A. Moreno (Argentina), L. Villari (Italy) and C. H. Shultz (U.S.A.), and glaciologists, O. Orheim and T. Hughes (U.S.A.) and L. S. Goverukha (U.S.S.R.). An independent visit was also made by two Chilean geologists, F. Munizaga and H. Moreno, during the same period. Several preliminary accounts of the 1970 activity at Deception Island have already been published (e.g. Baker and McReath, 1971; González-Ferrán and others, 1971; Shultz, 1972).

A. THE 1970 VENTS

The 1970 craters lie within an arcuate zone at the foot of the caldera wall around the edge of Telefon Bay from Goddard Hill to Cross Hill (Fig. 29). There was a considerable overlap between the 1970 vents and those of the 1967 activity. The 1970 craters can conveniently be considered in three separate groups.

1. *New craters at the foot of Goddard Hill, north of the 1967 land centre*

This is a group of seven craters which are aligned roughly in an east–west direction. Their rim diameters range from about 50 to 300 m. and the maximum depth is about 150 m. Six of them cluster closely together so that their rims partly coalesce. The vents have been blasted through older pyroclastic debris and the inner slopes of the craters have a conical form quite unlike those of Telefon Bay (Plate VIId). Three of them have crater lakes at the bottom. The largest of the group is the easternmost one which has developed within a glacier and has a sheer ice wall nearly 100 m. high on its northern side. An arcuate zone around the northern periphery of this crater is intensely crevassed and its floor is covered by debris from alluvial fans. The crater of the 1967 land centre was completely obliterated by a mudflow which was apparently associated with the opening up of the new craters. The mudflow evidently occurred rather late in the eruption, since it is not covered by pyroclast fall debris. About 1 km. to the west of these craters are two much older ones, pre-dating the recent series of eruptions, whose lakes were drained as a result of the 1970 activity.

2. *Telefon Bay craters*

In this area there was a chain of vents running along the foot of the exposed part of the caldera wall (Plate VIIc). The activity was, at least to start with, dominantly submarine and it resulted in the formation

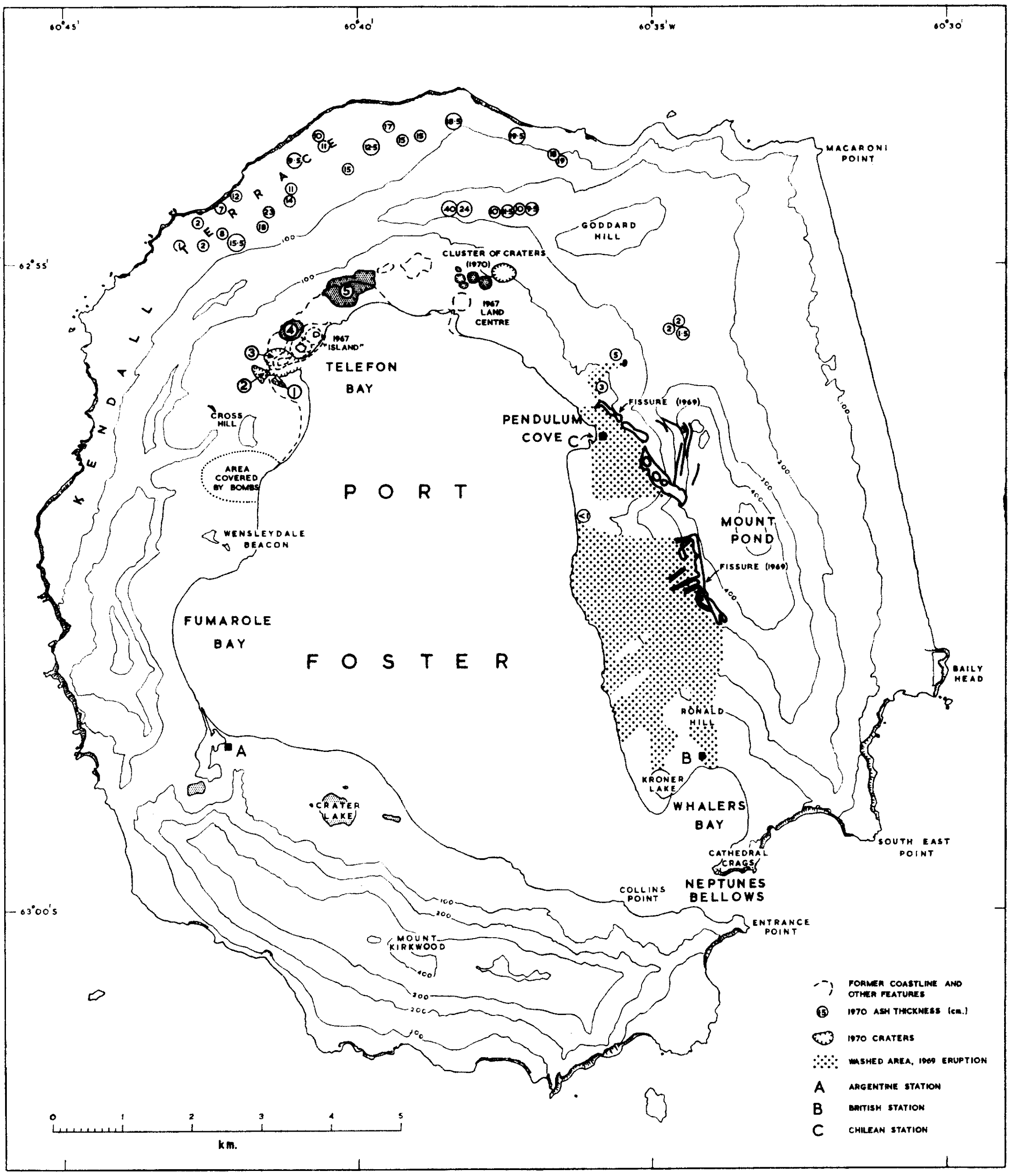

FIGURE 29

Location of the 1970 eruptive centres and thickness of pyroclastic deposits measured on Kendall Terrace and Goddard Hill (in cm.).

of a new strip of land about 1,700 m. long by 400 m. wide but nowhere more than about 12 m. a.s.l. The most obvious of the surviving craters and associated features in this zone are shown in Fig. 30, and for convenience they are numbered 1 to 5 in Fig. 35 in a clockwise sequence (Baker and McReath, 1971, p. 6). As suggested by the new topography, there must have been a number of other ephemeral craters which were destroyed or filled in by the products of the later craters. Although the 1970 activity added slightly to the total surface area of Deception Island, it also caused the partial destruction of the island which had formed in 1967 in Telefon Bay. The island was almost cut in two along its length so that only the south-eastern half remains. The surviving parts of the craters have been partially filled with new debris and then left like hanging valleys in the steep cliffs (Plate VIIb). The island was also truncated at both its north-eastern and

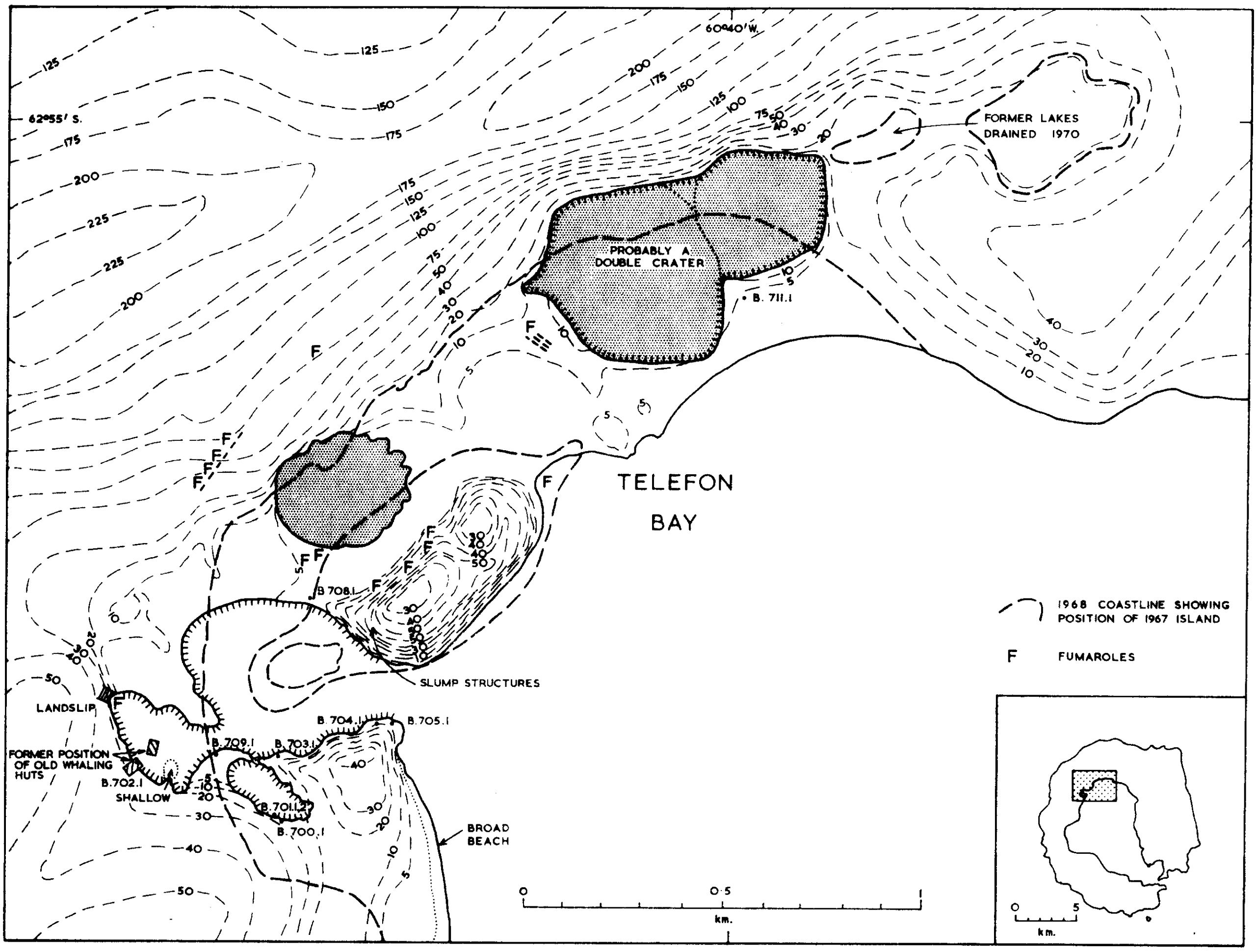

FIGURE 30

Topographical sketch map of the changes in Telefon Bay brought about by the volcanic eruption of August 1970. Contours are in metres. Sample sites are also shown, e.g. B.705.1.

south-western ends; only the long south-east-facing coast was essentially unaffected by these changes. The remnant now incongruously occupies the edge of the new strip of low land (Figs. 30 and 31, Plate VIa).

The following are notes on individual craters or features numbered in Fig. 35:

1. This is a water-filled feature which probably consists of at least two coalescing craters. It measures approximately 250 m. north-west to south-east by 100 m. north-east to south-west. On its southern side, the cliffs are about 20 m. high but elsewhere they are lower than this. At the low northern end, a narrow channel between two spits connects it with crater 3 and also permits the entry of sea-water from Port Foster (Plate VIb).

2. This is a larger but probably also a composite crater, elongated in the same direction as crater 1. It measures 300 m. north-west to south-east by a maximum of about 200 m. north-east to south-west. It tapers north-westward to a conspicuous landslip, where the sea-water is agitated by strong fumarolic activity and the temperature in December 1970 was 60° C. The water connects with crater 3 through a 50 m. channel in the south-east rim (Plate VId) and this eventually joins with Port Foster. The south-western part of crater 2 contains an area of shallow water, probably representing rims between adjacent eruptive vents. The cliffs forming the western side of crater 2 are about 25 m. high. 3 m. a.s.l. at the foot of this wall wooden posts were protruding from the pyroclastic debris. At this level the pyroclasts had clearly been re-worked as sedimentary structures such as current bedding were apparent. The posts are believed to have formed parts of the old whalers'

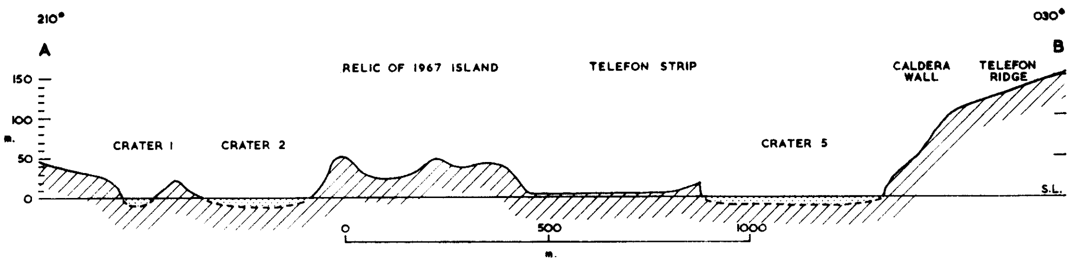

FIGURE 31

Topographical profile across the north-western part of Telefon Bay in December 1970. The vertical scale is twice the horizontal scale.

huts which are shown on the D.O.S. map (1 : 25,000, D.O.S. 310, 1960). Remnants of these huts were observed during the investigation of the 1967 eruption and it is believed that the west wall of crater 2 coincides with the position of the huts. They were situated near the bottom of a broad open valley and the re-distributed deposits seen in the new cliff probably represent older alluvial material. The former position of the two huts has been superimposed on the new topographical sketch map in Fig. 30.

3. This crater is centred on and represents a much enlarged version of what was formerly the south-westernmost crater of the 1967 island. It is sub-circular with a diameter of about 400 m., and it connects with Port Foster through a 150 m. wide channel at its eastern end. In the south-west, it connects through narrower channels with craters 1 and 2. To the north and west, the crater rim is only about 8 m. a.s.l. but the eastern channel is flanked by high cliffs, which on the northern side belong to the remnants of the 1967 island (Plate VIc).
4. This is a gently shelving depression occupied by a lake whose surface is only about 2 m. a.s.l. It almost certainly represents the site of one of the craters responsible for the partial destruction of the 1967 island. However, the crater was subsequently filled in by the products of later activity. The semi-circular structure, which lies to the east of this and to the north of the island relic (Fig. 30), is undoubtedly the remains of another eruptive centre. In December 1970, there was a fumarolic area on the gently rising ground west of crater 5. Gases were issuing from a series of north-west to south-east trending fissures in the unconsolidated pyroclastic deposits which form this new stretch of ground (Plate VIa).
5. This is by far the largest of the new craters formed in 1970. Its position partly overlaps with what was formerly Telefon Bay, but it has also cut back into Telefon Ridge (Plate VIIa). It is clearly a composite structure and was in all probability composed of two major craters, the largest of which forms the western part of the existing structure. The major axis of the composite structure is aligned in a west-south-west to east-north-east direction and has a length of about 770 m. Perpendicular to this, the shorter axes are 300 m. in the eastern half and 450 m. in the western half. The high walls of the northern side of the crater pass up into the steep slopes of Telefon Ridge, but elsewhere, especially around the southern periphery which is new land, the walls are vertical and between 2 and 12 m. high. The southernmost point of this crater is separated from Telefon Bay by a narrow isthmus of land only 9 m. wide. From the seashore the slope up to the crater is very gentle (*c.* 5°) but it steepens noticeably as the rim itself is approached. Although there is no direct connection with Port Foster, the lake of crater 5 is virtually at sea-level and the porosity of the intervening pyroclasts probably allows the tidal influence to be felt.

Steep-sided volcanic cones of the sort that formed the 1967 island are conspicuously absent from the new land area. The maar-like craters, which have almost vertical walls, are set in a generally flat and almost featureless belt of pyroclastic deposits. Approaching the large crater 5 there is only a very slight increase in gradient in the last few metres up to the lip of the crater; the profile suggests at least a marginally greater accumulation of debris nearer to the vent. The absence of volcanic cones may perhaps be attributed to the phreatic nature of the activity in which the vents were continually susceptible to the in-rush of cold sea-water. The large explosions which this induced probably resulted in a wider dispersal of pyroclastic fragments than is usual with a subaerial vent. On the other hand, contemporaneous subsidence could have counteracted any tendency for cone formation as appears to have happened at the 1967 land centre (p. 26). The maar-like craters of Telefon Bay contrast with the subaerial coalescing cones of the 1970 centres near Goddard Hill.

3. *Between Cross Hill and Wensleydale Beacon*

Fresh volcanic bombs cover an area about 1 km. across lying between Cross Hill and Wensleydale Beacon. The largest bomb measured had a mean diameter of 22 cm., which is comparable with the size of many of the larger bombs around crater 5 of the Telefon Bay land strip. There was, however, no evidence of a continuous bomb cover between the area under discussion and the southernmost part of the Telefon Bay strip. Instead, this is an isolated area of relatively large bombs, often quite densely concentrated on the surface and yet with no traces of a source crater. The distribution of these bombs and the size variations of the larger fragments are illustrated in Figs. 32 and 33. Data for the density of bomb cover over the surface and for the maximum size distribution show that both the largest bombs and the greatest concentration of fragments occur in an area about 200 m. inland and 700 m. south of the summit of Cross Hill. As shown in

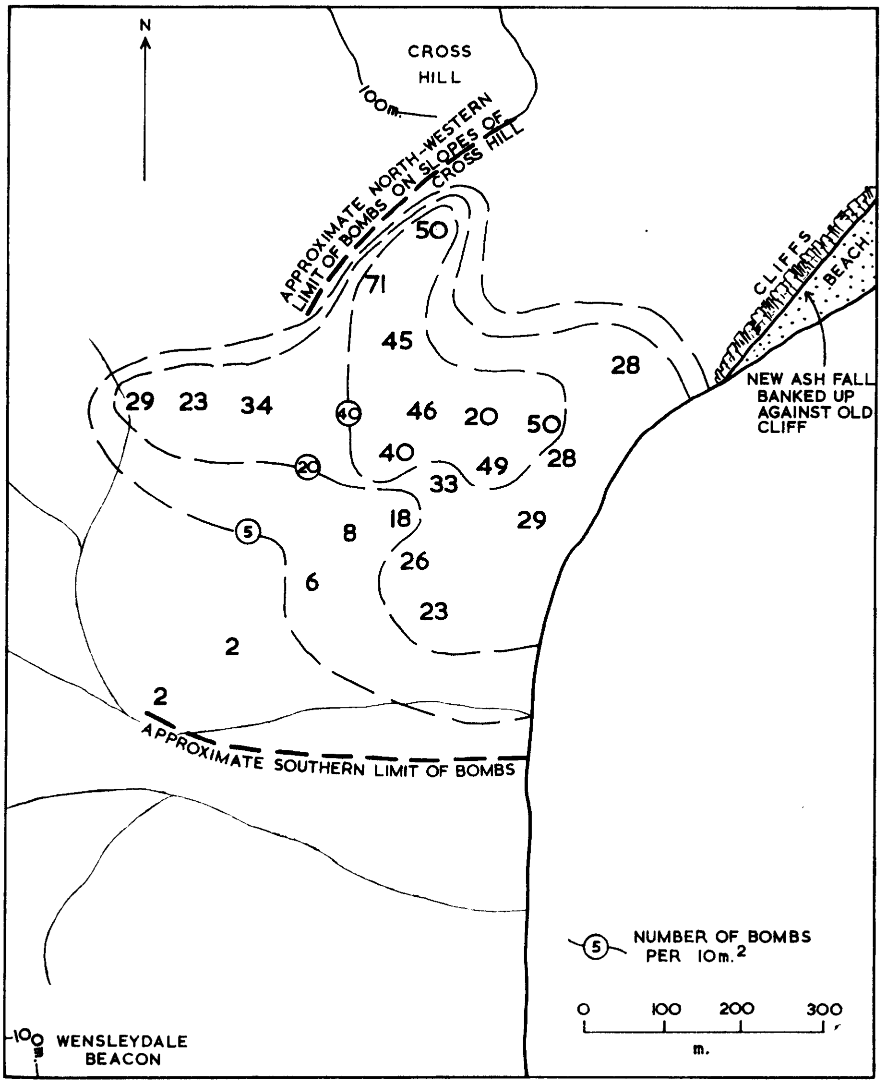

FIGURE 32

Sketch map showing the density of bomb cover over the area between Cross Hill and Wensleydale Beacon.

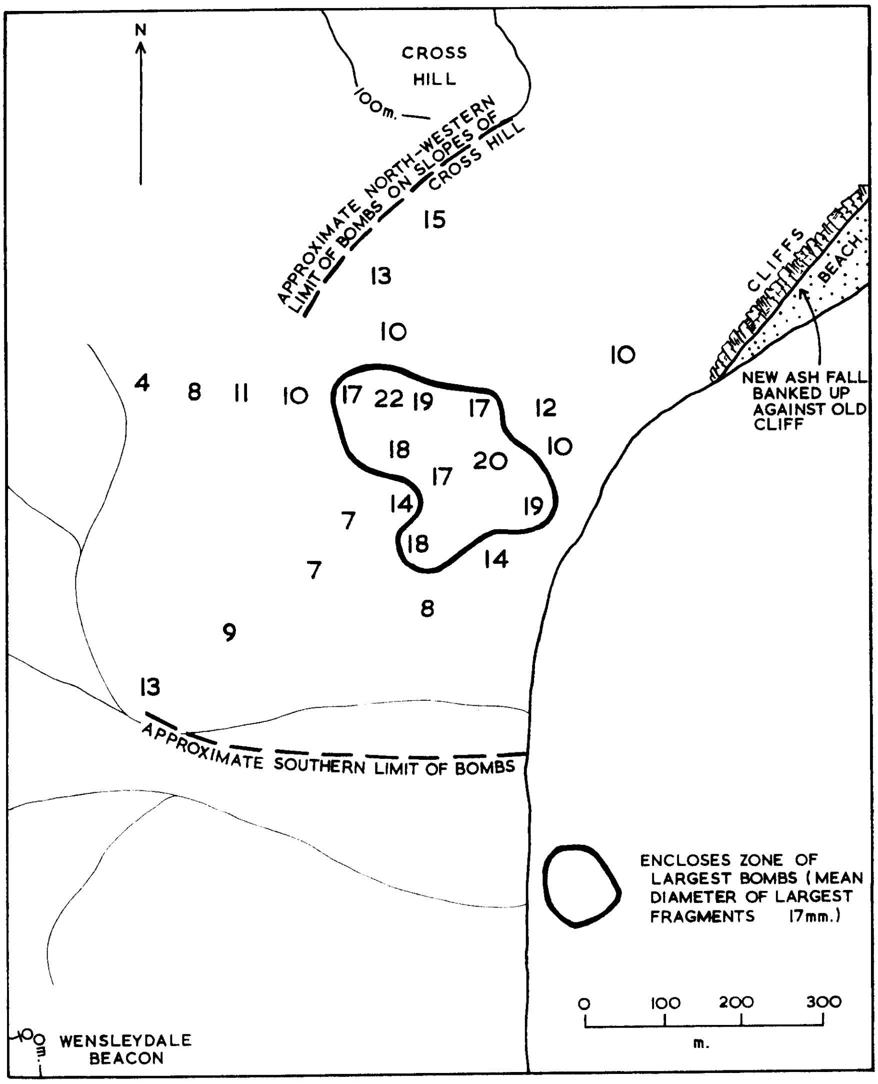

FIGURE 33

Sketch map showing the mean diameter of the largest bombs (in cm.) over the area between Cross Hill and Wensleydale Beacon.

Fig. 32, the density of bomb cover at the foot of the steep slope on the south side of Cross Hill is anomalously high; this is caused by the accumulation of bombs which have rolled down the slope.

It is concluded from this evidence that these bombs were discharged from another eruptive vent, presumed to have been located near to the shore but now concealed by Port Foster. Such a centre could be regarded as an extension of the arcuate trend to which the remainder of the 1970 vents conform.

B. THE 1970 PYROCLASTIC DEPOSITS

1. *Distribution*

As with the two preceding eruptions, the 1970 activity was entirely pyroclastic and there were no lava flows. Particular difficulty was encountered in compiling an isopach map for these deposits. The new vents were all located at the northern end of Deception Island and the ejecta had been carried in a northerly direction. This severely limited the area over which the thickness of the new ash fall could be measured (Fig. 29). A further complication was that the deposits had obviously been emitted from a large number of quite widely spaced vents.

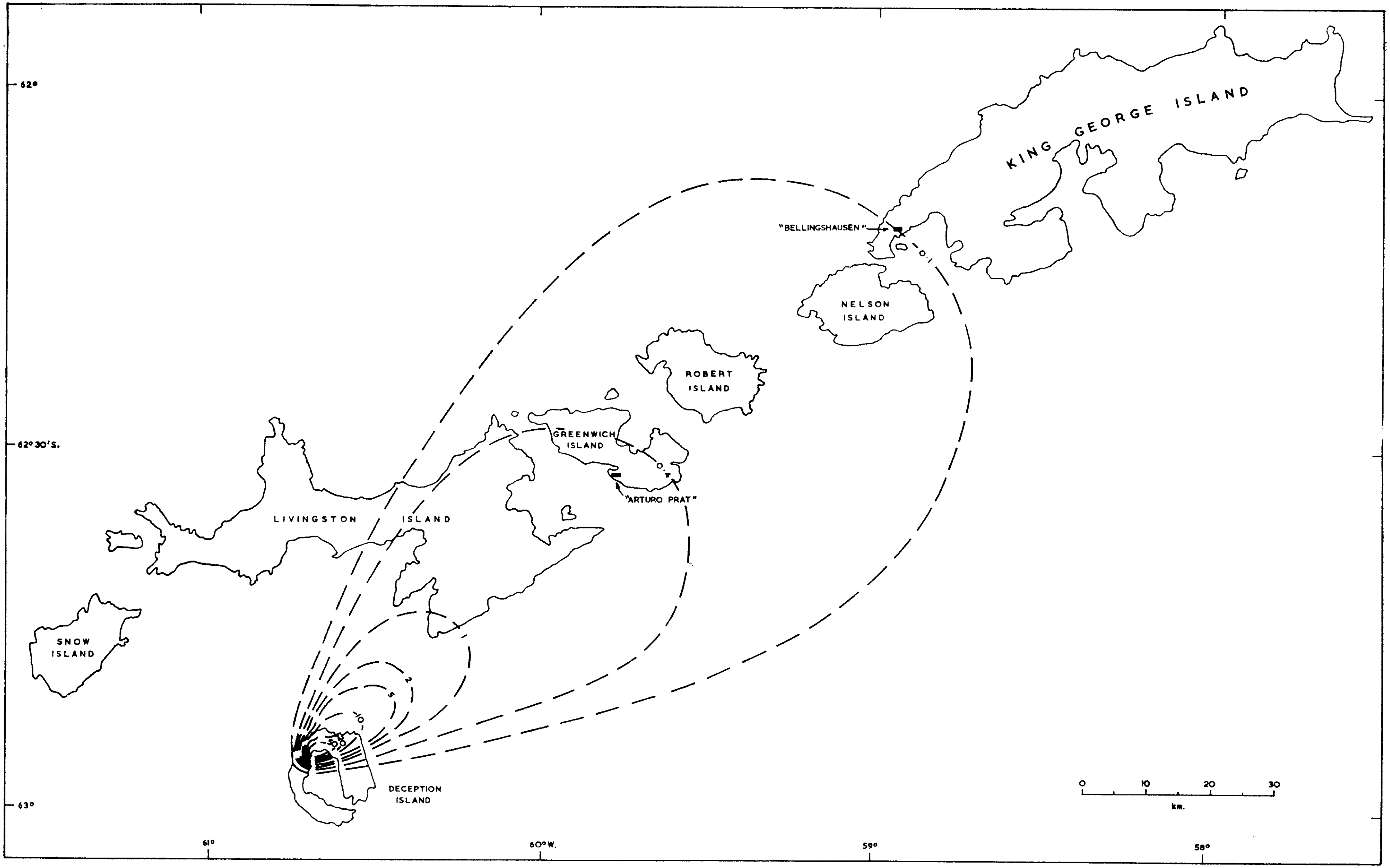

FIGURE 34

Isopachs (in cm.) for the 1970 pyroclastic deposits of Deception Island.

Detailed thickness determinations on Deception Island showed that the measurable ash fall was confined to a northerly sector of the island between the central part of Kendall Terrace and Pendulum Cove. South of Wensleydale Beacon and Pendulum Cove the ash fall was negligible. For instance, glaciologists working on Mount Kirkwood failed to recognize an ash layer which they could attribute to the 1970 eruption.

Since, on this occasion, a very large proportion of the ash fell outside Deception Island, the form of the isopachs in Fig. 34 is partly controlled by the evidence obtained from other islands in the South Shetland Islands group. For example, a sharp boundary between ash-covered and ash-free snow could be seen trending across the south-eastern part of Livingston Island. It is also known that approximately 4 mm. of dust fell on Arturo Prat station, Greenwich Island, and about 1 mm. on Bellingshausen station, King George Island.

The evidence of thickness variations and distribution derived from Deception Island and adjacent islands is thus consistent with an isopach pattern extending north-eastward along the axis of the South Shetland Islands. Ash from the 1970 eruption was thus distributed under the influence of a south-westerly wind, which carried most of the material out over the caldera rim between Goddard Hill and Telefon Ridge into Bransfield Strait.

The 1970–71 seasonal melt was unusually early and abnormally pronounced on Deception Island, causing widespread re-distribution of the pyroclast-fall deposits by small streams and mudflows (Plate IXd). Re-working of the pyroclast deposits by long-shore drift was responsible for the formation of the new wide beaches north-east of Cross Hill (Plate VIb). However, towards the eastern end of Kendall Terrace, the thicker blanker of ash provided effective insulation and a number of reliable ash thicknesses with unambiguous snow bases were obtained in this area. Quite apart from the problem of re-distribution, any individual ash sample is likely to be a composite one, incorporating material emitted from more than one of the numerous 1970 vents.

2. *Size analyses*

For the reasons outlined above, grain-size studies were confined to the surface bombs of the Telefon Bay strip and the area between Cross Hill and Wensleydale Beacon. Even so, it is apparent on the Telefon Bay strip that these bombs were emitted from different craters. Fig. 35 shows the mean diameter of the largest bombs collected at a number of localities in this area. The size value recorded on this map is an average of three mutually perpendicular axes measured on the largest bomb obtainable at a particular site (the site is a circle 10 m. in diameter). The values for the average diameters are plotted graphically, having been projected on to a single line of section A–B along the length of the Telefon Bay strip. The distribution of

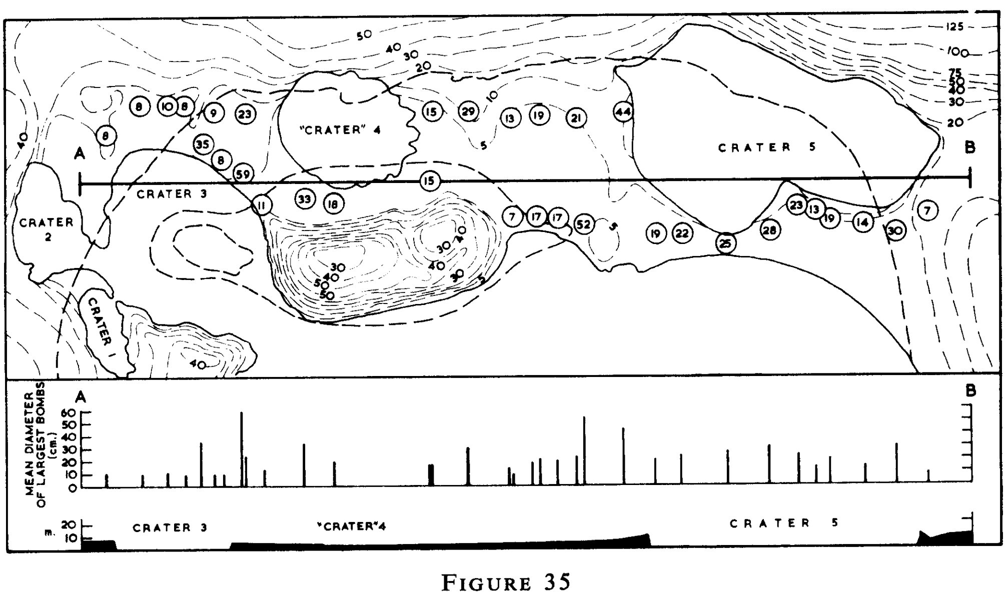

FIGURE 35

Mean diameter of largest bombs (in cm.) at individual localities shown by circled figures. These figures are projected on to the line of section A–B to illustrate the distribution of largest bombs across the new Telefon Bay strip.

TABLE VI

CHEMICAL ANALYSES OF BOMBS EMITTED DURING THE 1970 ERUPTION

	B.701.2	B.702.1	B.704.1	B.711.1	B.710.1	B.707.1
SiO_2	59·3	59·5	59·5	59·3	58·7	58·0
TiO_2	1·61	1·62	1·65	1·75	1·60	1·91
Al_2O_3	15·8	16·0	16·1	15·9	15·8	15·9
Fe_2O_3	2·24	2·31	2·59	2·89	2·45	2·38
FeO	5·40	5·33	5·09	5·13	5·18	6·00
MnO	0·18	0·17	0·17	0·18	0·17	0·18
MgO	2·34	2·42	2·39	2·46	2·29	2·72
CaO	5·06	5·02	5·17	5·26	5·00	5·73
Na_2O	5·92	6·17	5·91	5·90	5·89	5·46
K_2O	1·08	1·09	1·08	1·03	1·09	0·98
H_2O+	0·47	0·49	0·55	0·11	0·50	0·37
P_2O_5	0·41	0·40	0·42	0·41	0·42	0·37
TOTAL	99·81	100·52	100·62	100·32	99·09	100·00
			C.I.P.W. NORMS			
Qz	6·90	5·75	7·23	7·28	6·83	6·53
Or	6·38	6·44	6·38	6·09	6·44	5·79
Ab	50·09	52·20	50·00	49·92	49·83	46·20
An	13·36	12·75	14·22	13·87	13·46	15·99
Di	7·50	7·87	7·14	7·82	7·09	8·27
Hy	7·86	7·66	7·24	6·77	7·36	8·92
Mt	3·25	3·35	3·75	4·19	3·55	3·45
Il	3·06	3·08	3·13	3·32	3·04	3·63
Ap	0·97	0·94	0·99	0·97	0·99	0·87
H_2O	0·45	0·47	0·53	0·09	0·48	0·35
Diff. index	63	64	64	63	63	59

B.701.2 South side of crater 1.
B.702.1 South-west side of crater 2.
B.704.1 South side of crater 3.
B.711.1 South-east side of crater 5.
B.710.1 South side of Cross Hill.
B.707.1 100 m. west of largest new crater; north of land centre,

bomb sizes shows two maxima, one between craters 3 and 4 and the other on the western side of the composite crater 5. The size-distribution data for the enigmatic zone between Cross Hill and Wensleydale Beacon (Fig. 33) suggest an independent origin from a vent in Port Foster, as discussed on p. 57.

3. *Composition*

The 1970 bombs are composed largely of dark scoriaceous glass and plagioclase microlites with occasional microphenocrysts of plagioclase, clinopyroxene, magnetite and very occasionally small rounded olivines (Plate Xe and f). In appearance, the bombs show a closer resemblance to the rough crusty bombs of the 1967 island than they do to the well-formed spindle bombs erupted from the 1969 fissure.

The chemical analyses of the 1970 bombs (Table VI) do not show such a wide compositional spread as did the 1969 bombs. All the analysed samples lie within the range 58·0–59·5 per cent SiO_2 and have a differentiation index of between 59 and 64. Their normative plagioclase is in the oligoclase range and they are perhaps best regarded as a type of mugearite. There are some significant differences between the samples; for instance, products from vents close to the 1967 land centre are more basic in composition than those near the site of the 1967 island (Table VIII). All of these analyses fall between the compositions for the 1967 land centre and those for the 1967 island and are more siliceous than all but the northernmost of the 1969 bombs.

4. *Accessory blocks*

Associated with the primary magmatic material in the Telefon Bay area, and especially common around the group of craters to the south-west of the 1967 island, are accessory blocks which in order of abundance are:

i. Grey aphyric lava apparently similar to types present on Stonethrow and Telefon Ridges.
ii. Yellow tuffs similar to those which form the outer cliffs of Deception Island.
iii. A greenish tuff which varies from coarse and agglomeratic to fine-grained and is a type so far unrecorded on the island.
iv. A reddish vesicular lava similar to the lavas of the "Whalers Bay Group".
v. A coarse-grained plagioclase-pyroxene xenolith, which was found in one large block of dark grey lava. This xenolith is discussed further in the section on geochemistry (p. 69).

VI. GEOCHEMISTRY OF DECEPTION ISLAND

By

I. McREATH

HAWKES (1961) considered that the Deception Island suite represents a local sodic deviation from the normal basalt–andesite–dacite–rhyolite association of the circum-oceanic regions. At the time that report was written the high-sodium, high-alumina basalt type found at Deception Island was uncommon in world-wide Tertiary or Recent volcanism, but it is now apparent that this basalt type is characteristic of the Recent province north-west of the Antarctic Peninsula (González-Ferrán and Katsui, 1971). However, the total suite remains unusual.

Since Hawkes's report was published, it has also become evident that in circum-oceanic regions the more normal progression in chemical character, as the distance of the volcanic centre from the trench increases, is towards enrichment in K_2O (Dickinson and Hatherton, 1967) and towards a silica-undersaturated alkaline character (Kuno, 1966).

The aim of the present study was to test the validity of Hawkes's views and to attempt to explain the genesis of the unusual basalt type and the subsequent evolution of the suite.

A. SETTING

The South Shetland Islands have exhibited a number of phases of igneous activity from the Jurassic to mid-Tertiary times. The composition of the products (Adie, 1964) suggests that this area has formed the boundary between two converging lithospheric plates during that period. A recent geophysical reconstruction of the area implies that the most recent period of underthrusting may have continued until about 10 m. yr. ago (Barker and Griffiths, 1972). It seems likely, therefore, that frictional heat generated at the interface between underthrust and overthrust plates (Minear and Toksoz, 1970) may still be in the process of dissipating by upward conduction.

Bransfield Strait and the associated trough are extensional grabens, whose north-western fault boundaries coincide with a number of topographical highs of which Deception Island is the sole large subaerial feature to the south-east and Penguin Island (of similar basalt type to that of Deception Island) is a smaller feature to the north-west. This lineation continues eastward to the South Orkney Islands; it is of interest that the granite of Cornwallis Island (Rex and Baker, 1973) shows a high Na_2O/K_2O ratio, which is the most prominent feature of the Deception Island suite.

The Drake Passage area appears to be underlain by normal oceanic crust (Barker and Griffiths, 1972) but the structure beneath the South Shetland Islands is more complex. At Deception Island, both gravity (Davey, 1971) and seismic (Ashcroft, 1972) studies have suggested the presence of an 8–10 km. thickness of acid or intermediate volcanic rocks underlain by a similar thickness of basic rocks, with the Mohorovičić discontinuity at about 20 km.

B. PREVIOUS WORK

The main features of the mineralogy and petrology have been described in detail by Hawkes (1961) and González-Ferrán and Katsui (1970). Except for the recognition that anorthoclase is a phenocrystic constituent in some of the acid rocks, little was added to the overall picture, presented by these authors, during the course of the present work. Table VII gives a summary.

Feldspars in some of the basalts are highly calcic with core compositions reaching An_{90-92}. These feldspars are frequently associated with an olivine of composition Fo_{70-80} (Plate XIa). Such an association has been considered by Lewis (1971) to be characteristic of the calc-alkaline suite. Later feldspars become more sodic than is usually found in the calc-alkaline suite; for example, at Deception Island the andesites have feldspars whose cores are generally more sodic than An_{60}, whilst in calc-alkaline andesites core compositions are in the range An_{65-85} with an average of about An_{70}.

Table VIII
PREVIOUS CHEMICAL ANALYSES OF ROCKS FROM DECEPTION ISLAND

	1	2	3	4	5	6	7	8	9	10	11	12	13	14	15	16
SiO_2	49·72	49·84	50·18	50·63	50·65	51·81	52·42	52·93	52·96	53·10	53·50	54·22	54·48	54·9	56·89	57·2
TiO_2	1·50	1·32	1·54	1·67	1·78	1·63	2·26	2·29	1·78	1·81	1·65	1·88	1·83	2·07	1·79	1·89
Al_2O_3	17·91	19·37	17·75	17·59	17·67	17·04	16·31	15·86	14·89	17·34	17·62	15·61	17·15	16·1	16·07	15·8
Fe_2O_3	3·04	3·42	3·56	2·38	2·50	2·16	2·72	2·01	6·33	2·42	2·58	2·37	2·77	2·98	1·81	2·82
FeO	6·17	3·69	5·79	6·34	6·14	6·58	8·24	8·90	4·69	6·97	6·07	7·93	6·97	6·95	7·08	5·67
MnO	0·18	—	0·14	0·17	0·16	0·11	0·30	0·11	0·15	—	—	0·17	—	0·18	0·08	0·18
MgO	6·10	4·71	6·68	5·56	5·82	5·22	3·60	3·63	4·68	3·34	4·39	3·63	2·86	3·67	2·79	2·73
CaO	10·64	12·35	9·19	10·22	10·14	9·91	7·64	7·60	8·65	7·56	9·22	7·82	6·05	7·25	5·89	5·76
Na_2O	3·77	2·50	3·92	4·12	4·10	4·23	5·25	5·03	4·38	4·45	4·15	5·00	4·45	5·02*	5·89	5·58
K_2O	0·50	0·87	0·49	0·44	0·52	0·55	0·61	0·64	0·60	0·81	0·75	0·85	0·91	0·73	0·94	0·96
P_2O_5	0·33	0·11	0·34	0·29	0·30	0·29	0·48	0·35	0·34	0·29	0·36	0·27	0·32	0·29	0·21	0·36
H_2O+	0·22	} 1·79	0·22	0·34	0·11	0·25	0·42	0·42	0·26	0·84	—	0·19	0·96	0·09	0·56	0·23
H_2O-	0·12		0·18	0·14	0·04	0·04	0·11	0·04	0·04	—	—	0·23	—	†	0·08	†
S	—	—	—	—	—	—	—	—	—	—	—	—	—	—	0·06	—
Total	100·20	99·97	99·98	99·89	99·93	99·82	100·36	99·75	99·75	98·96	100·29	100·17	98·75	100·20	100·14	99·18

	17	18	19	20	21	22	23	24	25	26	27	28	29	30	31	32
SiO_2	57·45	58·0	58·06	58·7	59·3	59·3	59·5	59·5	59·51	60·62	61·0	66·21	67·40	67·71	68·28	69·01
TiO_2	1·91	1·91	2·02	1·60	1·75	1·61	1·62	1·65	1·45	1·51	1·26	0·62	0·60	1·00	0·70	0·58
Al_2O_3	15·88	15·9	15·82	15·8	15·9	15·8	16·0	16·1	15·32	16·22	15·7	15·52	15·41	14·65	15·95	14·21
Fe_2O_3	2·97	2·38	1·68	2·45	2·89	2·24	2·31	2·59	1·50	1·76	1·19	1·02	1·16	1·59	2·00	2·33
FeO	5·12	6·00	6·50	5·18	2·13	5·40	5·33	5·09	5·08	5·67	5·50	4·13	3·81	3·29	1·82	2·89
MnO	0·16	0·18	0·18	0·17	0·18	0·18	0·17	0·17	0·16	—	0·17	0·17	0·13	—	—	—
MgO	2·78	2·72	3·13	2·29	2·46	2·34	2·42	2·39	2·14	1·62	1·71	0·63	0·36	0·85	0·09	0·62
CaO	5·42	5·73	5·40	5·00	5·26	5·06	5·02	5·17	3·93	4·18	4·11	2·40	1·88	2·34	1·78	2·11
Na_2O	6·50	5·46	6·40	5·89	5·90	5·92	6·17	5·91	7·00	6·25	6·23*	6·87	7·27	6·09	7·03	6·30
K_2O	1·00	0·98	1·03	1·09	1·03	1·08	1·09	1·08	1·20	1·20	1·23	1·71	1·99	1·99	1·75	2·07
P_2O_5	0·46	0·37	0·40	0·42	0·41	0·41	0·40	0·42	0·44	0·24	0·42	0·21	0·21	0·16	0·07	0·12
H_2O+	0·54	0·37	1·00	0·50	0·11	0·47	0·49	0·55	1·98	} 0·56	0·18	0·21	0·07	} 0·16	} 0·24	} 0·09
H_2O-	0·08	†	0·08	†	†	†	†	†	0·24		†	0·18	0·04			
S	—	—	—	—	—	—	—	—	—	—	—	—	—	—	—	—
Total	100·27	100·00	100·50	99·09	100·32	99·81	100·52	100·62	99·98	99·86	98·70	99·94	100·83	99·83	99·71	100·23

* Analysed by F. Buckley.
† Samples dried at 110° C.

1. OG.232 Almost aphyric basaltic andesite with olivine; north of Cross Hill (González-Ferrán and Katsui, 1971).
2. Doleritic basalt (Gourdon, 1914).
3. OG.229 Basaltic andesite with olivine; west coast (González-Ferrán and Katsui, 1971).
4. OG.356 Aphyric basaltic andesite; Macaroni Point (González-Ferrán and Katsui, 1971).
5. B.163.1 Olivine-basalt; Stonethrow Ridge (Hawkes, 1961).
6. B.103.3 Olivine-basalt; near Collins Point (Hawkes, 1961).
7. OG.244 Basaltic andesite with olivine; Pendulum Cove (González-Ferrán and Katsui, 1971).
8. Basaltic andesite (Barth and Holmsen, 1939).
9. B.213.3 Olivine-basalt; Crater Lake (Hawkes, 1961).
10. Pyroclastic deposits of "1917 eruption" (Orheim, 1971c).
11. Labradorite-basalt (Gourdon, 1914).
12. OG.354 Aphyric andesite; north of Mount Pond (González-Ferrán and Katsui, 1971).
13. Pyroclastic deposits of "1912 eruption" (Orheim, 1971c).
14. B.571.1 "Basaltic andesite"; 1969 eruption (Baker and McReath, 1971). (See also Table X.)
15. Two-pyroxene andesite (bandaite) (Barth and Holmsen, 1939).
16. B.428.1 Andesitic bomb; 1967 eruption (Baker and McReath, 1971). (See also Table X.)
17. D-15b Andesitic bomb; 1967 eruption (Valenzuela and others, 1970).
18. B.707.1 Andesitic bomb; 1970 eruption (Baker and McReath, 1971). (See also Table X.)
19. D-7 Andesitic pumice; 1967 eruption (Valenzuela and others, 1970).
20. B.710.1 Andesitic bomb; 1970 eruption (Baker and McReath, 1971). (See also Table VI.)
21. B.711.1 Andesitic bomb; 1970 eruption (Baker and McReath, 1971). (See also Table X.)
22. B.701.2 Andesitic bomb; 1970 eruption (Baker and McReath, 1971). (See also Table VI.)
23. B.702.1 Andesitic bomb; 1970 eruption (Baker and McReath, 1971). (See also Table VI.)
24. B.704.1 Andesitic bomb; 1970 eruption (Baker and McReath, 1971). (See also Table VI.)
25. D-1 Andesitic ash; 1967 eruption (Valenzuela and others, 1970).
26. Andesite (Gourdon, 1914).
27. B.276.1 Andesitic bomb; 1967 eruption (Baker and McReath, 1971). (See also Table X).
28. OG.226 Glassy pyroxene-dacite; Cross Hill (González-Ferrán and Katsui, 1971).
29. B.111.4 Oligoclase-andesite; west-north-west of Collins Point (Hawkes, 1961).
30. Trachyandesite (Gourdon, 1914).
31. Tridymite-santorinite (Barth and Holmsen, 1939).
32. Trachyandesite (Gourdon, 1914).

TABLE VII
MINERALOGY OF THE DECEPTION ISLAND VOLCANIC ROCKS

Type	*Occurrence*	*Texture*	*Mineralogy*
Basalt—olivine normative	All episodes except most recent	Usually weakly porphyritic to aphyric Intersertal or intergranular, rarely hyaline groundmasses	Phenocrysts in order of abundance: Feldspar cores An_{80-90}, rims An_{35-40} Olivine Fo_{70-82}, usually about Fo_{75-77} Clinopyroxene diopsidic augite, sub-calcic augite, pigeonite (rare) Orthopyroxene usually absent Opaque minerals usually absent Groundmass in usual order of abundance: Feldspar An_{40-60} Clinopyroxene: augite, sub-calcic augite, pigeonite Opaque ores Olivine K-feldspar, biotite (rare)
Basalt—quartz normative	All episodes except most recent	Intersertal or intergranular, rarely hyaline groundmasses	As above, but olivine is a minor phenocryst constituent and absent in the groundmass
Basaltic andesite	All episodes	Intersertal or intergranular, rarely hyaline groundmasses. Pyroclasts have glassy groundmasses	Feldspar phenocrysts are An <60 and generally <50 Olivine generally absent Hypersthene *c.* En_{60}
Andesite—acid andesite	Recent episodes particularly intra-caldera	Moderately porphyritic	Phenocrysts are largely feldspar An_{30-40} Microphenocrysts of olivine Fo_{40-50}, orthopyroxene *c.* En_{60}
Dacite	Recent episodes intra-caldera	Porphyritic with trachytic fine-grained or hyaline groundmasses	Phenocrysts are largely feldspar, albite-oligoclase. Anorthoclase present Microphenocrysts of orthopyroxene, olivine Fo_{20-15}, opaque ore minerals Groundmass of albite-oligoclase, K-feldspar and glass, heavily dusted with opaque minerals

The ferromagnesian assemblage follows a course of compositional evolution similar to that found during strong tholeiitic fractionation of basalt magma. The replacement of olivine by orthopyroxene in the middle members, and the re-appearance of moderately to highly fayalitic olivines in the later members, corresponds closely to the sequence found in the Skaergaard intrusion by Wager and Deer (1939), but at Deception Island magnetite does not become more than a trace phenocrystic constituent.

About 30 major-element analyses have been published (Table VIII) which show a series from high-alumina olivine-tholeiite to quartz-saturated intermediate and acid rocks, maintaining a high Na_2O content throughout. A conspicuous silica gap separates andesites (*c.* 61 per cent SiO_2) from the more acid rocks (>66 per cent SiO_2). Overall, the suite shows moderate iron enrichment. Within the scatter at the basic end, there is some indication that two basalt series may be present.

C. ANALYSED SPECIMENS

Whole-rock samples were selected to cover the total history of volcanic evolution with the exception of the earliest tuffs, which are the subject of another section of this report (p. 14). Localities and approximate stratigraphical positions are summarized in Table IX. As in previous studies, considerable emphasis has been placed upon *in situ* lavas, although these may represent a small proportion of the subaerial volcano.

The choice of samples for the study of early formed minerals is limited. Minerals were separated by

TABLE IX

STRATIGRAPHICAL COLUMN AND LOCALITIES OF ANALYSED SPECIMENS FROM DECEPTION ISLAND

Unit, episode	*Locality*	*Samples analysed*		*Number in Table X*
1970 eruption	"Land centre" area	B.707.1	Andesitic bomb	18
	"Island centre" area	B.711.1	Andesitic bomb	19
1969 eruption	Mount Pond	B.571.1	Basaltic andesite bomb	15
		B.556.1	Andesitic bomb	16
1967 eruption	"Island centre"	B.276.1	Andesitic bomb	20
		B.317.1	Dacitic pumice	23
	"Land centre"	B.428.1	Andesitic bomb	17
1842 (?) eruption	Mount Kirkwood	B.416.1	Almost aphyric basalt	5
		B.417.1	Aphyric basaltic andesite	13
Undifferentiated post-caldera	Cross Hill	B.429.2	Porphyritic dacite	22
	Collins Point	B.431.1	Dacite	21
	Kendall Terrace	B.352.3	Almost aphyric basalt	1
Caldera collapse				
Commencement of caldera collapse	Fumarole Bay	B.413.4	Yellow tuff	10
		B.413.5	Grey tuff	9
	Cathedral Crags	B.357.1	Porphyritic basalt dyke	6
		B.420.1	Pumiceous tuff	7
Secondary centres	Macaroni Point	B.422.1	Yellow tuff	4
	Baily Head	B.405.1	Yellow tuff	12
		B.403.1	Almost aphyric basalt	8
Strato-volcano	Stonethrow and Telefon Ridges	B.309.1	Porphyritic basalt	11
		B.311.1	Scoriaceous basaltic andesite	14
	Neptunes Bellows	B.432.1	Almost aphyric basalt	2
	Argentine station	B.408.4	Almost aphyric basalt	3
Outer coast tuff	Cliffs of outer coast			

conventional means from one basalt (B.411.2), whose phenocryst mineralogy is fairly representative of that found in other basalts, and from two blocks (B.304.1 and 712.1) whose textures suggest an origin by crystal accumulation.

Samples of coarse-grained intermediate and acid plutonic blocks, thought to have originated from the sub-volcanic basement, were studied in order to evaluate their relationships to the intermediate and acid extrusive rocks, and to other intrusive bodies in this area.

D. ANALYTICAL METHODS

Major elements were analysed by X-ray fluorescence spectrometry using a simple fusion technique described by Padfield and Gray (1971), except for Na_2O, FeO and $H_2O\pm$, which were analysed by conventional chemical methods. Trace elements (Rb, Sr, Y, Zr and Ni) were determined by X-ray fluorescence in whole-rock samples, and the remaining elements in whole rocks and all elements in separated minerals were analysed by optical spectrography using the method described by Rooke and Fisher (1962). Details of the performance usually expected may be found in the references. A few semi-quantitative and qualitative electron-microprobe scans were made on selected mineral phases.

Initial strontium isotope ratios were determined by mass spectrometry, using prior ion-exchange separation, which is a standard technique at the University of Leeds. It is assumed that the Deception Island volcano is a relatively young structure and that no correction for Rb decay since formation is necessary.

E. Whole-rock Analyses

1. *Major elements*

The most significant new feature revealed in this study is the demonstration of the co-existence of two basalt types (Table X) distinguished by differences in Al_2O_3 and total iron oxide contents. These distinctions are most readily seen on the variation diagrams (Figs. 36 and 37). The two types are frequently intimately associated in space (e.g. at Baily Head: B.403.1 and 405.1). Types transitional between the extremes are also present. Since many of the basalts are either almost or completely aphyric, the differences in composition must be due to differences in magma source or history (Plate XIb–d).

The tuffs commonly have a 3–15 per cent total-water content. When the analyses are corrected to a water-free basis (Table X, Nos. 4, 7, 9, 10 and 12), they may also be separated into high- or low-alumina types. While the tuffs are not completely aphyric, their analyses plot close to the "liquid lines of descent" defined by the aphyric basalts.

The distinction between high-alumina and high-iron types becomes blurred at intermediate compositions. In the intermediate and acid ranges, few samples are aphyric but the scatter on the variation diagrams is small except for Na_2O. In these rocks the principal phenocryst phase is a plagioclase, usually more sodic than An_{65}, which shows considerable variation in modal proportions and may explain this scatter. When compared with the other acid rocks, the most acid specimen (B.317.1; Table X, No. 23) appears to be anomalous in a number of respects, particularly in the low abundances of the alkali elements. Since specimen B.317.1 is relatively aphyric, the "anomalies" may be in part a reflection of the porphyritic nature of the other acid rocks (Plates XIe and f, and XIIa and b), which contain albite-oligoclase and anorthoclase as the principal phenocrysts. Other features of specimen B.317.1, such as the lower concentrations of iron and TiO_2, may be the result of further fractionation of the ferromagnesian minerals.

The gap in silica content between the andesites and dacites has only been marginally reduced. The gap is undoubtedly real and is potentially a major obstacle to any model of magma evolution based upon fractional crystallization. For most elements, the acid rock compositions (except for that of specimen B.317.1) appear to lie on direct continuations of the main trends, although for Na_2O there is a change in rate of increase with increasing SiO_2 content.

The FMA diagram (Fig. 37) confirms the general trend of iron enrichment observed by other authors. but the continuity of the trend is dependent on a few points which lie between the area towards the "M" apex (occupied by high-alumina basalts) and the origin of the main trend from high-iron basalts to dacites. This trend shows only minor iron enrichment.

2. *Trace elements*

The behaviour of the trace elements follows the now well-established distinction between elements which are readily accepted into the lattices of crystallizing phases, and therefore become depleted in liquids derived by fractional crystallization, and those which are rejected by crystallizing species, and hence become enriched in derivative liquids. The group Co, Cr, Ni and V become depleted in later members of the sequence, while V is concentrated and Ni depleted in the high-iron basalts relative to the high-alumina types. Sr is also depleted during differentiation and is concentrated in the high-alumina types. If the high-alumina and high-iron types are related by processes of fractional crystallization, these relations suggest that the high-iron type is most likely to have been derived from the high-alumina type by fractionation of plagioclase and olivine.

In contrast, Li, Rb, Ba, Y and Zr undergo steady enrichment throughout the series. The tuffs appear to be somewhat enriched in Rb, and depleted in Y and Zr compared with other basalts, but they are similar in other respects (Fig. 36).

3. *Strontium isotope ratios*

The initial $^{87}Sr/^{86}Sr$ ratios of basalts have previously been determined by Halpern (1970) and Faure and others (1971), who found values in the range 0·703–0·704. Most basalts analysed in this study, including a tuff, and intermediate and acid rocks have ratios lying within, or close to, this range when allowance is made for the observed analytical imprecision ($\pm 0\cdot0007$). One high-alumina basalt (B.432.1) has a value significantly lower than any other (Table XI).

While the total range of isotopic compositions is significant and may indicate subtle differences in source

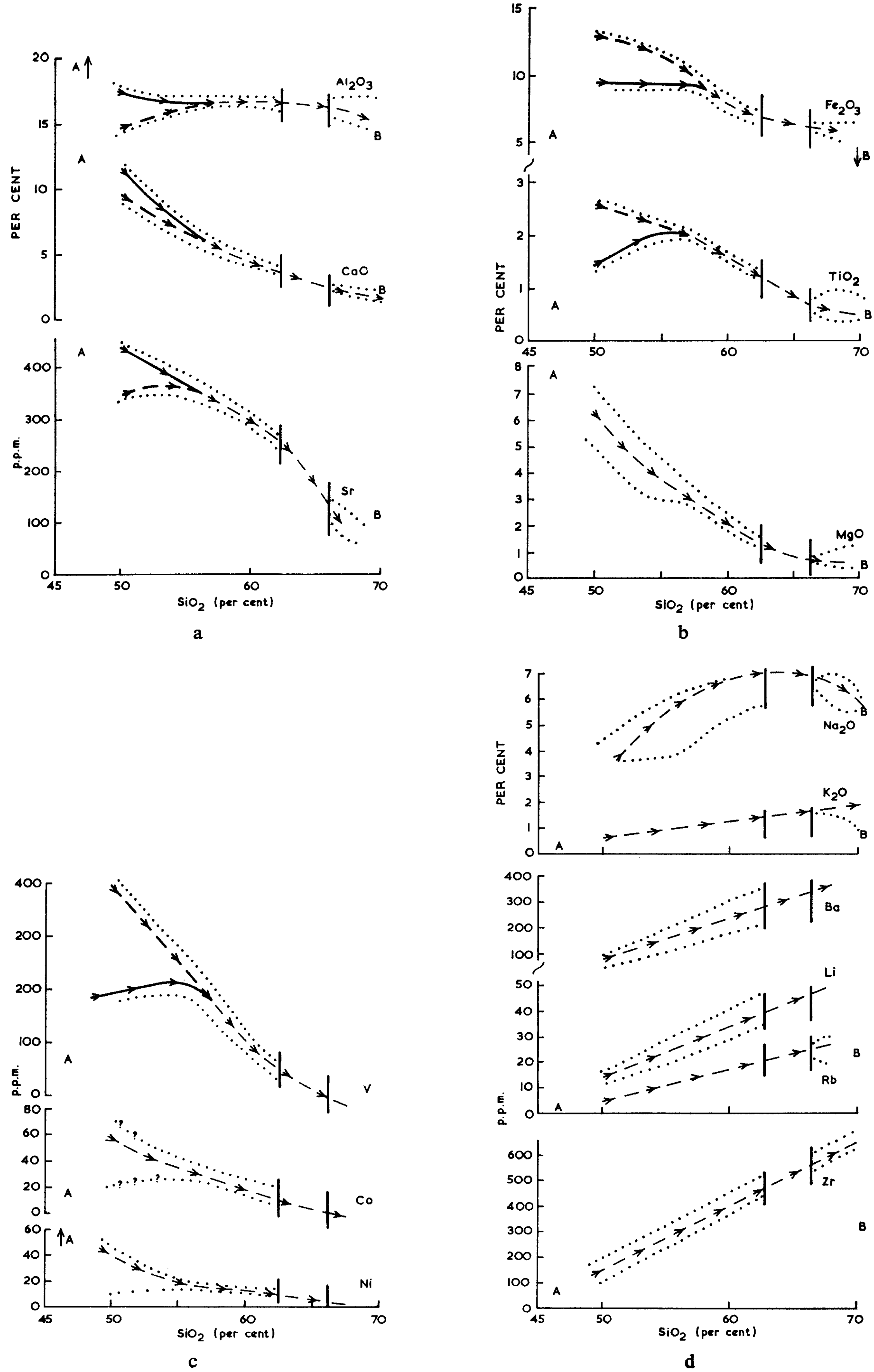

FIGURE 36

a–d. Variation diagrams for Deception Island.

A = B.304.1 (see p. 69).

B = B.317.1.

Envelope of compositions.

— — — — High-iron trend. } where separable.

———— High-alumina trend. } where separable.

. . . . Main trend (questionable at the acid end; see text).

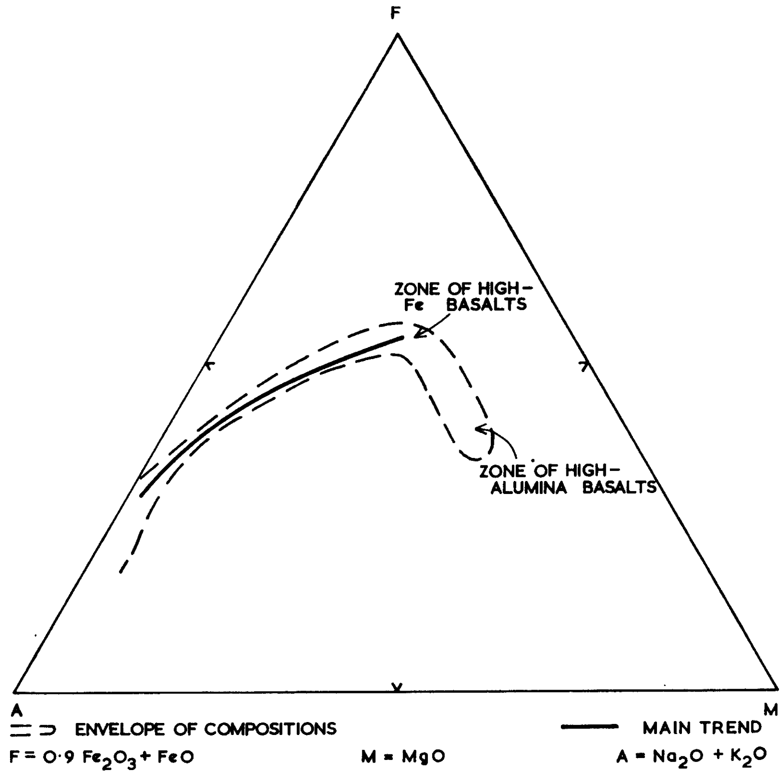

FIGURE 37
FMA diagram for the volcanic rocks of Deception Island.

TABLE XI
INITIAL STRONTIUM ISOTOPE RATIOS FOR ROCKS FROM DECEPTION ISLAND

Sample number	$^{87}Sr/^{86}Sr$*
Basic rocks	
B.304.1	0·7036
B.357.1	0·7035
B.413.4	0·7028
B.432.1	0·7018
Intermediate rocks	
B.276.1	0·7041
B.571.1	0·7046
Acid rocks	
B.420.2	0·7043
B.429.2	0·7028
B.431.1	0·7037

* Normalized to $^{88}Sr/^{86}Sr = 8·375$.

composition or magma history, the data suggest that all magmas are derived from isotopically similar "primitive" sources. Re-fusion of old continental sialic material is unlikely to be a source for the most acid rocks and, unless processes operate which allow leaching of Na_2O from sialic basement while Sr remains fixed, interaction of basaltic magmas with sialic material is unlikely to be the source of the high observed Na_2O concentrations. Furthermore, although some of the samples probably originated from vents close to sea-level and the tuff (B.413.4) is extensively hydrated, there is no evidence in the form of high

TABLE X

CHEMICAL ANALYSES AND SELECTED NORMS FOR ROCKS FROM DECEPTION ISLAND

	High-alumina types					*High-iron types*						*Basaltic andesite*					*Andesite*				*Dacite*	
	1	2	3	4	5	6	7	8	9	10	11	12	13	14	15	16	17	18	19	20	21	22
SiO_2	50·3	51·7	52·4	52·8	53·2	50·2	51·7	51·7	52·2	52·3	52·4	54·5	54·7	54·2	54·9	56·2	57·2	58·0	59·3	61·0	62·6	67·5
TiO_2	1·60	1·65	1·80	1·94	1·81	2·54	2·08	2·34	2·34	2·49	2·14	1·78	1·93	2·34	2·07	1·97	1·89	1·91	1·75	1·26	1·14	0·72
Al_2O_3	17·7	17·3	16·8	17·0	17·1	15·3	16·3	15·6	14·7	15·1	15·3	17·0	16·3	15·3	16·1	15·9	15·8	15·9	15·9	15·7	15·6	14·8
Fe_2O_3†	9·57	1·95	9·95	10·4	2·08	12·3	10·9	2·04	11·4	12·1	11·4	9·51	9·92	4·20	2·98	9·77	2·82	2·38	2·89	1·19	0·31	1·39
FeO		6·72			7·05			8·87						6·39	6·95		5·67	6·00	2·13	5·50	6·15	3·16
MnO	0·16	0·15	0·17	0·17	0·17	0·19	0·19	0·19	0·19	0·20	0·19	0·18	0·17	0·18	0·18	0·17	0·18	0·18	0·18	0·17	0·17	0·15
MgO	6·50	5·96	5·59	4·82	5·25	5·23	5·52	4·86	4·72	4·08	5·20	4·85	4·06	3·86	3·67	3·12	2·73	2·72	2·46	1·71	1·45	0·70
CaO	10·3	10·2	9·68	8·34	9·32	9·10	8·03	8·75	8·55	8·25	9·02	6·69	7·75	7·12	7·25	6·47	5·76	5·73	5·26	4·11	3·59	1·98
Na_2O	3·48	4·06	3·24	3·66	3·41	3·64	3·13	3·74	3·66	3·42	3·60	3·50	4·02	4·27	5·02*	5·36	5·58*	5·46	5·90	6·23*	6·66	6·96
K_2O	0·46	0·44	0·49	0·72	0·51	0·53	0·85	0·51	0·55	0·75	0·48	0·89	0·74	0·77	0·73	0·85	0·96	0·98	1·03	1·23	1·44	1·80
H_2O+	0·07	0·07	0·13	‡	0·02	0·20	‡	0·02	‡	‡	0·23	‡	0·37	0·07	0·09**	0·47**	0·23**	0·37**	0·11**	0·18**	0·29	0·14
H_2O-		0·14			0·02			0·10						0·01							0·00	0·13
P_2O_5	0·25	0·24	0·29	0·28	0·29	0·34	0·31	0·37	0·33	0·33	0·26	0·34	0·29	0·37	0·36	0·34	0·36	0·37	0·41	0·42	0·37	0·16
TOTAL	100·39	100·58	100·54	100·13	100·23	99·57	99·01	99·09	99·64	99·02	100·22	99·24	100·25	99·08	100·30	100·64	99·18	100·00	97·32	98·70	99·77	99·59
Li	16	12	12	—	—	15	—	13	—	—	15	—	—	16	16	20	—	—	30	30	44	48
Rb	4	5	6	12	6	5	10	7	14	15	8	10	7	8	9	12	15	13	14	17	21	29
Ba	120	100	110	—	175	125	—	125	—	—	160	—	160	160	185	180	—	—	195	250	340	340
Sr	450	415	375	420	360	340	355	350	325	355	330	390	340	365	320	335	340	320	305	270	240	135
Y	23	26	27	15	27	32	15	30	25	20	36	20	—	37	33	38	41	40	42	46	50	57
Co	19	18	20	33	40	22	35	28	—	34	46	32	38	40	26	26	—	—	29	30	9	5
Ni	29	§	§	31	§	20	25	§	§	28	18	28	§	15	15	13	11	tr	10	10	§	§
Cr	75	§	§	—	§	75	—	§	—	—	50	—	§	40	30	25	—	—	25	25	§	§
V	175	165	170	—	140	350	—	240	—	—	215	—	140	270	275	195	—	—	57	55	40	tr
Zr	145	150	170	95	165	190	110	195	190	120	205	125	—	225	210	310	305	305	305	370	410	535

C.I.P.W. NORMS

	2	5	8	14	15	16	18	20	21	22
Qz	—	3·67	1·60	6·53	2·57	2·84	6·56	7·56	6·73	14·67
Or	2·60	3·01	3·01	4·55	4·37	5·02	5·85	7·27	8·51	10·64
Ab	34·35	28·85	31·64	36·97	42·47	45·35	46·20	52·71	56·35	58·89
An	27·69	29·85	24·28	19·86	18·95	16·82	15·96	11·25	8·43	3·83
Di	17·34	11·83	13·79	10·56	12·36	10·87	8·12	5·58	5·95	4·14
Hy	4·37	15·85	16·38	9·24	10·31	11·57	8·97	8·63	10·04	3·38
Ol	7·50	—	—	—	—	—	—	—	—	—
Mt	2·83	3·02	2·96	6·09	4·32	2·33	3·45	1·73	0·45	2·02
Il	3·13	3·44	4·44	4·44	3·87	3·74	3·62	2·47	2·17	1·37
Ap	0·57	0·68	0·87	0·87	0·66	0·80	0·90	1·04	0·87	0·40
H_2O	0·14	0·02	—	—	0·78	—	0·35	0·16	0·27	0·26

* Analysed by F. Buckley. — Not determined. tr Trace.
† Where a single figure is reported, this represents total iron expressed as Fe_2O_3.
‡ Analysis is corrected to a water-free basis.
§ Material was probably contaminated during the preparation of the sample.
** Dried at 110° C.
Optical spectrographic analyses of Cr, V, Ba and Li in tuffs could not be performed because of explosive evolution of water during arcing.

1. B.352.3 Almost aphyric basalt; Kendall Terrace.
2. B.432.1 Almost aphyric basalt; Neptunes Bellows.
3. B.408.4 Almost aphyric basalt; Argentine station.
4. B.422.1 Yellow tuff; Macaroni Point.
5. B.416.1 Almost aphyric basalt; Mount Kirkwood.
6. B.357.1 Porphyritic basalt dyke; Cathedral Crags.
7. B.420.1 Pumiceous tuff; Cathedral Crags.
8. B.403.1 Almost aphyric basalt; Baily Head.
9. B.413.5 Grey tuff; Fumarole Bay.
10. B.413.4 Yellow tuff; Fumarole Bay.
11. B.309.1 Porphyritic basalt; Stonethrow Ridge.
12. B.405.1 Yellow tuff; Baily Head.
13. B.417.1 Aphyric basaltic andesite; Mount Kirkwood.
14. B.311.1 Scoriaceous basaltic andesite; Telefon Ridge.
15. B.571.1 Basaltic andesite bomb; Mount Pond.
16. B.556.1 Andesitic bomb; Mount Pond.
17. B.428.1 Andesitic bomb; "Land centre".
18. B.707.1 Andesitic bomb; "Land centre" area.
19. B.711.1 Andesitic bomb; "Island centre" area.
20. B.276.1 Andesitic bomb; "Island centre".
21. B.431.1 Dacite; Collins Point.
22. B.429.2 Porphyritic dacite; Cross Hill.
23. B.317.1 Dacite pumice; "Island centre".

initial ratios (*c.* 0·709) that complete isotopic exchange with sea-water took place. However, a high initial magmatic Sr content would be likely to obscure the effects of partial equilibration.

4. *Acid plutonic blocks*

Samples of coarse-grained plutonic blocks have been found amongst surface detritus at a number of localities, particularly the youthful Kendall Terrace lava platform (Plate XIIc). Petrographically, the blocks range from diorite through granodiorite, tonalite to granite. The most characteristic feature of these rocks is the intense alteration of the cores of the plagioclase phenocrysts. Products of alteration include, in approximate order of abundance, sericite, chlorite and epidote. Whatever the cause of this alteration, the products are capable of fixing the majority of mobilized cations with the exception of sodium. Many of the corroded plagioclases are mantled by a rim of alkali-feldspar, which would act as an effective sink.

Compared with the acid volcanic rocks, the acid intrusive rocks have much higher K/Na and Rb/Sr ratios, with a much higher concentration of Rb (Table XII). In contrast, Zr is lower. Data on the individual mineral phases are not available but it does not seem likely that the plutonic blocks represent the intrusive equivalent, nor any product of crystal accumulation in the formation of the acid extrusive rocks.

Petrographically, the plutonic rocks closely resemble members of the Andean Intrusive Suite, described from nearby Livingston Island by Hobbs (1968) and from the adjacent Antarctic Peninsula by Adie (1955). In major- and trace-element contents they are closely comparable to the analyses of the Andean Intrusive Suite given by Adie (1955, p. 24–25).

TABLE XII
CHEMICAL ANALYSES OF PLUTONIC BLOCKS FROM DECEPTION ISLAND

	B.351.1	B.313.2	B.316.2
SiO_2	60·1	70·6	75·3
TiO_2	0·66	0·35	0·21
Al_2O_3	17·1	14·0	13·3
Fe_2O_3	5·79	2·36	1·64
MnO	0·11	0·04	0·05
MgO	3·30	0·52	0·35
CaO	5·87	1·65	1·57
Na_2O	4·10	4·36	4·36
K_2O	2·07	4·60	3·40
$H_2O\pm$	0·69	0·49	0·43
P_2O_5	0·20	0·03	0·05
TOTAL	99·99	99·00	100·26
Rb	61	300	155
Sr	560	285	175
Y	19	40	29
Ni	17	4	tr
Zr	180	280	92

tr Trace.

F. Mineral Analyses

Modal data for the host rocks are given in Table XIII. In specimen B.304.1 (Plate XIId), the interstitial material and to a lesser extent the rims of the phenocrysts have been subject to high-temperature alteration. The entrained fluid has been quenched rather rapidly, as shown by the presence of feather-like aggregates (quench structures) of fine-grained feldspar, or more rarely calcic scapolite, and clinopyroxene (Plate XIIe). This block was ejected during the course of the formation of the 1967 island. It is possible that the invading fluid species were present in the magma which gave rise to those products. Alternatively, the alteration could be autometasomatic involving hydrous fluids concentrated during the crystallization of the assemblage in specimen B.304.1.

The phenocrysts in specimen B.411.2 are fresh but fragments of quench structures are present. In specimen B.712.1, which occurred as a cognate xenolith in a fine-grained lava block ejected during the 1970 eruption,* the rims of some of the clinopyroxenes, and areas in plagioclase adjacent to cracks and margins, show signs of lower-temperature alteration. A single localized area, where apparently serpentine is developed, could be pseudomorphic after olivine. However, the overall proportion is very small.

In all cases, seriously altered material could be readily detected in grains, which were removed by hand-picking prior to mechanical separation. Fine-density "cuts" were taken during heavy-liquid separation to minimize the possibility of contamination of phenocryst material by alteration products.

1. *Major elements*

Comment need only be made on the composition of the clinopyroxene in specimen B.712.1. Although Al_2O_3 contents in the range 4·5–6 per cent (TiO_2 contents <1 per cent) and FeO/MgO ratios between *c.* 0·4 and 0·6 are characteristic of the early clinopyroxenes of the calc-alkaline suite (Lewis, 1967; McReath, 1972), the clinopyroxene of specimen B.712.1 is much less calcic. In this respect, it resembles the early clinopyroxenes of the island-arc tholeiite suite, though it is more aluminous than is common in this series (Baker, 1966; McReath, 1972). The analysis, before normalization, shows a low total $(Ca^{2+}+Mg^{2+}+Fe^{2+})SiO_3$, suggesting that much of the iron must be present as Fe^{3+}. If this supposition is correct, the analysis will plot in a position removed from the normal tholeiitic clinopyroxene trend (Brown, 1967) towards the sub-calcic augite field. This is not unreasonable on the basis of the observed phenocryst mineralogy (Table XIII).

2. *Minor elements*

The high concentrations of Al_2O_3 and CaO in the olivines, and of FeO in the plagioclases, should be noted. There is some doubt as to the exact significance of the values found for Al_2O_3 in the olivines, but it is believed that at least part of these concentrations may be present in the crystal structure. The high concentrations of CaO are compatible with an origin at low pressures (Simkin and Smith, 1970; Nicholls and others, 1971).

The concentration of FeO in plagioclases from island-arc volcanic rocks is related both to the concentration of iron in the magmas and to the extent of oxidation of the iron (McReath, 1972). There is possibly also a temperature effect (Lewis, 1969). The low concentration of FeO in the plagioclase of specimen B.304.1 may be due, therefore, to a low iron-oxidation state and a lower concentration of iron in the magma compared with that which crystallized the plagioclase of specimen B.411.2. If the plagioclase of specimen B.712.1 crystallized at a lower temperature than that of specimen B.304.1, which seems likely on the basis of the observed mineralogy, the parent magma for specimen B.712.1 probably has both a high iron content and a relatively high oxidation ratio.

3. *Trace elements*

The concentrations of Cr in the olivines compare with those found in olivines from ultramafic nodules (Mercy and O'Hara, 1967) rather than those of island-arc volcanic rocks, where concentrations of less than 20 p.p.m. are usual (McReath, 1972) and distribution coefficients for chromium partition between olivine and liquid are much less than unity. In non-accumulative basalts, observed olivine/liquid distribution coefficients for Ni lie in the range 13–17 (Häkli and Wright, 1967; Henderson and Dale, 1970; McReath, 1972). Therefore, it follows that both olivines must have crystallized from magmas with higher Ni concen-

* Samples collected and kindly donated by Dr. L. Villari.

TABLE XIII
CHEMICAL ANALYSES AND MODAL DATA FOR CUMULATE BLOCKS FROM DECEPTION ISLAND

	B.304.1			B.411.2				B.712.1	
	Whole rock	*Olivine*	*Plagioclase*	*Whole rock*	*Groundmass*	*Olivine*	*Plagioclase*	*Clinopyroxene*	*Plagioclase*
SiO_2	46·7	40·0	46·0	53·5	54·0	37·8	45·8	50·0	50·0
TiO_2	0·69	0·06	0·07	1·23	1·48	0·10	0·08	0·80	0·10
Al_2O_3	23·3	0·20	34·2	18·3	18·2	0·82	33·5	5·41	32·2
FeO	5·10	10·5	0·42	8·58	9·39	18·7	0·63	9·32	0·66
MnO	0·08	0·18	0·01	0·13	0·16	0·33	0·02	0·22	0·01
MgO	7·82	48·0	tr	5·05	3·55	39·3	?tr	17·3	tr
CaO	12·8	0·43	18·2	9·53	8·89	0·59	17·8	15·8	15·2
Na_2O	—	—	1·32	3·81	—	—	1·30	0·44	3·03
K_2O	0·12	—	0·02	0·57	0·68	—	0·04	0·06	0·09
TOTAL	99·51	99·37	100·29	100·70	(94·35)	97·64	99·24	99·45	101·38
Ba	27	—	51	120	115	n.d.	41	20	±10
Sr	425	—	635	375	300	n.d.	650	7	605
Co	14	115	n.d.	15	21	160	n.d.	45	n.d.
Ni	*	1,800	5	*	10	620	10	150	±10
Cr	*	480	tr	*	70	280	tr	470	n.d.
V	72	10	n.d.	150	265	10	n.d.	250	n.d.
Zr	60	tr	7	195	—	—	7	—	—

MODES

	B.304.1 *Phenocryst only*	B.304.1 *Whole rock*	B.411.2 *Whole rock*	B.712.1 *Whole rock*
Plagioclase	61·5	75·6	12·6	70
Olivine	9·7	11·8	1·7	—
Clinopyroxene	0·7	10·5	2·5	28
Opaque minerals	tr	2·1	tr	2
Interstitial minerals	28·1	—	—	tr
Groundmass	—	—	83·3	—
Plagioclase; An per cent	88	—	88	73
Olivine; Fo per cent	90	—	78	—
Clinopyroxene	—	—	—	$Ca_{31}Mg_{48}Fe_{21}$

* Below limits of sensitivity.
tr Trace.
n.d. Not determined.

trations than any observed in surface lavas. It may be estimated that hypothetical parent magmas are likely to contain between 130 and about 200 p.p.m. Ni, if only small amounts of olivine fractionation are allowed to produce the early high-alumina basalts, and the parent will obviously be more basic than any observed basalt.

Similarly, for Ni partition between clinopyroxene and liquid, distribution coefficients in the range 2–5 have been found (Häkli and Wright, 1967; Ewart and Taylor, 1969; McReath, 1972). On this basis, therefore, the assemblage represented by specimen B.712.1 could have crystallized from one of the more basic Deception Island magmas.

Applying the same arguments, using the distribution of Sr between plagioclase and liquid ($K_D = 1 \cdot 5–2 \cdot 8$; Ewart and Taylor, 1969; Philpotts and Schnetzler, 1970; McReath, 1972), suggests that the plagioclase of specimens B.304.1 and 411.2 could have crystallized from magmas of slightly lower Sr content than the most basic high-alumina basalts, while that of specimen B.712.1 most probably crystallized from a basaltic andesite magma, taking into account the previous restrictions imposed by the Ni concentration in the clinopyroxene.

The groundmass of specimen B.411.2 is depleted in Co and Ni compared with basaltic types of similar SiO_2 content, and observed distribution coefficients are considerably higher than the normal range. This implies that the groundmass of specimen B.411.2 is the product of excessive fractionation of olivine.

The trace-element data suggest, therefore, that there are more basic precursors for the Deception Island magmas. The earlier phases of magmatic evolution are probably governed by fractionation of olivine and possibly calcic bytownite/anorthite, while later evolution is controlled by fractionation of sodic bytownite.

G. Discussion

1. *Comparisons*

The general pattern of major- and trace-element abundances in the Deception Island basalts suggests that they are at a stage of evolution away from mantle compositions similar to that represented by the circum-oceanic basalts. In particular, the Ni/Co and V/Cr ratios in basalts lie within the ranges regarded by Taylor and others (1969) as being characteristic of high-alumina basalt in island arcs. The Na_2O contents compare with the highest and K_2O with the lowest found in Recent arcs. The total-alkali content approaches that found in some alkaline series and this affinity is further strengthened by the high concentrations of Ti, Zr and Sr found. These characteristics are essentially transitional, however, and this is emphasized, for example, on a diagram of Ti *vs* Zr (Fig. 38; after Pearce and Cann, 1971), which shows that the fields of the Deception Island extrusive rocks are distinct both from calc-alkaline or island-arc tholeiite material, on the one hand, and typical alkaline material on the other.

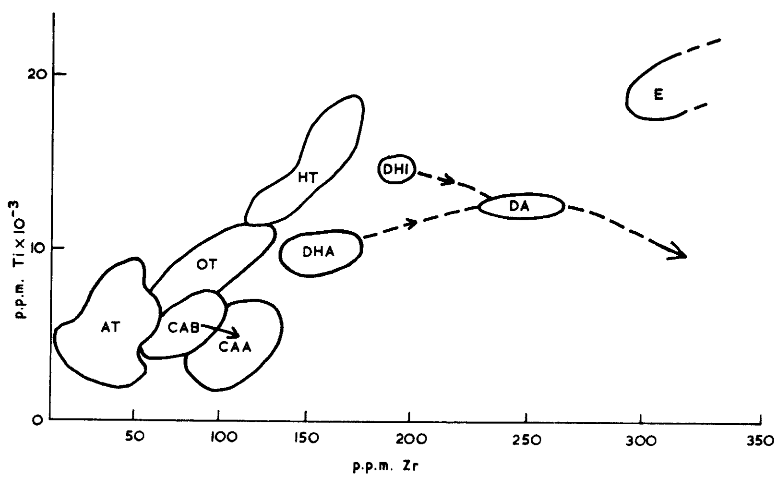

FIGURE 38

Titanium-zirconium relations in some volcanic rocks (after Pearce and Cann, 1971).
AT arc tholeiite; OT ocean tholeiite; HT Hawaiian tholeiite; CAB calc-alkali basalts; CAA calc-alkali andesites; E Easter Island; DHA Deception Island, high-alumina basalts; DHI Deception Island, high-iron basalts; DA Deception Island, andesites. Tie lines represent fractionation trends.

While the overall trend of iron enrichment throughout the suite invites comparison with the island-arc tholeiite suite (Jakes and Gill, 1970), the total resemblance is only passing (see Table XIV, columns g and h).

Some close parallels are observed. Major-element trends are closely similar to those found in the Quaternary lavas of Santorini (Nicholls, 1971*a*), which are unique in the Aegean area (Nicholls, 1971*b*). In a recent study of the rocks of Mount Ararat, Lambert and Holland (personal communication) have described a high-alumina basalt which has many features in common with the Deception Island high-alumina basalt types; in particular, high Na_2O/K_2O, Sr, Ba and Zr compared to circum-oceanic types. The high-alumina basalt appears chemically well separated from the remainder of the suite, which compares more closely with a normal calc-alkaline acid andesite–dacite succession. The relation between the basalt and the remainder of the suite is therefore obscure. Although the area is one of much late Tertiary and Quaternary activity, little information is available to show how widespread the development of this basalt type might be.

TABLE XIV

COMPARATIVE DATA

	Mantle	*Oceanic basalts*				*Alkali-basalts*		*Calc-alkali*		*Tholeiitic*	
	a	b	±	c	±	d	±	e	f	g	h
SiO_2	43·6 – 45·2	49·34	0·54	49·21	0·74	47·41	3·08	51·7	50·9	51·91	52·0
TiO_2	0·04 – 0·7	1·49	0·39	1·39	0·28	2·87	0·24	—	1·0	0·79	1·11
Al_2O_3	2·5 – 4·2	17·04	1·78	15·81	1·50	18·02	1·71	16·9	19·4	15·58	16·7
Fe_2O_3	0·5 – 1·5	1·99	0·65	2·21	0·74	4·17	1·16	11·6	3·7	12·9	12·0
FeO	6·5 – 8·2	6·82	1·50	7·19	1·25	5·80	1·17		5·4		
MnO	0·1 – 0·2	0·17	0·03	0·16	0·08	0·16	0·03	—	0·2	0·19	0·20
MgO	37·5 – 41·5	7·19	0·67	8·53	1·98	4·79	1·35	6·5	4·7	5·00	5·51
CaO	2·2 – 3·1	11·72	0·69	11·14	0·78	8·65	0·91	11·0	10·5	11·36	10·3
Na_2O	0·2 – 0·6	2·73	0·20	2·71	0·19	3·99	0·41	3·1	3·2	3·05	2·15
K_2O	0·03 – 0·1	0·16	0·06	0·26	0·17	1·66	0·38	0·4	0·5	0·20	0·46
Rb	0·2 – 2	<10		20		33		9·6		9	15
Sr	1 – 50	130	25	123	46	815	375	328	250	123	138
Ba	0·4 – 18	14	7	12	8	498	136	115	136	—	85
Co	100 – 250	32	3	—	—	25	5	40	27	—	38
Ni	1,500 – 3,100	97	19	123	56	51	33	25	17	19	16
Cr	1,600 – 3,500	297	73	296	80	67	57	40	49	—	46
V	40 – 100	292	57	289	73	252	32	255	275	—	308
Zr	30 – 45	95	35	100	42	333	48	100	80	25	108

± Signifies standard deviation.

a. Range of some estimates of mantle composition, based on data and summaries given by Paul (1970) and a calculation by Rea (1970), using a pyrolite model and data from various sources.
b and d. From Engel and others (1965). b: high-alumina type of oceanic ridges; d: alkali-basalts of seamounts.
c. High-iron oceanic ridge tholeiite; from Melson and others (1968).
e. Aphyric high-alumina basalt [*sic*], K-trig, Taupo, New Zealand; from Taylor and others (1969).
f. Average porphyritic basalts, St. Kitts; quoted by Rea (1970).
g. Basalt, Zavodovski Island, South Sandwich Islands.
h. Average basalt, Visokoi Island; data from Baker (in press) and McReath (1972).

TABLE XV

CHEMICAL ANALYSIS OF A WARNER-TYPE HIGH-ALUMINA BASALT

(Data from Yoder and Tilley (1962) and Nicholls (1965); trace elements (one analysis) from Nockolds and Allen (1953).)

		Trace elements (p.p.m.)	
SiO_2	48·0	Li	5
TiO_2	0·8	Sr	400
Al_2O_3	18·1	Ba	20
Fe_2O_3	9·6	Y	20
MgO	9·8	Co	50
CaO	11·5	Ni	225
Na_2O	2·5	Cr	225
K_2O	0·09	V	175
		Zr	50

are effectively removed from the crystalline solids and transported to higher levels. Here, the typical mineralogy of the surface rocks, characterized by more sodic plagioclases, develops.

The proposed evolutionary sequence differs from that observed in the normal calc-alkaline series (Lewis, 1971; McReath, 1972) primarily in the absence of amphibole at any stage and in the low quantities of magnetite involved. The presence of amphibole is essential both for the maintenance of a low rate of enrichment in Na_2O and for the production of voluminous quantities of siliceous derivatives, while the presence of small quantities of magnetite (*c.* 5–10 per cent) can prevent iron enrichment (cf. Osborn, 1959) but it is also essential if extreme silica enrichment is to be produced. Although the later stages of the evolution of calc-alkaline suites probably take place under low-pressure conditions, it is apparent that in many cases the evolution is under high partial pressures of water, which causes the modal plagioclase to be much more calcic than the normative composition. At Deception Island, it is proposed that in the later stages of evolution the partial water pressure remained low or that during the separation stage mentioned above volatiles were lost. Under these circumstances, the feldspars produced are much more sodic but at least part of the differences between calc-alkaline andesitic plagioclases and those of Deception Island must be due to response of the crystallizing system to the high Na_2O contents in the andesitic liquids.

3. *Acid rocks*

Although a variety of reasons for the absence of parts of an igneous rock suite have been advocated from time to time, cases where the gap is between intermediate and acid rocks are rare. Although complete separation of a sodic plagioclase (sodic labradorite/andesine) from an andesitic magma could result in the reduction of the rate of increase in Na_2O with increasing SiO_2 content observed between the andesites and dacites, the viscosity of the acidic magmas might prevent this effective separation. Direct derivation of the acidic magmas at depths (possibly under low volatile pressures) when viscosities would be reduced, followed by a short period of imperfect fractionation at higher levels after the loss of volatiles, might be a possible mechanism.

The extreme compositional discontinuity between the andesitic bombs (B.276.1) and pumice (B.317.1) of the 1967 eruption suggests that liquid immiscibility may be present. The immiscibility could be generated by fortuitous meeting of two separately differentiated magma pockets immediately prior to eruption, but the possibility that it is generated during late magma evolution under low total and partial water pressures cannot be discounted.

4. *General implications*

The limits of conditions for magma genesis or equilibration previously discussed lead to the conclusion that the decisive processes take place within the topmost upper mantle or the lower crust. If the primary magma genetic process involved the partial melting of a plagioclase–amphibole assemblage to produce the parental basalt, a probable means of genesis of the source rock would be invasion of the basaltic layer between *c.* 10 and 20 km. (p. 62) underneath Deception Island by hydrous volatile phases derived from the down-going slab. The amphibolitization process would probably require the crust to be sufficiently hot to make the process kinetically feasible, but not hot enough to produce partial melting. With the slow dissipation of frictional heat in an underthrust system which has come to rest, some time lag between amphibolitization and the commencement of melting would be expected. If no further influx of volatiles accompanies the onset of partial melting, the earliest phase to melt under the essentially anhydrous conditions would be amphibole. Unless the earliest volatile-rich liquid is immediately tapped from the source region, later conditions would approach, though not achieve, those for water-saturated conditions. Both plagioclase and amphibole would melt. High degrees of partial melting under these circumstances may not be required to produce a basaltic magma, though melting might have to be extensive to produce a high-alumina olivine-tholeiite. Some additional source of heat may be required to produce such a melt.

For the proposed subsequent fractionation path, sufficient hydrous volatile phases must be retained early in the evolution to maintain highly calcic plagioclase compositions, but at the same time the volatile pressure must remain fairly low to prevent the suppression of plagioclase as a near-liquidus phase. In the case of many of the basalts, magma release direct from source to surface is required.

The situation of Deception Island close to a graben fault may explain a number of features. Efficient separation of phenocrysts from magma may be promoted by seismic activity, and release of magma from depth may be aided by movement at the fault. In addition, frictional heat developed during fault movement could promote the degrees of partial melting required to produce the hypothetical parent magma.

Other features discussed, notably the low-pressure stage, require that high-level magma chambers are formed and maintained. The historical evidence suggests that this has probably only been possible subsequent to caldera collapse but that the size of magma chamber involved is probably small. That the magma chambers are capable of sustained independent existence has been discussed previously (p. 73). Some evidence that such a magma chamber may still be present is provided by heat-flow measurements (Orheim, 1971*c*).

H. Summary and Conclusions

In important major features and detail, the Deception Island suite differs from the typical calc-alkaline suite. It is suggested, however, that the same general process of magma genesis—partial melting of hydrated oceanic crust and equilibration under intermediate or low-pressure conditions ($<$10 kbar)—operate. The differences are explained most satisfactorily if it is assumed that volatile loss takes place throughout magma evolution at both deep and shallow levels, under which conditions amphibole, the most critical fractionating phase involved in the evolution of the calc-alkaline suite from high-alumina basalt, fails to form.

VII. CONCLUSIONS

1. Deception Island, formerly a large strato-volcano with flanking parasitic cones, was transformed by caldera subsidence. The principal episode of collapse was preceded by the eruption of pyroclast flows but minor movements on the caldera fault appear to have continued to the present time. Post-caldera activity has occurred both high on the caldera rim, usually as lava flows, and on the inner part of the caldera wall around Port Foster, generally forming pyroclastic cones.
2. The basaltic lavas of Deception Island are similar to the late Tertiary and Quaternary lavas of the James Ross Island group and associated islands on the eastern side of the Antarctic Peninsula. However, Deception Island is unique in having a differentiated suite of rocks in which the Na-rich, K-poor character is amplified. This chemical identity of the Deception Island lavas has persisted throughout its history, though more acid differentiates are confined to post-caldera times.
3. The recent eruptions have all occurred on the inside of the caldera and their arcuate disposition around the caldera wall suggests that the ring fracture is still active.
4. The eruptions were entirely pyroclastic which is normal on Deception Island for vents close to sea-level such as those of 1967 and 1970. Explosive eruptions from the much higher 1969 fissure may have been induced by contact of the magma with glacial melt water.
5. The 1967 and 1969 eruptions are known to have been preceded by enhanced seismic activity over a period of a few weeks. The high water temperatures and strong fumarolic activity recorded around Telefon Bay in December 1968 may be more accurately construed as foreshadowing the 1970 eruption rather than as being residual after the 1967 event.
6. There is a relationship between the chemical composition of a sample and the geographical position of its source vent. The most siliceous products were emitted from the area of the 1967 island in Telefon Bay and the more basic ejecta came from the southerly part of the 1969 fissure. Clear evidence of lateral variation in composition can be seen in all three eruptions and the trends are mutually consistent.
7. Material erupted from any particular part of the fissure system appears to become more basic with time, e.g. the 1967 bombs from the new island had *c.* 61 per cent SiO_2, whereas the 1970 bombs from this site had 59 per cent SiO_2.
8. The spatial and temporal variations in composition indicate that the ring fractures are tapping zones of variously differentiated magma and that they do not have direct access to a large uniform magma reservoir.
9. During the three recent eruptions only a very small volume of magma has escaped ($\sim 0 \cdot 2$ km.^{3}). Probably only small volumes were actually emplaced into the upper part of the ring-fault system, thus favouring relatively rapid cooling and differentiation.
10. The evidence is open to a number of interpretations, and one model is as follows:

    Magma first enters the ring fracture system in the north, gradually moving upwards and differentiating. Farther south, magma penetrates later and less effectively into the caldera fault zone. The result is an arcuate dyke-like body of magma reaching higher up the fracture in the north but being retained at lower levels farther south. Surface activity commenced over the apex of this arcuate magma body when the most differentiated material was emitted and created the 1967 island. The structural movement which had triggered the 1967 eruption (such as a hinge-like motion of the caldera floor) now propagated southward along the eastern limb of the caldera, allowing small quantities of less differentiated magma to reach the surface in its course, hence the more basic eruptive rocks of 1969 (Fig. 39).
11. The ash–ice stratigraphy suggests a pattern, over the past two centuries, of several eruptions in one decade followed by several decades without eruptions (Orheim, 1971*b*, p. 85). There is, however, no particular reason for supposing that the present series of eruptions has come to an end. The anomalous occurrence of bombs south of Cross Hill, and also the open rifts reported by Shultz (1971, p. 84) in this area, suggests the possibility of activity spreading down the west flank of the caldera.

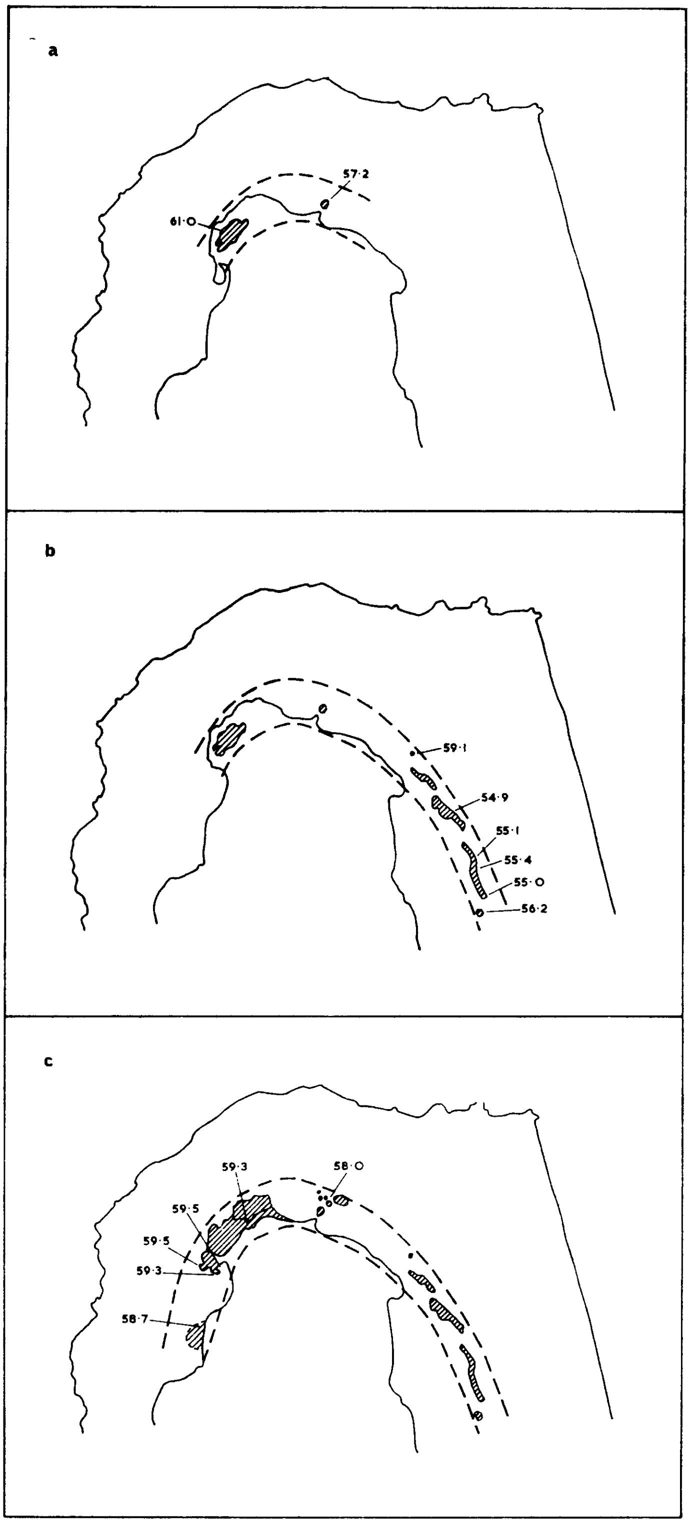

FIGURE 39

Summary diagrams of events on Deception Island, 1967–70. Figures represent SiO_2 values of erupted bombs.

a. An arcuate magma body moves up the caldera fault system. The most differentiated part of the melt is erupted from the highest part of the body to form the new island in Telefon Bay (4–6 December 1967). At the same time the fracture system extended eastward in an arc around Telefon Bay, allowing less differentiated magma to erupt at the land centre.

b. The fracture system propagates southward down the eastern side of Deception Island. A hinge-like motion of the caldera floor may have allowed less differentiated magma from greater depths to be tapped farther south. The more basic magma was erupted along the fissure which opened up on 21 February 1969. The shoreline heats up in the vicinity of Cross Hill, suggesting that magma is also rising in the caldera fault zone on the north-western side of the island.

c. In August 1970 eruptions occurred at several vents in the vicinity of the 1967 island and land centre, and also farther south down the western limb of Deception Island. As in 1967, products erupted on the north-western side of Telefon Bay were more siliceous than those erupted on the north-eastern side.

12. The recent series of eruptions has demonstrated that the main hazards to human life and property are the floods of melt water released during subglacial eruptions. They have also shown that the most convenient sites for scientific stations, low on the shores around Port Foster, are also the most vulnerable to the effects of such eruptions. No part of the island can be considered immune from the possible influence of volcanism, though the ring-fracture zone is undoubtedly the most likely site for an outbreak to occur. This includes, for instance, the possibility of an eruption in Neptunes Bellows with the far-reaching effects that this would have on the life and role of the island.
13. It would obviously be unwise to construct any new stations, air strips or harbour installations at Deception Island. The policy of only allowing parties to remain on the island whilst a means of rapid evacuation exists is also one that should be continued.

VIII. ACKNOWLEDGEMENTS

WE thank the Royal Society and the Natural Environment Research Council for financial support. We are most grateful to the Chairman of the Royal Society's Volcanological Research Committee, Professor J. Sutton, F.R.S., and also to Mr. G. E. Hemmen for their help in the initial planning and organization of the expeditions.

For repeated logistic support we are indebted to the British Antarctic Survey and we are grateful to Sir Vivian Fuchs and Dr. R. J. Adie for the close interest they have maintained in the Deception Island work. We are especially indebted to Dr. Adie for his invaluable help with the organization of the expeditions and with the preparation of this publication.

For logistic support on other occasions we are indebted to the Instituto Antártico Argentino and its Director, General J. E. Leal; also to the Argentine Navy, particularly Capitan Juan Carlos Dupuy and the officers and crew of *Zapiola*. We are also grateful to the Royal Navy (H.M.S. *Endurance*) for help on the occasion of our first visit in 1968. For their repeated help, we thank the Masters of the British Antarctic Survey ships *John Biscoe* and *Shackleton*, Captain J. Cole and Captain D. H. Turnbull.

We are grateful to all of the British Antarctic Survey members who helped us during our visits to Deception Island; we much appreciated having the use of the British Antarctic Survey station and were fortunate in being able to talk with several eye-witnesses to the eruptions. We gratefully acknowledge the help of W. Stocks, D. Snell, J. O'Toole, A. Spencer, J. Newman, I. Curphey and G. Higgins.

We are much indebted to our colleagues N. J. Collins, O. H. S. Darling, A. N. Bushell, B. Gargate, C. G. Smith, R. B. Ledingham and D. Parnell. We are also grateful for discussions with N. H. Fourcade, O. González-Ferrán, L. S. Goverukha, T. Hughes, H. Moreno, J. A. Moreno, F. Munizaga, O. Orheim, C. M. Scarfe, C. H. Shultz and L. Villari. Thanks are due to R. St. J. Lambert and J. G. Holland for permission to refer to their recent work on Mount Ararat.

For kindly undertaking some of the chemical analyses we thank F. Buckley, J. G. Holland, A. Gray and J. Wigley.

We are grateful to Professor E. A. Vincent for the use of laboratory facilities in the Department of Geology and Mineralogy, University of Oxford, during the earlier stages of this project.

Part of this work was undertaken during the tenure of the Royal Society Mackinnon Research Studentship by P.E.B. Two of the authors [M.R.H. and I.McR.] took part in this project during tenure of Natural Environment Research Council Research Studentships which are gratefully acknowledged.

IX. REFERENCES

ADIE, R. J. 1955. The petrology of Graham Land: II. The Andean Granite–Gabbro Intrusive Suite. *Falkland Islands Dependencies Survey Scientific Reports*, No. 12, 39 pp.

————. 1964. The geochemistry of Graham Land. (*In* ADIE, R. J., *ed. Antarctic geology.* Amsterdam, North-Holland Publishing Company, 541–47.)

————. 1971. Evolution of volcanism in the Antarctic Peninsula. (*In* ADIE, R. J., *ed. Antarctic geology and geophysics.* Oslo, Universitetsforlaget, 137–41.)

ASHCROFT, W. A. 1972. Crustal structure of the South Shetland Islands and Bransfield Strait. *British Antarctic Survey Scientific Reports*, No. 66, 43 pp.

BAKER, P. E. In press. The South Sandwich Islands: II. Petrology and geochemistry. *British Antarctic Survey Scientific Reports.*

————. *and* I. MCREATH. 1971*a*. 1970 volcanic eruption at Deception Island. *Nature, Lond.* (*Phys. Sci.*), **231**, No. 18, 5–9.

————. *and* ————. 1971*b*. Geological investigations on Deception Island. *Antarct. Jnl U.S.*, **6**, No. 4, 85–86.

————. *and* ————. 1972. Investigation of the 1970 volcanic activity at Deception Island, South Shetland Islands. *Polar Rec.*, **16**, No. 100, 67–71.

————., DAVIES, T. G. *and* M. J. ROOBOL. 1969. Volcanic activity at Deception Island in 1967 and 1969. *Nature, Lond.*, **224**, No. 5219, 553–60.

————., GONZÁLEZ-FERRÁN, O. *and* M. VERGARA. 1973. Paulet Island and the James Ross Island Volcanic Group. *British Antarctic Survey Bulletin*, No. 32, 89–95.

BARAGAR, W. R. A. *and* A. M. GOODWIN. 1969. Andesites and Archean volcanism of the Canadian Shield. (*In* MCBIRNEY, A. R., *ed.* Proceedings of the andesite conference. *Bull. Ore. St. Dep. Geol. miner. Ind.*, No. 65, 121–42.)

BARKER, P. F. *and* D. H. GRIFFITHS. 1972. The evolution of the Scotia Ridge and Scotia Sea. *Phil. Trans. R. Soc.*, Ser. A, **271**, No. 1213, 151–83.

BARTH, T. F. W. *and* P. HOLMSEN. 1939. Rocks from the Antarctandes and the Southern Antilles. Being a description of rock samples collected by Olaf Holtedahl 1927–1928, and a discussion of their mode of origin. *Scient. Results Norw. Antarct. Exped.*, No. 18, 64 pp.

BONATTI, E. 1965. Palagonite, hyaloclastites and alteration of volcanic glass in the ocean. *Bull. volcan.*, Sér. 2, **28**, Pt. 3, 257–69.

BREW, D. A. *and* L. J. P. MUFFLER. 1965. Upper Triassic undevitrified volcanic glass from Hound Island, Keku Strait, southeastern Alaska. (*In* Geological Survey research 1965. *Prof. Pap. U.S. geol. Surv.*, No. 525-C, C38–43.)

BROWN, G. M. 1967. Mineralogy of basaltic rocks. (*In* HESS, H. H. *and* A. POLDERVAART, *ed. Basalts: the Poldervaart treatise on rocks of basaltic composition. Vol. 1.* New York, London, Sydney, John Wiley & Sons: Interscience Publishers, 103–62.)

CASERTANO, L. 1964. Volcanic activity at Deception Island. (*In* ADIE, R. J., *ed. Antarctic geology.* Amsterdam, North-Holland Publishing Company, 33–47.)

CLAPPERTON, C. M. 1969. The volcanic eruption at Deception Island, December 1967. *British Antarctic Survey Bulletin*, No. 22, 83–90.

DAVEY, F. J. 1971. Marine gravity measurements in Bransfield Strait and adjacent areas. (*In* ADIE, R. J., *ed. Antarctic geology and geophysics.* Oslo, Universitetsforlaget, 39–45.)

DICKINSON, W. R. *and* T. HATHERTON. 1967. Andesitic volcanism and seismicity around the Pacific. *Science, N.Y.*, **157**, No. 3794, 801–03.

EMSLIE, R. F. 1971. Liquidus relations and subsolidus reactions in some plagioclase-bearing systems. *Yb. Carnegie Instn Wash.*, **69** (for 1969–70), 148–55.

ENGEL, A. E., ENGEL, C. G. *and* R. G. HAVENS. 1965. Chemical characteristics of oceanic basalts and the upper mantle. *Geol. Soc. Am. Bull.*, **76**, No. 7, 719–33.

EWART, A. *and* S. R. TAYLOR. 1969. Trace element geochemistry of the rhyolitic volcanic rocks, central North Island, New Zealand. Phenocryst data. *Contr. Miner. Petrol.* (*Beitr. Miner. Petrogr.*), **22**, No. 2, 127–46.

FAURE, G., HILL, R. L., JONES, L. M. *and* D. H. ELLIOT. 1971. Isotope composition of strontium and silica content of Mesozoic basalt and dolerite from Antarctica. (*In* ADIE, R. J., *ed. Antarctic geology and geophysics.* Oslo, Universitetsforlaget, 617–24.)

FOURCADE, N. H. 1971. Volcanic evolution at Deception Island: studies during 1970–1971. *Antarct. Jnl U.S.*, **6**, No. 4, 86.

GONZÁLEZ-FERRÁN, O. 1971. Distribution, migration and tectonic control of Upper Cenozoic volcanism in west Antarctica and South America. (*In* ADIE, R. J., *ed. Antarctic geology and geophysics.* Oslo, Universitetsforlaget, 173–79.)

————. *and* Y. KATSUI. 1970. Estudio integral del volcanismo cenozoico superior de las Islas Shetland del Sur, Antártica. *Ser. cient. Inst. antárt. chileno*, **1**, No. 2, 123–74. [*Contrnes Inst. antárt. chileno*, No. 22.]

————., MUNIZAGA, F. *and* H. MORENO. 1971*a*. Sintesis de la evolución volcánica de Isla Decepción y la erupción de 1970. *Ser. cient. Inst. antárt. chileno*, **2**, No. 1, 1–14. [*Contrnes Inst. antárt. chileno*, No. 24.]

————., ————. *and* ————. 1971*b*. 1970 eruption at Deception Island: distribution and chemical features of ejected materials. *Antarct. Jnl U.S.*, **6**, No. 4, 87–88.

GOURDON, E. 1914. Sur la constitution minéralogique des Shetlands du Sud. *C. r. hebd. Séanc. Acad. Sci., Paris*, **158**, No. 25, 1905–07.

GREEN, D. H. *and* W. HIBBERSON. 1970. The instability of plagioclase in peridotite at high pressure. *Lithos*, **3,** No. 3, 209–21.

HÄKLI, T. A. *and* T. L. WRIGHT. 1967. The fractionation of nickel between olivine and augite as a geothermometer. *Geochim. cosmochim. Acta*, **31,** No. 5, 877–84.

HALPERN, M. 1970. Rubidium-strontium dates and Sr^{87}/Sr^{86} initial ratios of rocks from Antarctica and South America: a progress report. *Antarct. Jnl U.S.*, **5,** No. 5, 159–61.

HAWKES, D. D. 1961. The geology of the South Shetland Islands: II. The geology and petrology of Deception Island. *Falkland Islands Dependencies Survey Scientific Reports*, No. 27, 43 pp.

HENDERSON, P. *and* I. M. DALE. 1970. The partitioning of selected transition element ions between olivine and groundmass of oceanic basalts. (*In* Geochemical application of crystal-field theory. *Chem. Geol.*, **5,** No. 4, 267–74.)

HOBBS, G. J. 1968. The geology of the South Shetland Islands: IV. The geology of Livingston Island. *British Antarctic Survey Scientific Reports*, No. 47, 34 pp.

HOLTEDAHL, O. 1929. On the geology and physiography of some Antarctic and sub-Antarctic islands. *Scient. Results Norw. Antarct. Exped.*, No. 3, 172 pp.

JAKES, P. *and* J. GILL. 1970. Rare earth elements and the island arc tholeiitic series. *Earth planet. Sci. Lett.*, **9,** No. 1, 17–28.

KUNO, H. 1950. Petrology of Hakone Volcano and the adjacent areas, Japan. *Bull. geol. Soc. Am.*, **61,** No. 9, 957–1019.

————. 1966. Lateral variation of basalt magma types across continental margins and island arcs. *Bull. volcan.*, Sér. 2, **29,** 195–222.

LEWIS, J. F. 1967. Unit-cell dimensions of some aluminous natural clinopyroxenes. *Am. Miner.*, **52,** Nos. 1 and 2, 42–54.

————. 1969. Composition, physical properties and origin of sodic anorthites from the ejected plutonic blocks of the Soufrière volcano, St. Vincent, West Indies. *Contr. Miner. Petrol.* (*Beitr. Miner. Petrogr.*), **21,** No. 3, 272–94.

————. 1971. Composition, origin and differentiation of basalt magma in the Lesser Antilles. (*In* DONNELLY, T. W., *ed.* Caribbean geophysical, tectonic, and petrologic studies. *Mem. geol. Soc. Am.*, No. 130, 159–79.)

MCREATH, I. 1972. *Petrogenesis in island arcs.* Ph.D. thesis, University of Leeds, 110 pp. [Unpublished.]

MELSON, W. G., THOMPSON, G. *and* TJ. H. VAN ANDEL. 1968. Volcanism and metamorphism in the mid-Atlantic ridge, 22°N latitude. *J. geophys. Res.*, **73,** No. 18, 5925–41.

MERCY, E. [L. P.] *and* M. J. O'HARA. 1967. Distribution of Mn, Cr, Ti and Ni in co-existing minerals of ultramafic rocks. *Geochim. cosmochim. Acta*, **31,** No. 12, 2331–41.

MINEAR, J. W. *and* M. N. TOKSÖZ. 1970. Thermal regime of a downgoing slab and new global tectonics. *J. geophys. Res.*, **75,** No. 8, 1397–419.

MOORE, J. G. 1966. Rate of palagonitization of submarine basalt adjacent to Hawaii. (*In* Geological Survey research 1966. *Prof. Pap. U.S. geol. Surv.*, No. 550-D, D163–71.)

NELSON, P. H. H. 1966. The James Ross Island Volcanic Group of north-east Graham Land. *British Antarctic Survey Scientific Reports*, No. 54, 62 pp.

NICHOLLS, G. D. 1965. Petrological and geochemical evidence for convection in the Earth's mantle. *Phil. Trans. R. Soc.*, Ser. A, **258,** No. 1088, 168–79.

NICHOLLS, I. A. 1971*a*. Petrology of Santorini volcano, Cyclades, Greece. *J. Petrology*, **12,** Pt. 1, 67–119.

————. 1971*b*. Santorini volcano, Greece; tectonic and petrochemical relationships with volcanics of the Aegean region. *Tectonophysics*, **11,** No. 5, 377–85.

NICHOLLS, J., CARMICHAEL, I. S. E. *and* J. C. STORMER. 1971. Silica activity and P_{total} in igneous rocks. *Contr. Miner. Petrol.* (*Beitr. Miner. Petrogr.*), **33,** No. 1, 1–20.

NOCKOLDS, S. R. *and* R. ALLEN. 1953. The geochemistry of some igneous rock series. *Geochim. cosmochim. Acta*, **4,** No. 3, 105–42.

OLSACHER, J. 1956. Contribución al conocimiento geológico de la Isla Decepción. (*In* OLSACHER, J., DIAZ, H. *and* M. TERUGGI. Contribución a la geología de la Antártida occidental. *Publnes Inst. antárt. argent.*, No. 2, 19–76.)

ORHEIM, O. 1970. Glaciological investigations on Deception Island. *Antarct. Jnl U.S.*, **5,** No. 4, 95–97.

————. 1971*a*. International volcanological expedition to Deception Island. *Antarct. Jnl U.S.*, **6,** No. 4, 82–83.

————. 1971*b*. Glaciological studies at Deception Island and Livingston Island. *Antarct. Jnl U.S.*, **6,** No. 4, 85.

————. 1971*c*. Volcanic activity on Deception Island, South Shetland Islands. (*In* ADIE, R. J., *ed. Antarctic geology and geophysics.* Oslo, Universitetsforlaget, 117–20.)

OSBORN, E. F. 1959. Role of oxygen pressure in the crystallization and differentiation of basalt magma. *Am. J. Sci.*, **257,** 609–47.

PADFIELD, T. [D.] *and* A. GRAY. 1971. Major element rock analysis by X-ray fluorescence—a simple fusion method. *Philips Analytical Equipment Bulletin*, **FS 35,** 4 pp.

PAUL, D. K. 1970. *A study of ultramafic inclusions in basalt and their application to the upper mantle composition.* Ph.D. thesis, University of Leeds, 154 pp. [Unpublished.]

PEARCE, J. A. *and* J. R. CANN. 1971. Ophiolite origin investigated by discriminant analysis using Ti, Zr, and Y. *Earth planet. Sci. Lett.*, **12,** No. 3, 339–49.

PHILPOTTS, J. A. *and* C. C. SCHNETZLER. 1970. Phenocryst-matrix partition coefficients for K, Rb, Sr, and Ba, with applications to anorthosite and basalt genesis. *Geochim. cosmochim. Acta*, **34,** No. 3, 307–22.

REA, W. J. 1970. *The geology of Montserrat, British West Indies.* D.Phil. thesis, University of Oxford, 196 pp. [Unpublished.]

REX, D. C. 1971. K-Ar determinations on volcanic and associated rocks from the Antarctic Peninsula and Dronning Maud Land. (*In* ADIE, R. J., *ed. Antarctic geology and geophysics.* Oslo, Universitetsforlaget, 133–36.)

————. *and* P. E. BAKER. 1973. Age and petrology of the Cornwallis Island granodiorite. *British Antarctic Survey Bulletin*, No. 32, 55–61.

ROOBOL, M. J. 1973. Historic volcanic activity at Deception Island. *British Antarctic Survey Bulletin*, No. 32, 23–30.

ROOKE, J. M. *and* A. M. FISHER. 1962. Validity of spectrographic determinations of trace elements in granite G-1 and diabase W-1. *Geochim. cosmochim. Acta*, **26**, No. 2, 335–42.

SHULTZ, C. H. 1970. Petrology of the Deception Island volcano, Antarctica. *Antarct. Jnl U.S.*, **5**, No. 4, 97–98.

———. 1971. Petrologic and volcanologic investigation of Deception Island. *Antarct. Jnl U.S.*, **6**, No. 4, 83–84.

———. 1972. Eruption at Deception Island, Antarctica, August 1970. *Geol. Soc. Am. Bull.*, **83**, No. 9, 2837–42.

SIMKIN, T. *and* J. V. SMITH. 1970. Minor-element distribution in olivine. *J. Geol.*, **78**, No. 3, 304–25.

TAYLOR, S. R., KAYE, M., WHITE, A. J. R., DUNCAN, A. R. *and* A. EWART. 1969. Genetic significance of Co, Cr, Ni, Sc, and V content of andesites. *Geochim. cosmochim. Acta*, **33**, No. 2, 275–86.

THORARINSSON, S. 1958. The Oraefajökull eruption of 1362. *Acta nat. islandica*, **2**, No. 2, 99 pp.

VALENZUELA, E., CHÁVEZ, L. and F. MUNIZAGA. 1968. Informe preliminar sobre la erupción de Isla Decepción ocurrida en diciembre de 1967. *Bol. Inst. antárt. chileno*, No. 3, 5–16.

———., ———. *and* ———. 1970. Actividad volcánica en Isla Decepción, Antártica, 1967. *Ser. cient. Inst. antárt. chileno*, **1**, No. 1, 25–40. [*Contrnes Inst. antárt. chileno*, No. 18.]

VILJOEN, M. J. *and* R. P. VILJOEN. 1969. The geology and geochemistry of the lower ultramafic unit of the Onverwacht Group and a proposed new class of igneous rocks. (*In* HAUGHTON, S. H. *and others*. Upper Mantle Project, South African National Committee Symposium, Pretoria, July 1969. *Spec. Publs geol. Soc. S. Afr.*, No. 2, 55–85.)

WAGER, L. R. *and* W. A. DEER. 1939. Geological investigations in East Greenland. Pt. III. The petrology of the Skaergaard intrusion, Kangerdlugssuak, East Greenland. *Meddr Grønland*, **105**, No. 4, 1–352.

WILKES, C. 1845. *Narrative of the United States Exploring Expedition, during the years 1838, 1839, 1840, 1841, 1842*. Vols. I–V, Atlas. Philadelphia, Lea & Blanchard.

WILLIAMS, J. 1969. Volcanoes beneath the Antarctic ice. *Geogrl Mag., Lond.*, **41**, No. 7, 553–54.

YODER, H. S. 1969. Calcalkalic andesites: experimental data bearing on the origin of their assumed characteristics. (*In* MCBIRNEY, A. R., *ed.* Proceedings of the andesite conference. *Bull. Ore. St. Dep. Geol. miner. Ind.*, No. 65, 77–89.)

———. *and* C. E. TILLEY. 1962. Origin of basalt magmas: an experimental study of natural and synthetic rock systems. *J. Petrology*, **3**, Pt. 3, 342–532.

PLATE I

a. Whalers Bay and Cathedral Crags viewed from the lower slopes of Ronald Hill. In the middle distance are the remains of the old whaling station and the British Antarctic Survey station. Much of the debris on the lower ground was dropped by the lahar and flood which swept the area in February 1969.

b. The 1967 island viewed from the lower slopes of Telefon Ridge. In the distance steam rises from the land centre.

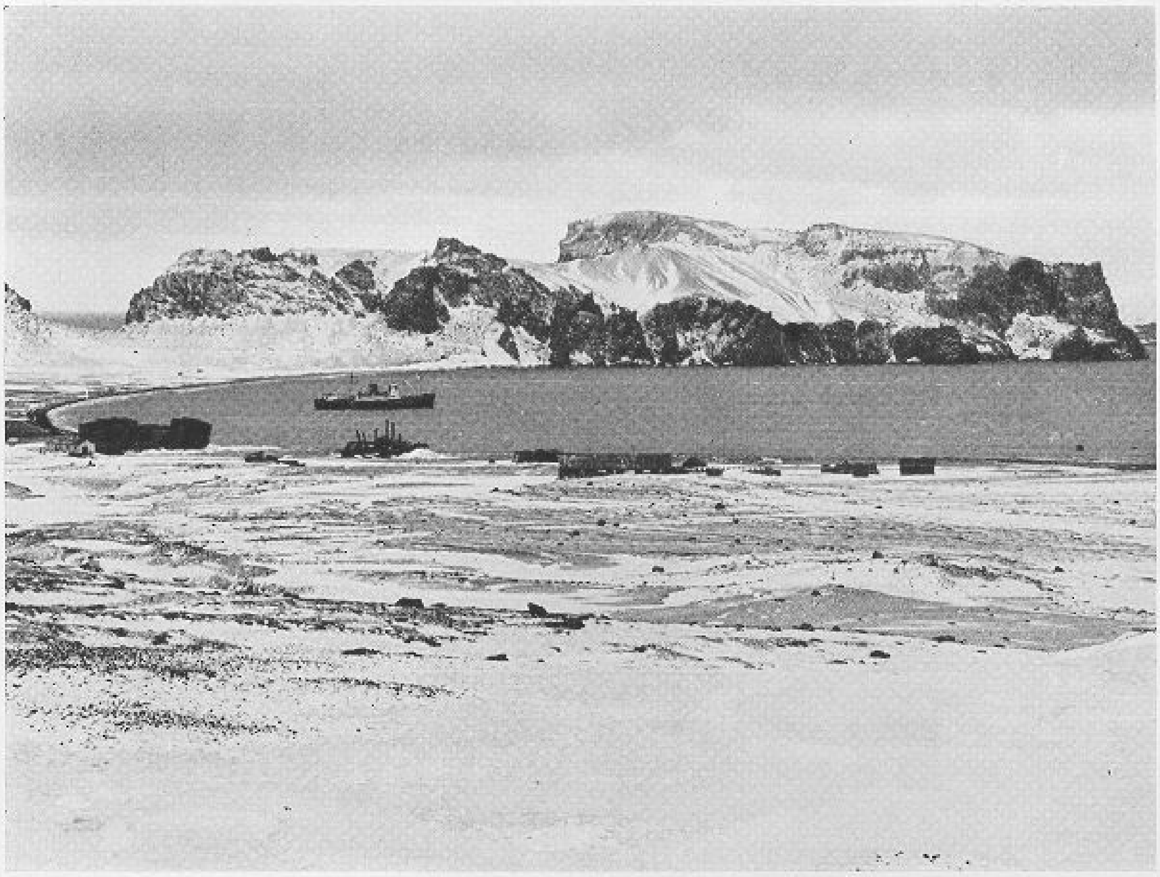

a

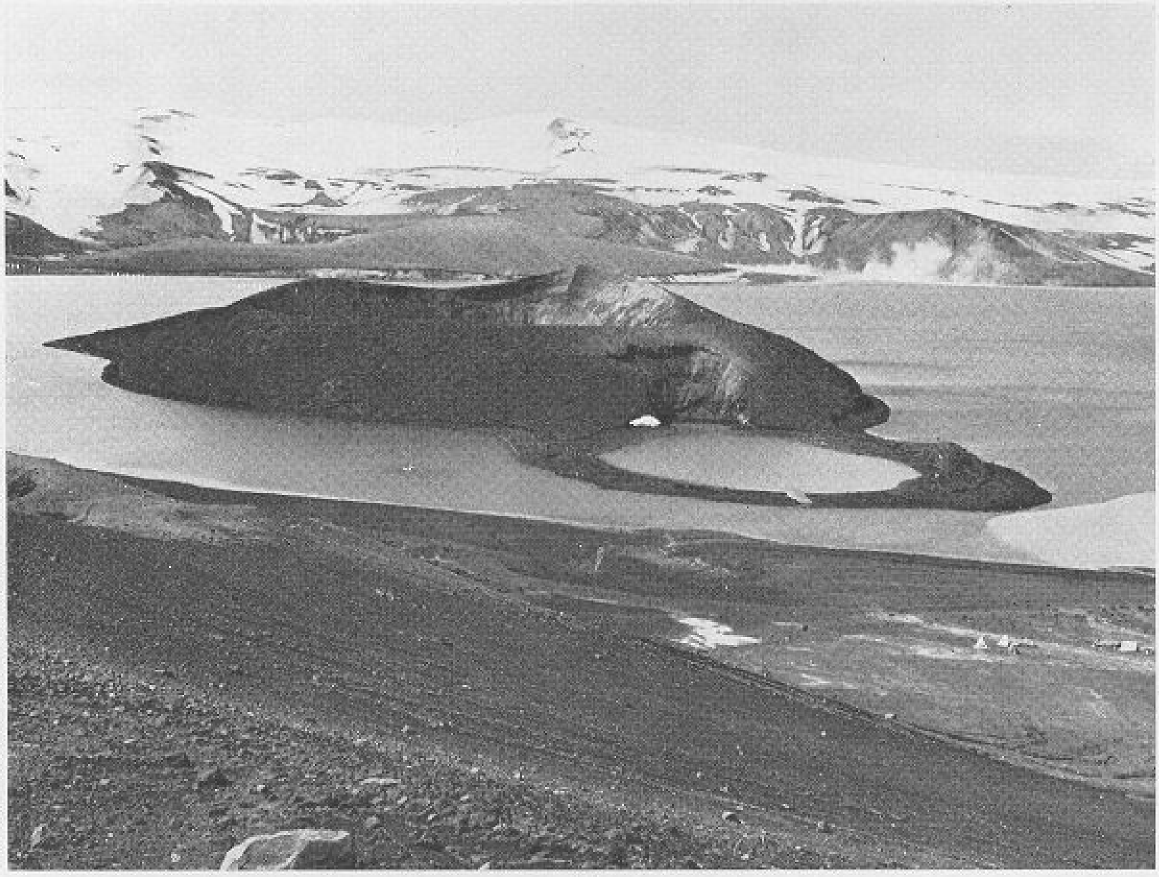

b

PLATE II

a. The northern part of Port Foster viewed from the north-east, showing Telefon Bay and the 1967 island. Beyond is the caldera wall, here formed by Stonethrow Ridge and Telefon Ridge. The two water-filled craters in the foreground were both drained during the subsequent 1970 eruption.

b. An oblique aerial view of the 1967 island from the south. Beyond is the northern part of the caldera wall.

c. An aerial view of the 1967 land centre from the north-west, showing the main water-filled crater and the new coastal embayment. Strong fumarolic activity is in evidence. The new gully, cut deeply into loosely consolidated pyroclastic deposits, can be seen in the bottom left of the picture.

d. Large bombs from the 1967 island litter the beach on the western side of Telefon Bay.

a

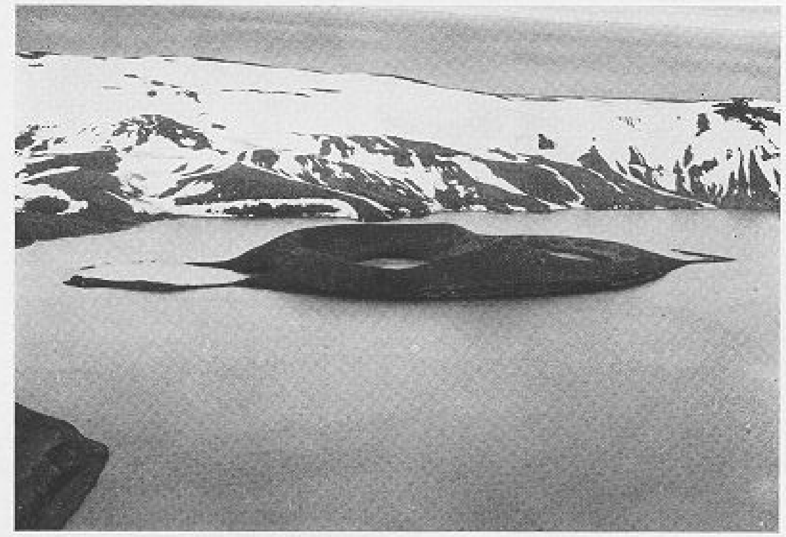

b

c

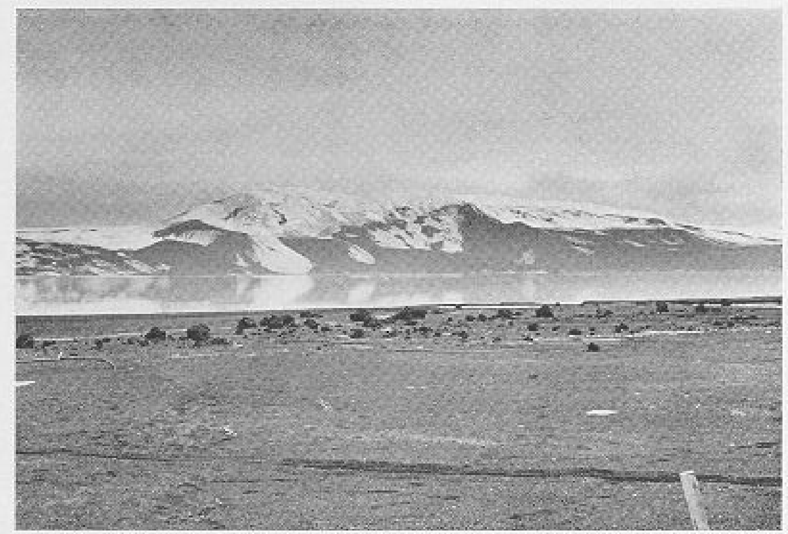

d

PLATE II

PLATE III

a. General view of the northern part of the 1969 fissure.

b. The widest and most active part of the 1969 fissure above Pendulum Cove. The vertical ice walls mark the north-eastern side of the chasm but the southern edge is blanketed by piles of scoria from which fumarolic gases issue.

c. Intense fumarolic activity from the 1969 ejecta on the south-western edge of the new fissure above Pendulum Cove.

d. The highly unstable ice bridge which spans the narrow northernmost section of the 1969 fissure. Note the figure in the lower central part of the picture for scale and also the dark dust/ash layers upon which Orheim (1971*c*) based his glacial stratigraphy.

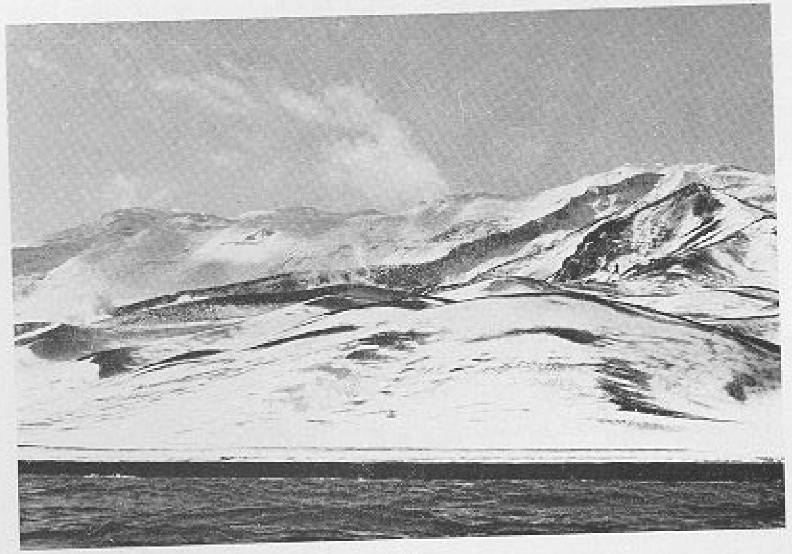

a

b

c

d

PLATE III

PLATE IV

a. Highly crevassed slopes south-west of Mount Pond near section D of the new fissure system. Erosion and gullying of the glacier have been accentuated by melt water generated in the 1969 activity.

b. The isolated "cirque" feature at the southern end of the 1969 fissure system (Fig. 25, B). The scattered ice blocks have been distributed by the flood of melt water. New pyroclastic deposits are exposed patchily at the surface.

c. Large blocks of ice and tuff, the debris of the 1969 flood and lahars, cover the low ground west of Ronald Hill.

d. Perched blocks of ice, left stranded by the passing flood waters, litter the hummocky ground between Pendulum Cove and Whalers Bay. This photograph was taken from about 2 km. north-west of Whalers Bay.

a

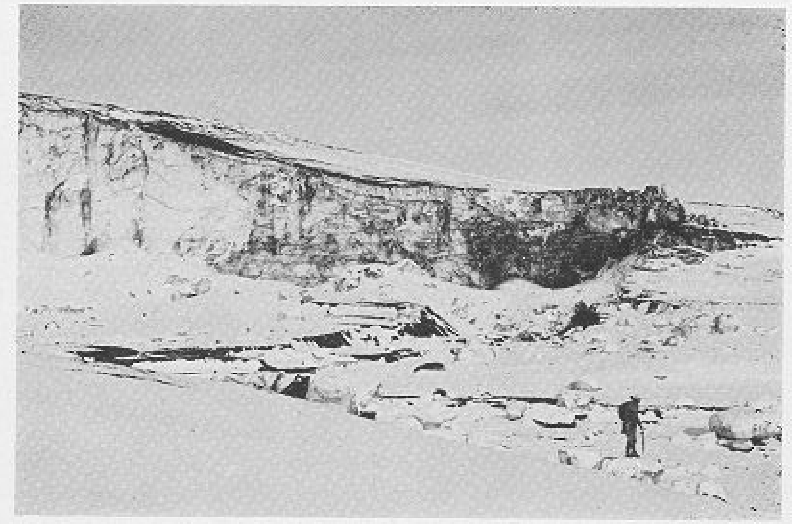

b

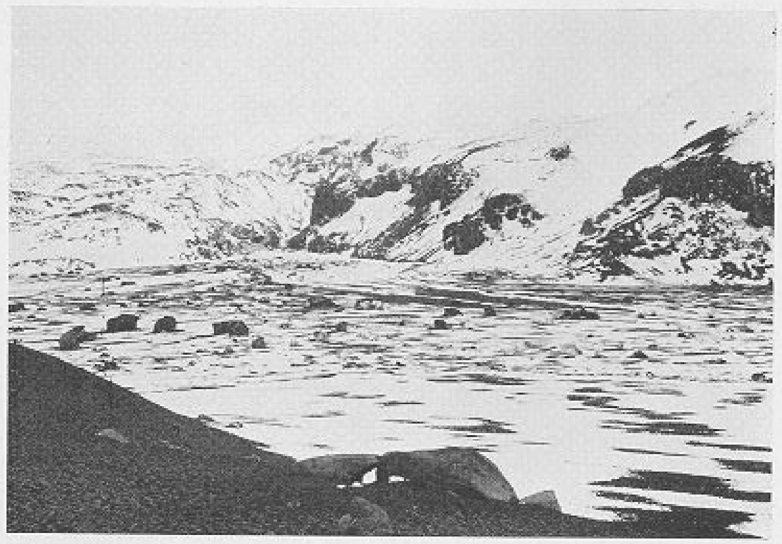

c

d

PLATE IV

PLATE V

a. Huts at the Chilean station, Pendulum Cove, blanketed by ash from the 1967 eruption. The ash is only about 50 cm. thick but it covers drifted snow which had been insulated during the 1967–68 summer.

b. Remnants of the Chilean station at Pendulum Cove after the 1969 eruption. Steam rises from section E of the new fissure in the background.

c. The tottering remains of the old whaling station and the British Antarctic Survey station after the 1969 flood.

d. A badly damaged section of "Biscoe House" at the British Antarctic Survey station after the 1969 flood and lahars. Cinders from the eruption cover the roof.

a

b

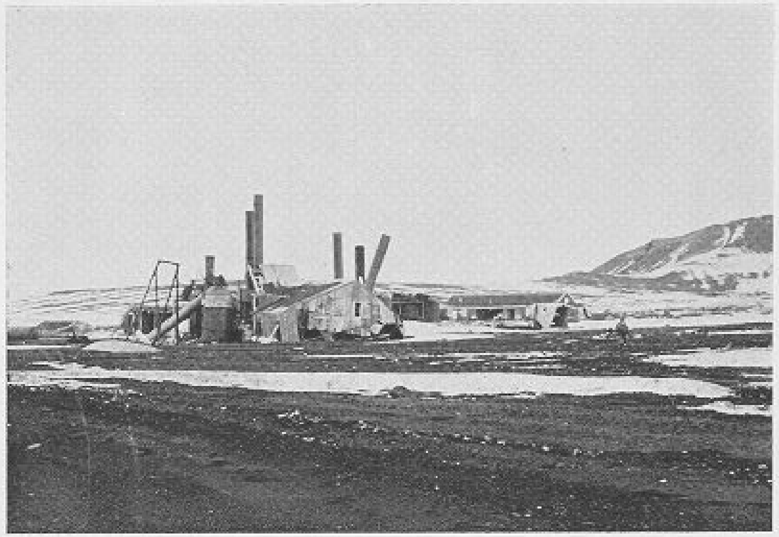

c

d

PLATE V

PLATE VI

a. View south-westward from the fumaroles beside the large double crater (5) of the 1970 eruption towards the relic of the 1967 island. Bombs erupted in 1970 litter the surface of the new strip of low ground which has been built out of Telefon Bay.

b. View southward to Cross Hill over the three craters which formed at the western end of the new strip of land in August 1970.

c. Looking north-eastward along the new strip of land in Telefon Bay. The lakes are: crater 3 in the bottom right, crater 4, and in the distance the composite crater 5. The hill to the right is the greatly reduced 1967 island.

d. View south-eastward over 1970 craters 2 (foreground) and 1, with crater 3 to the left. In the distance are Port Foster, Mount Pond, and at the far right Cathedral Crags.

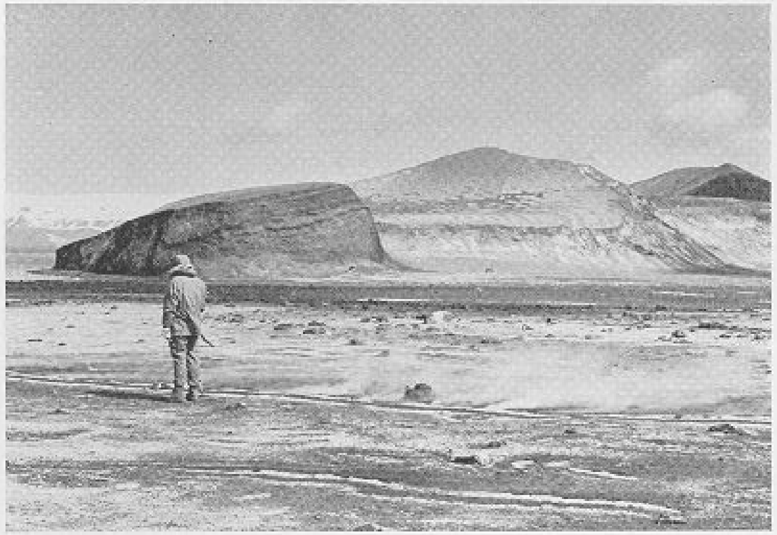

a

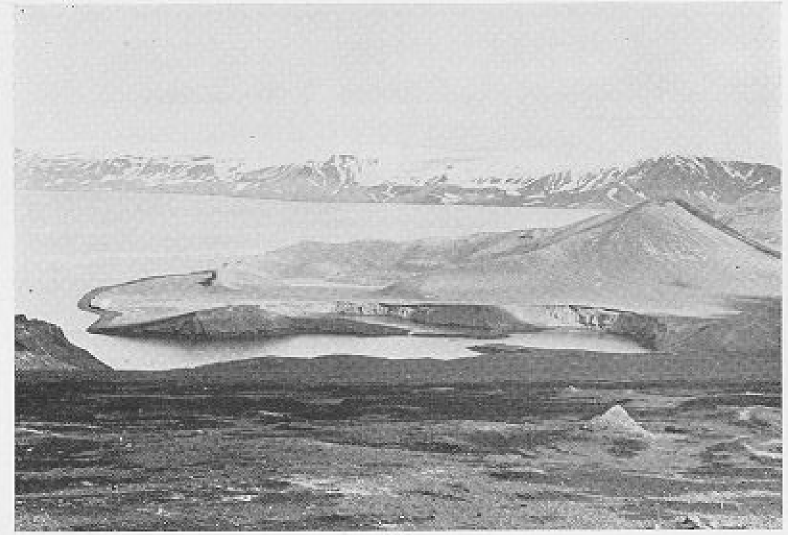

b

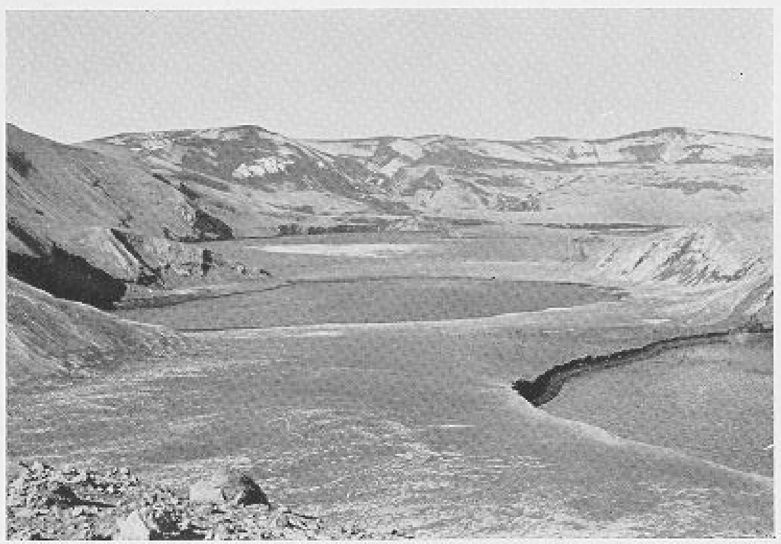

c

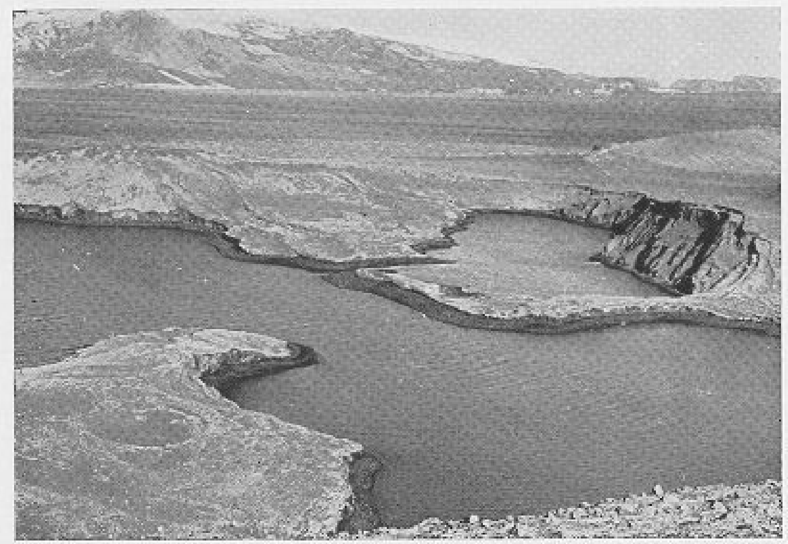

d

PLATE VI

PLATE VII

a. The new land strip in Telefon Bay viewed from the north-east. In the foreground is the largest of the new craters (5) and beyond are the other water-filled craters, the remains of the 1967 island, Cross Hill and the caldera wall (Stonethrow and Telefon Ridges).

b. View south-south-eastward from Telefon Ridge over the remains of the 1967 island. The 1970 "crater" 4 can be seen on the north side of the island (bottom right) and beyond is crater 3. Note that the island has been bisected longitudinally, preserving half of the 1967 crater 3 to the left of the highest ridge and part of crater 2 to the right. These craters have been further modified by the accumulation of debris from the 1970 eruption.

c. Aerial view of the western part of the new land strip in Telefon Bay. The remnant of the 1967 island with its partially preserved craters is clearly seen in the centre of the photograph. (Official U.S. Coast Guard photograph.)

d. 1970 craters north-east of the 1967 land centre. The largest of the new craters, cut into the glacier, is at the left; alluvial and mudflow deposits cover its floor. The 1967 land centre lies to the upper right. (Official U.S. Coast Guard photograph.)

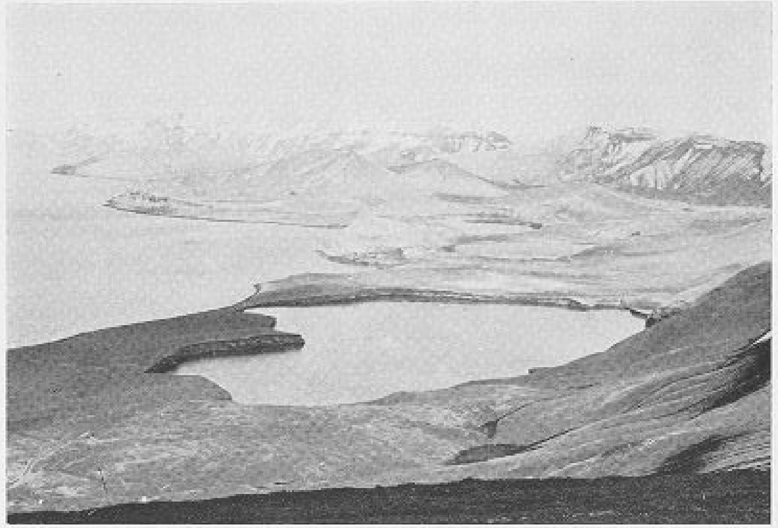

a

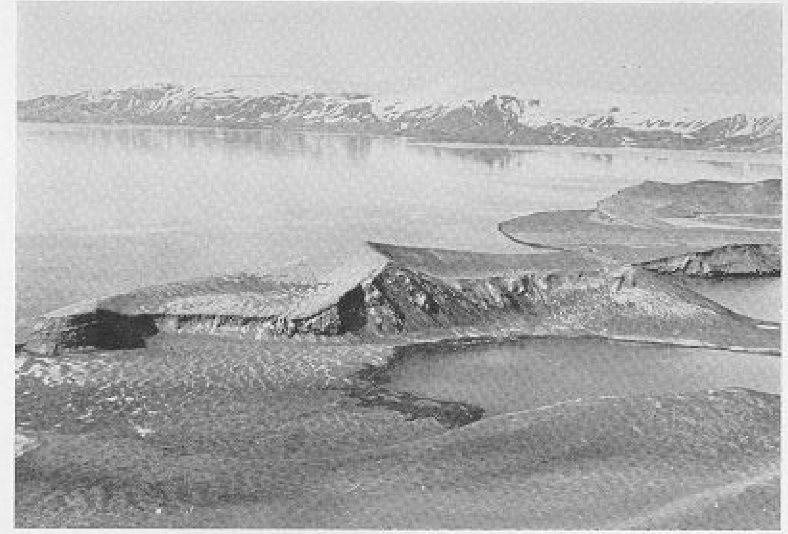

b

c

d

PLATE VII

PLATE VIII

a. 30·5 m. section of horizontally bedded grey tuffs showing large-scale subaqueous cross stratification (lower right corner) with symmetrical channel structures higher in the sequence. At the top the tuffs are interbedded with thin lavas and scoriaceous material; Vapour Col.

b. Enlargement of subaqueous cross stratification as in Plate VIIIa; Vapour Col.

c. Two weathered-out channel structures in the tuff sequence. The grain-size is extremely variable between beds; opposite the Argentine station, overlooking Port Foster.

d. 6 m. of re-distributed yellow tuffs showing variation in grain-size of the beds and (?) aeolian cross stratification; Argentine station.

PLATE VIII

a

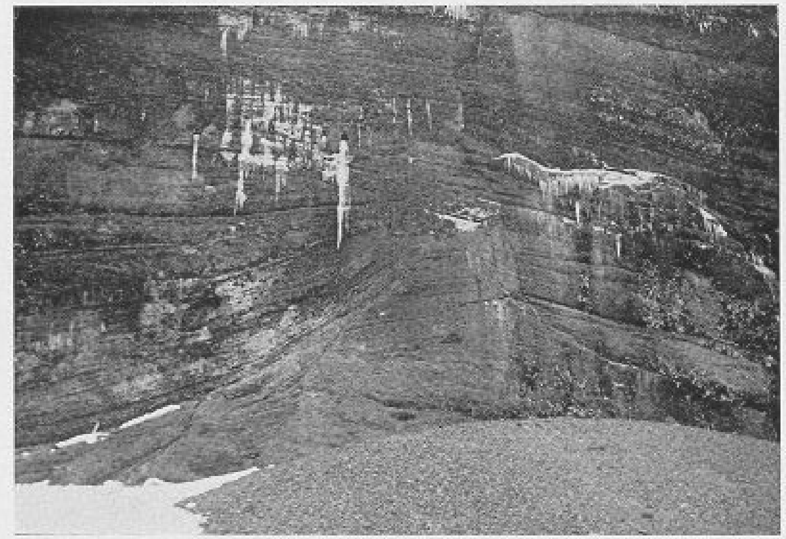

b

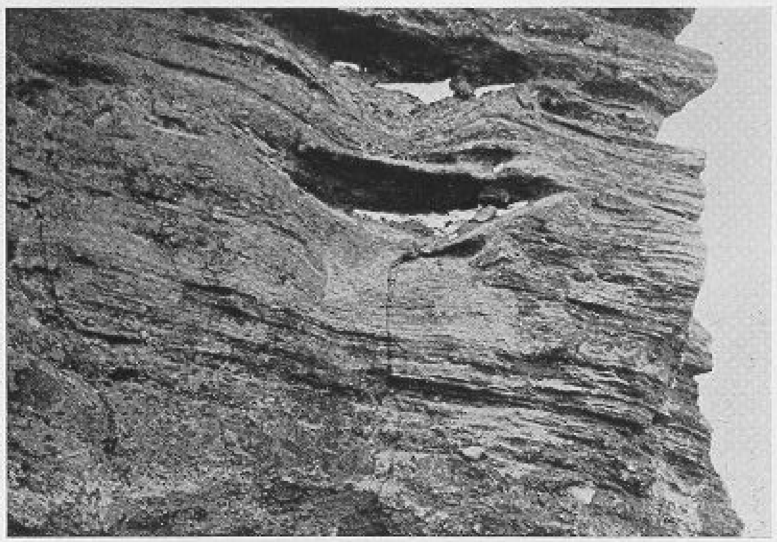

c

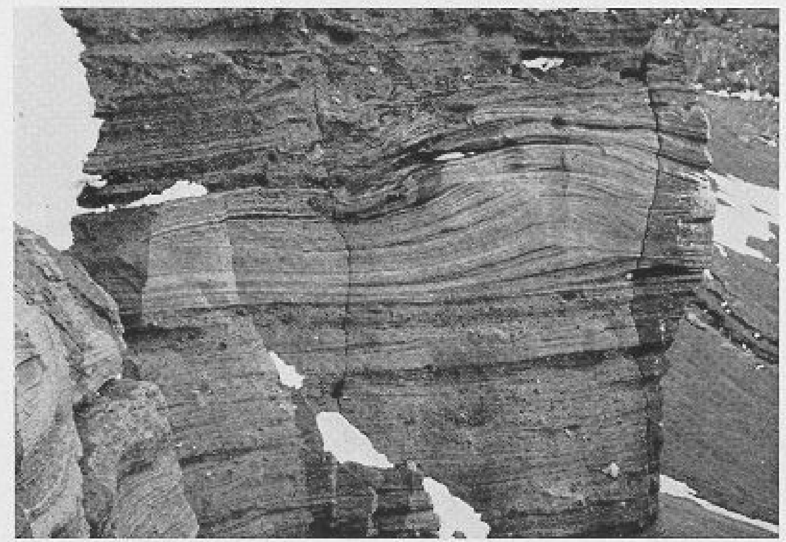

d

PLATE IX

a. Lightly welded pumiceous agglomerate forming the high cliffs on Fumarole Bay. It is thought to represent pyroclast flow deposits closely associated with caldera formation.

b. A large bomb on the slopes of crater 2, 1967 island.

c. A large contorted bomb, 1967 island.

d. 1970 pyroclastic deposits lying on top of snow on the steep north-western slopes of Goddard Hill, leading down to Kendall Terrace. The early melt had already caused appreciable erosion on the slopes by December 1970.

a

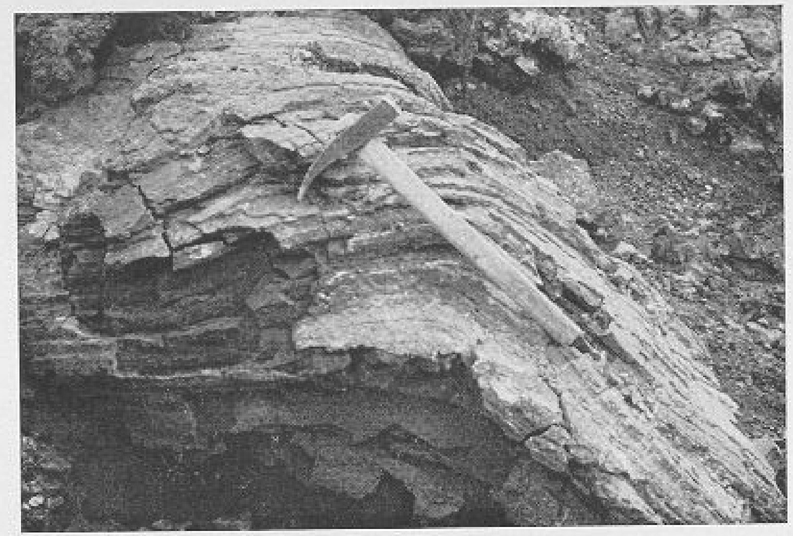

b

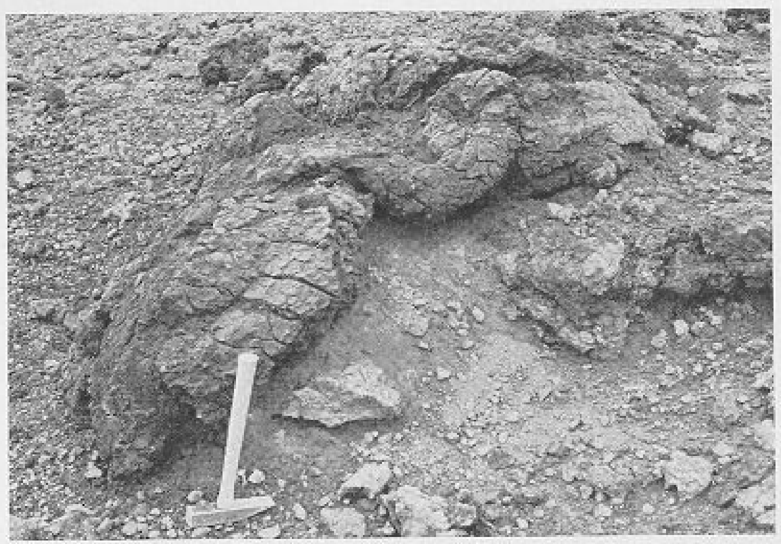

c

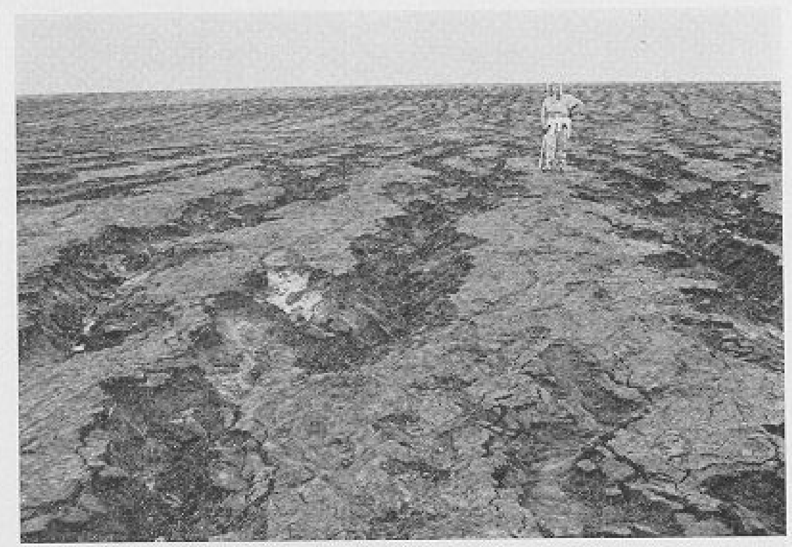

d

PLATE IX

PLATE X

a. Olivine-basalt from young Post-caldera Series (Whalers Bay Group of Hawkes (1961)); south end of Stonethrow Ridge. Olivine phenocryst partially altered to iddingsite in an intergranular matrix of plagioclase, clinopyroxene and magnetite, which also occurs on microphenocrysts. (B.410.2; ordinary light; ×30)

b. Post-caldera tuff; 0·5 km. south of the Argentine station, Fumarole Bay. Clinopyroxene and plagioclase phenocrysts in pale brown unaltered sideromelane. The vesicular glass contains microlites of feldspar and pyroxene. (B.802.1; ordinary light; ×30)

c. Outer Coast Tuff; eastern side of Stonethrow Ridge, 1 km. west of Wensleydale Beacon. Fragment of sideromelane with a broad pelagonite rim. Note vesicles and alignment of plagioclase microlites. Calcite forms much of the cement between the fragments. (B.815.1; ordinary light; ×30)

d. Vesicular bomb; north-west side of crater 2, 1967 island. Erupted December 1967. Phenocrysts of clinopyroxene, plagioclase and magnetite in a matrix of feldspar laths and pale brown glass. (B.276.1; ordinary light; ×75)

e. Bomb; west side of crater 2, 1970 eruption in Telefon Bay. Partly resorbed plagioclase phenocryst with smaller crystals of clinopyroxene and magnetite in a dark scoriaceous matrix. (B.702.1; ordinary light; ×30)

f. Bomb; west side of crater 2, 1970 eruption in Telefon Bay. Microphenocrysts of clinopyroxene and magnetite in a dark scoriaceous matrix. (B.702.1; ordinary light; ×75)

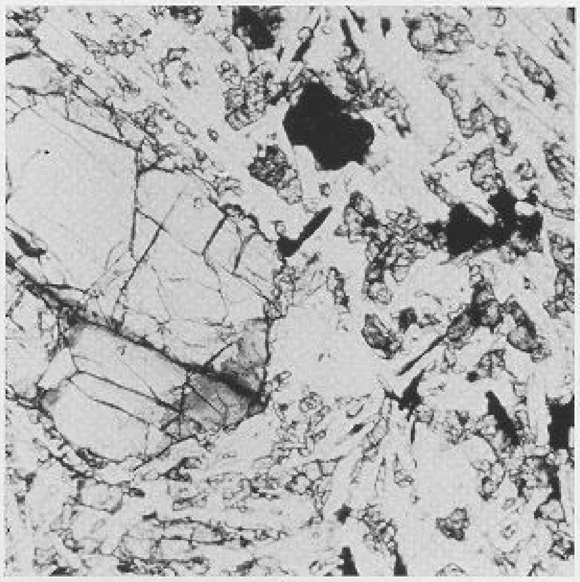

a

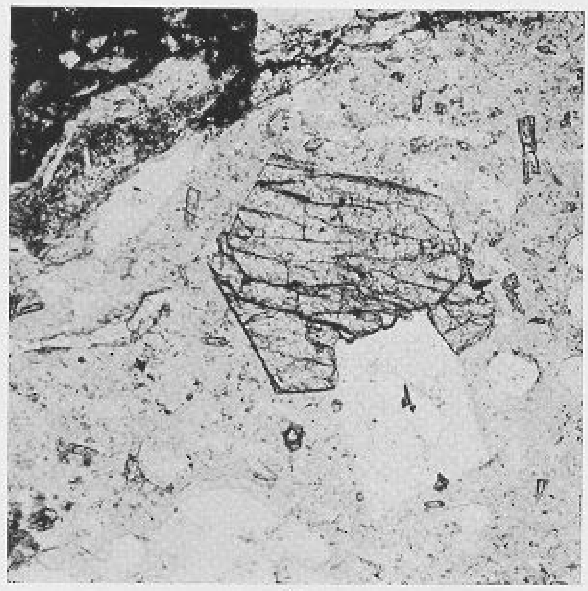

b

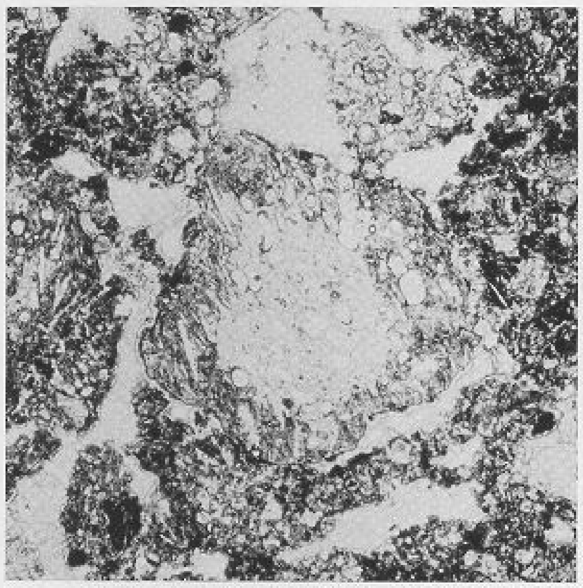

c

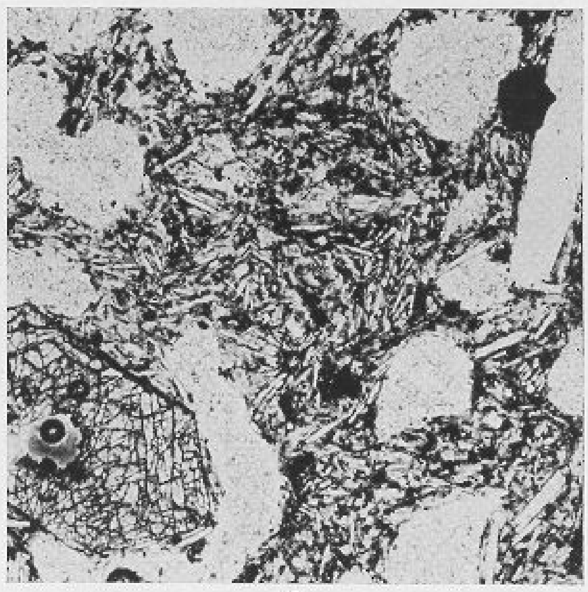

d

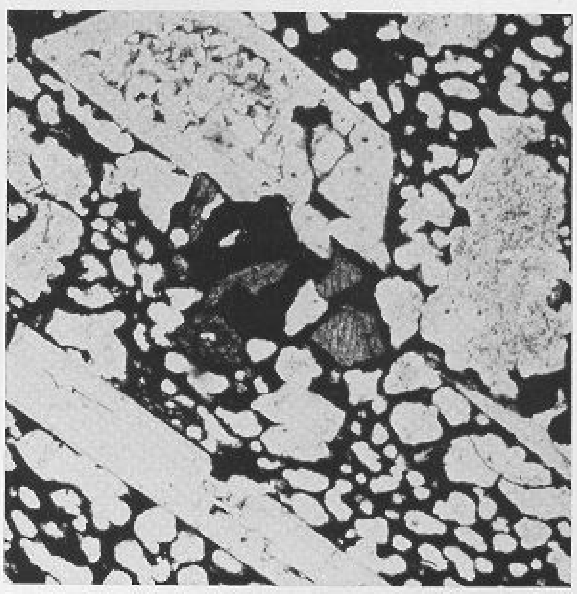

e

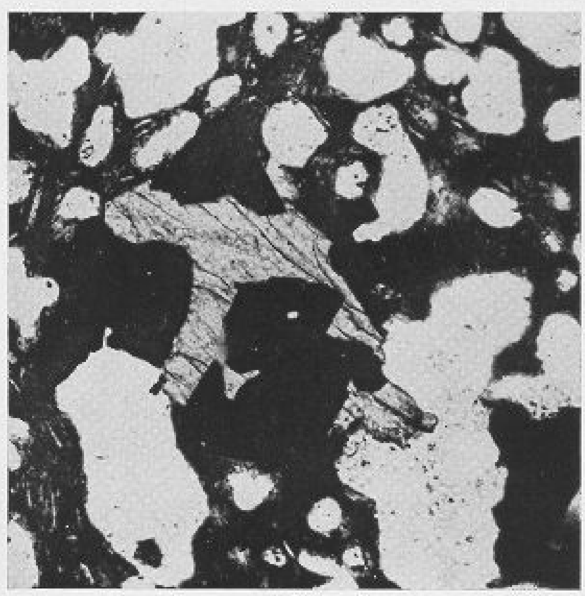

f

PLATE XI

a. Porphyritic olivine-basalt; 1 km. north of South East Point (loose block). Phenocrysts of olivine partly altered to serpentine and iddingsite in an intergranular fluidal matrix of plagioclase laths and clinopyroxene. (B.472.1; ordinary light; ×30)

b. Basalt; 1·5 km. north-west of Collins Point (block from glacier). Phenocryst of clinopyroxene in a fluidal matrix of plagioclase laths with granular pyroxene and magnetite. Occasional phenocrysts of olivine also occur. (B.434.1; ordinary light; ×75)

c. Aphyric basalt (high-alumina type); 1·5 km. west of Entrance Point. Plagioclase laths with granular clinopyroxene, olivine and magnetite. (B.432.1; ordinary light; ×140)

d. Basaltic dyke cutting Cathedral Crags pyroclastics; 200 m. north-east of Neptunes Window. Sub-parallel plagioclase laths enclosing granular clinopyroxene, olivine and magnetite. (B.426.1; ordinary light; ×75)

e. Dacite block; summit of Cathedral Crags. Phenocrysts of plagioclase (albite-oligoclase), clinopyroxene and magnetite in a microcrystalline to glassy base. (B.420.2; ordinary light; ×75)

f. Dacite; Cross Hill. Plagioclase (albite-oligoclase) and clinopyroxene phenocrysts in a microcrystalline to glassy base. (B.429.2; ordinary light; ×75)

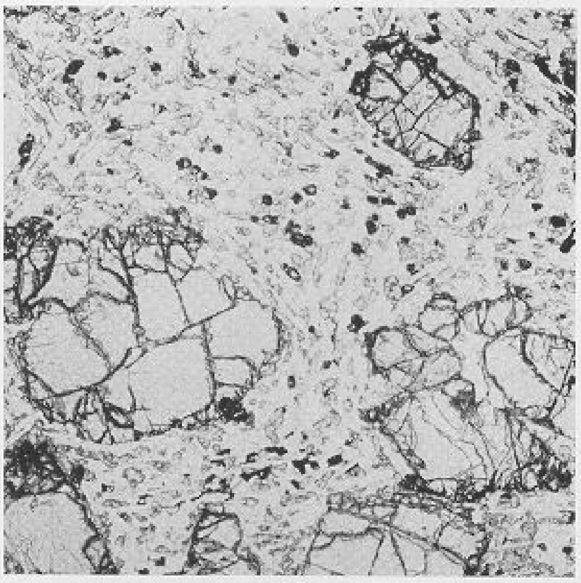

a

b

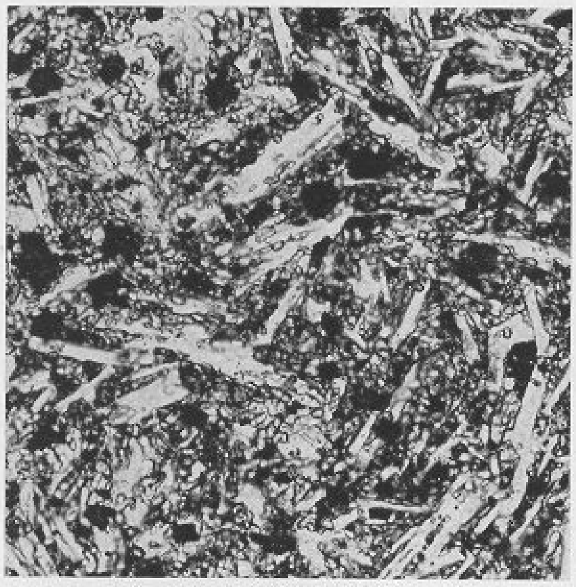

c

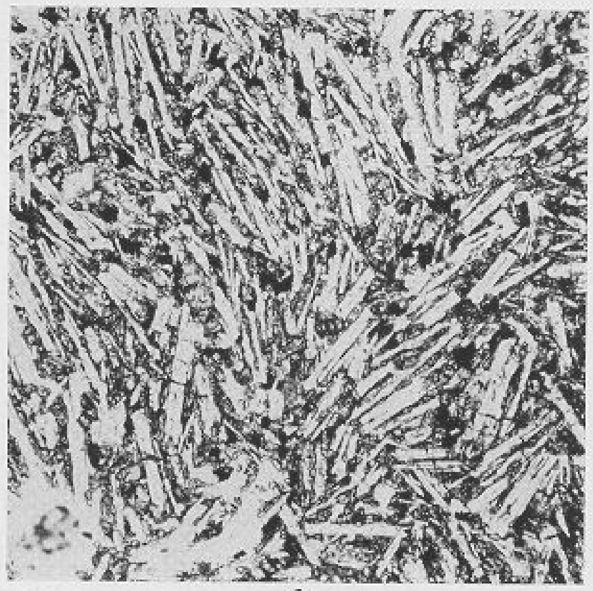

d

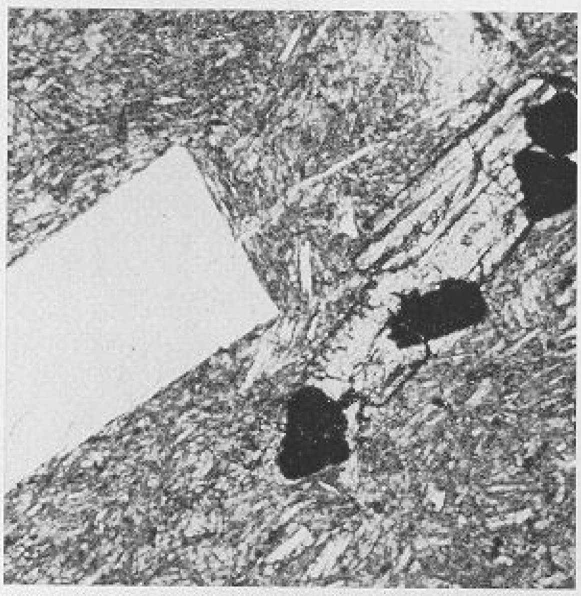

e

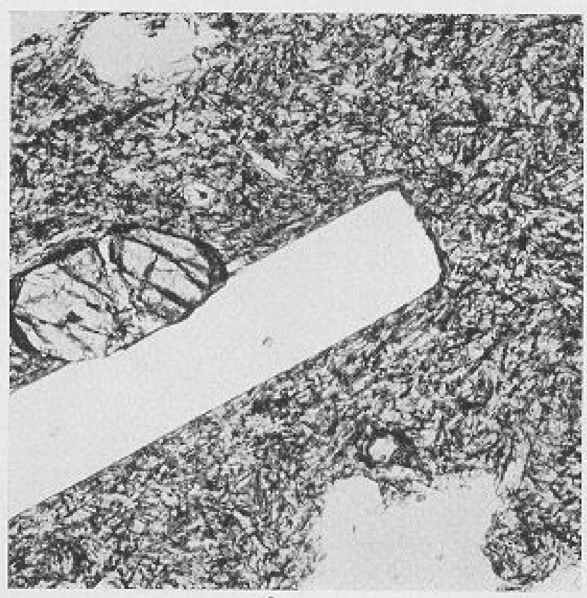

f

PLATE XII

a. Vesicular inclusion in Ronald Hill trachyte. Elongate plagioclase (albite-oligoclase) crystal with subhedral clinopyroxenes in a matrix of plagioclase and alkali-feldspar. (B.355.3; ordinary light; ×30)

b. Porphyritic dacite; east side of Cross Hill. Phenocrysts of plagioclase (albite-oligoclase), clinopyroxene and magnetite in a dark glassy base containing feldspar microlites. (B.429.1; ordinary light; ×75)

c. Ejected granodiorite block; above cliffs at south end of Kendall Terrace. Biotite, quartz and altered plagioclase. (B.316.1; ordinary light; ×30)

d. Cumulate block from 1967 island. Cumulus plagioclase (An_{88}) and olivine (Fo_{90}) with interstitial plagioclase and clinopyroxene. (B.304.1; X-nicols; ×30)

e. Cumulate block ejected from the new island in the 1967 eruption. High-temperature alteration of the matrix between the cumulus plagioclase and olivine. Feather-like quench aggregates of plagioclase, scapolite and clinopyroxene. (B.304.1; ordinary light; ×30)

f. Gabbro cumulate block; 1 km. south-west of Entrance Point. Plagioclase, clinopyroxene, olivine and magnetite with pale brown interstitial glass. (B.468.1; X-nicols; ×30)

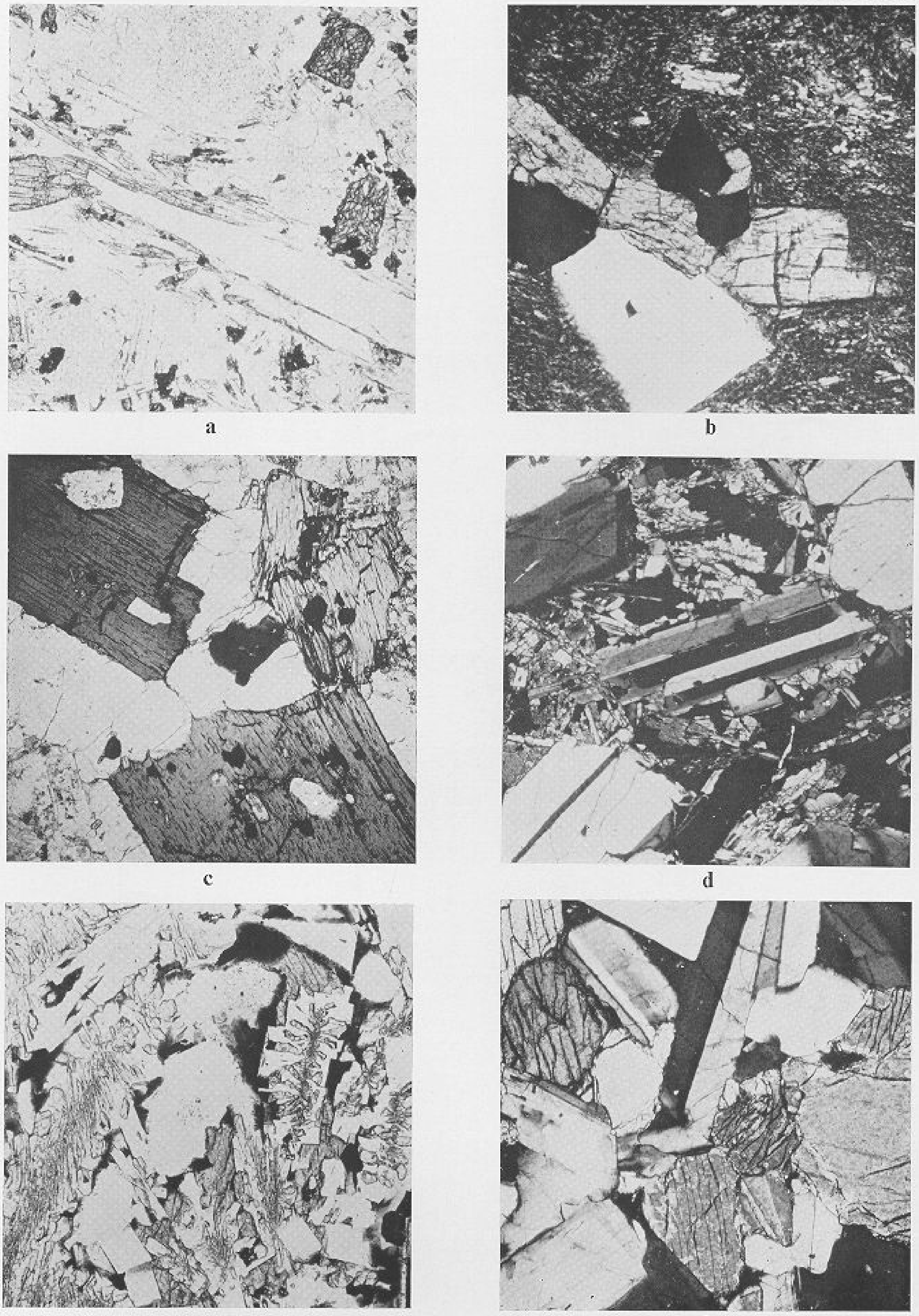
a b c d e f

PLATE XIII

An improvised seismograph utilizing a barograph and weighted boom was constructed by D. Snell, meteorologist at the British Antarctic Survey station in February 1969. This seismogram is the record produced by the instrument on the morning of 21 February. The event at the left of the chart, timed at 03.34 hr., is the strong earthquake which awakened men at the British station. The beginning of the eruption is marked by a relatively small seismic event at 09.50 hr. The low-amplitude disturbance between 10.00 and 10.30 hr. was probably caused by water and ice blocks entering the hut.

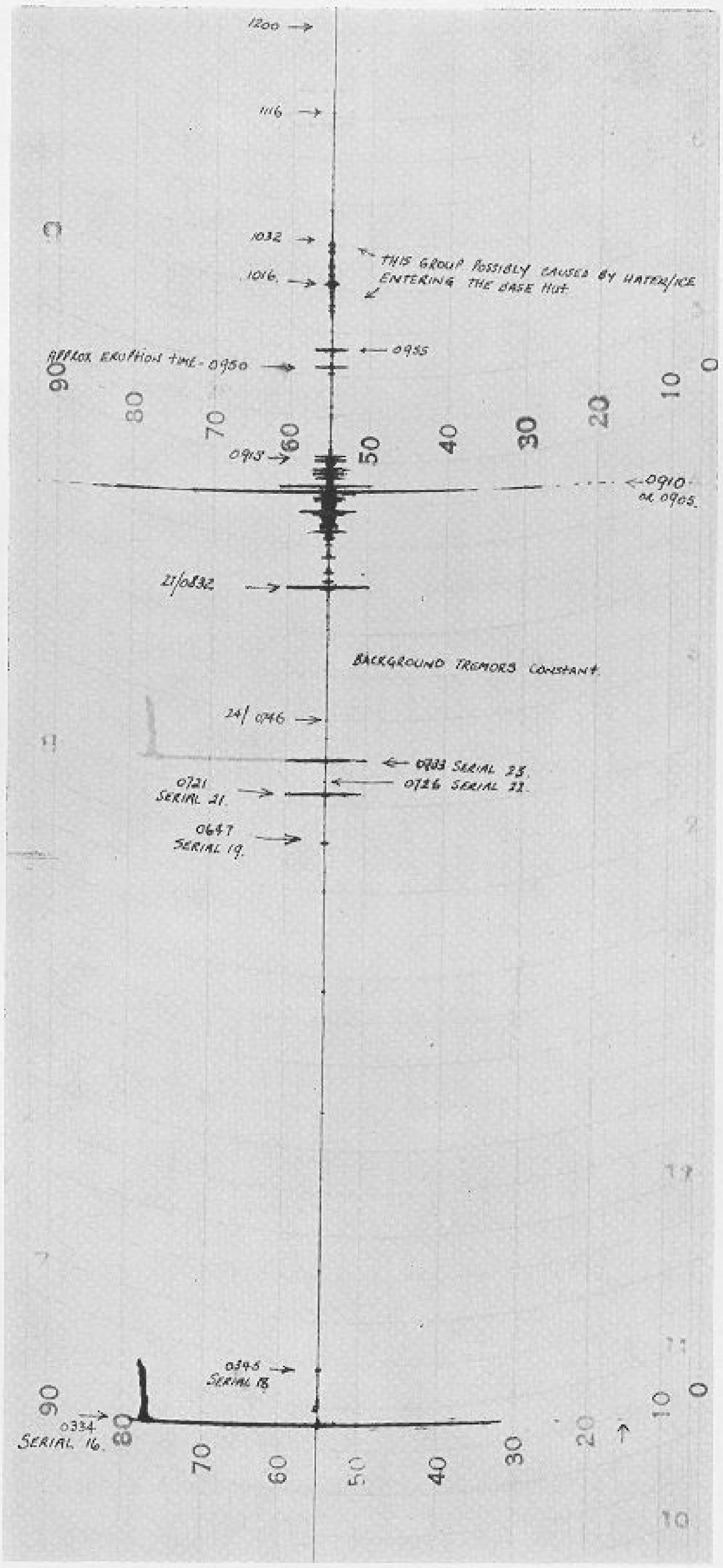
1200 →
1116 →
1032 →
1016. →
THIS GROUP POSSIBLY CAUSED BY WATER/ICE ENTERING THE BASE HUT
← 0955
APPROX ERUPTION TIME - 0950
0915 →
← 0910 or 0905.
21/0832 →
BACKGROUND TREMORS CONSTANT
24/0746 →
← 0733 SERIAL 23.
← 0726 SERIAL 22.
0721 SERIAL 21. →
0647 SERIAL 19. →
0345 SERIAL 18 →
0334 SERIAL 16.